SATELLITE OBSERVATIONS OF PHYTOPLANKTON VARIABILITY IN THE EASTERN EQUATORIAL PACIFIC

GENE CARL FELDMAN

1985

SATELLITE OBSERVATIONS OF PHYTOPLANKTON VARIABILITY IN THE EASTERN EQUATORIAL PACIFIC

A Dissertation presented

by

Gene Carl Feldman

to

The Graduate School

in Partial Fulfillment of the Requirements

for the Degree of

Doctor of Philosophy

in

Coastal Oceanography

Marine Sciences Research Center

State University of New York

at

Stony Brook

December 1985

STATE UNIVERSITY OF NEW YORK
AT STONY BROOK

THE GRADUATE SCHOOL

Gene Carl Feldman

We, the dissertation committee for the above candidate for the Doctor of Philosophy degree, hereby recommend acceptance of the dissertation.

J. R. Schubel, Advisor, Dean
Marine Sciences Research Center

Wayne E. Esaias, Chairman, Oceanographer
NASA / Goddard Space Flight Center

Richard T. Barber, Professor
Duke University Marine Laboratory

Malcolm J. Bowman, Associate Professor
Marine Sciences Research Center

David Halpern, Principal Research Associate
School of Oceanography and Department of Atmospheric Sciences
University of Washington

Charles R. McClain, Oceanographer
NASA / Goddard Space Flight Center

Akira Okubo, Professor
Marine Sciences Research Center

This dissertation is accepted by the Graduate School

The Graduate School

December 1985

Abstract of the dissertation

Satellite Observations of Phytoplankton Variability
in the Eastern Equatorial Pacific

by

Gene Carl Feldman

Doctor of Philosophy

in

Coastal Oceanography

Marine Sciences Research Center

State University of New York at Stony Brook

1985

The principal objective of this study is to assess the degree to which satellite ocean color observations can be used to improve our understanding of the patterns of biological production in the eastern equatorial Pacific Ocean. Specifically, observations from the Nimbus-7 Coastal Zone Color Scanner (CZCS) are used to quantify the variability of phytoplankton abundance over a wide range of time and space scales.

Mesoscale variability of phytoplankton biomass around the Galapagos Islands as well as the spatial extent of the region of enhanced phytoplankton production associated with the islands, is shown to be associated with large-scale oceanic and atmospheric circulation patterns. Satellite ocean color observations are used to document the effect of the 1982-83 El Nino on the distributions and abundances of phytoplankton throughout the eastern equatorial Pacific.

The structure and variability of coastal upwelling regions along the Peruvian coast are described through the use of CZCS imagery. A comparison between the patterns of phytoplankton distributions observed in the satellite images and those derived from shipboard observations, reveals that the offshore extent of the region of enhanced phytoplankton concentrations is significantly greater than previously described. In addition, the sharp transition from enhanced to oceanic conditions that is seen in the CZCS images suggests that physical rather than biological factors may control the shape and offshore extent of the region of enhanced phytoplankton abundances. Satellite data are also used to describe the short-term variability of the coastal upwelling system to changes in atmospheric forcing.

This study documents that significant interannual variability in the areal extent of the region of enhanced biological production, referred to as the productive habitat, exists even under non-perturbed (i.e. non-El Nino) conditions. Using some basic assumptions and the quantitative information contained in the CZCS data, it is shown how the increased spatial coverage offered by satellites may significantly reduce the errors associated with regional primary production estimates.

To my parents

for all the years of support, encouragement and love

Table of Contents

List of Figures

List of Plates

List of Tables

ACKNOWLEDGEMENTS

It is with my sincerest thanks and appreciation that I express my gratitude to all those people who, throughout the course of this project, have offered the support, the encouragement, the advice and the understanding that goes into an undertaking such as this. It is impossible to name everyone that has been a part of this project, so I would like to offer a collective thanks to everyone who, in one way or another, has helped me along the way.

One of the highlights of my graduate education has been the opportunity of interacting with the seven members of my committee. These individuals, outstanding in their respective fields, were always more than generous in their willingness to share their time and ideas. If the old saying about being able to tell something about a person by the company he keeps is true, then I have indeed been most fortunate.

I owe a special debt of gratitude to my advisor, J. R. Schubel, for refusing to accept my excuses for not returning to graduate school, and for having the confidence in me to allow me the independence to pursue my own research interests. I consider myself extremely fortunate to have had the opportunity of being associated with such a dedicated and dynamic individual.

Richard Barber challanged me to develop my own interpretations and ideas, and his enthusiasm for this project was

a constant source of encouragement. I am also grateful for the countless data reports and ship observations which gave me the confidence to believe that what I was seeing in the satellite images was real. Malcolm Bowman was always there to help unravel the complexities of physical oceanography and in particular, was of great help in improving my understanding of how flow patterns are affected by islands. Wayne Esaias encouraged me to think about the broader applications and significance of my work and made sure that my methods and assumptions were correct. Thanks for keeping me on track. David Halpern provided incalculable support and his willingness to share his knowledge and understanding of the oceanography of the equatorial ocean, as well as a multitude of oceanographic observations, is deeply appreciated. I want to thank Chuck McClain, for without whose active support I believe that this project could never have been undertaken. In more ways than I can name, I am deeply indebted to him for providing me with the opportunity to embark on this new and very exciting path. Through all phases of this project, Chuck has generously offered his support, guidance and encouragement. And finally, I want to express my appreciation to Akira Okubo for many things, but most of all, for being there when I needed someone to talk with. I thank him for sharing his wonderful perspective on many of the scientific questions raised in this study, and for his ability to place my often disjointed ideas into that beautifully logical sequence of steps that only

mathematicians seem to be able to come up with.

My thanks to Warren Hovis and Larry Crone for all their help during the early phase of this project and for giving me the opportunity to get 'hands on' experience at working with the CZCS data. Bruce Needham guided me through the maze of working with archived satellite data. Dennis Clark gave up more than just a few weekends to help me with my research, and I am deeply indebted to him for all his valuable advice and encouragement.

David Enfield, Oscar Guillen, Donald Hansen, Stan Hayes, Richard Legeckis, J. J. O'Brien, Carl Paul, Robert Rickleffs, James Sadler and Klaus Wyrtki were most generous in sharing their ideas, their expertise and their extensive data sets with me. I also appreciate the work of Paul Freitag, David Legler and Nancy Soreide for helping to put those data sets into the forms which were most useful to me. In addition, my thanks to Jane Kogelschatz, Francisco Chavez and Victoria Thayer for their help.

I want to express my appreciation to all those people at Goddard Space Flight Center who helped me with this project. In particular, I wish to thank Ed Szajna, John Sissala and Pam Anderson for their help in scheduling the CZCS coverage. My thanks to all the computer operators for their cheerful support through innumerable tape mounts. I would also like to express my deepest gratitude to Judy Fuh, and to thank her for the countless hours of help in coaxing the computer to do all those special little things I asked of it. Who would have thought that crossing

the equator with a computer would be almost as difficult as crossing it on a boat. I've now done both and I'm not sure which was worse.

Many students, faculty and staff at the Marine Sciences Research Center helped me in this work. In particular I would like to thank Bud Brinkhuis, Robert Cerrato, Bill Peterson and Bob Wilson. Also, a special note of thanks to Jeri Schoof for teaching me the ins and outs of grants management.

My appreciation to Stuart Finer for his helpful comments and suggestions on the early drafts of much of this work, and for correcting my often flagrant abuse of the English language. I am also grateful for his introducing me to the doctrine of "Occam's Razor" which has encouraged me to always try to provide the simplest explanation for any observed phenomenon...not to multiply explanations but, rather, to prune away declarations that are not supported by observation.

Without the incredible generosity of the Hurwitz family, who with good cheer provided food, shelter and oftentimes clothing, I cannot imagine how this project could have been carried out. It is certainly enough to have to put up with someone who would often not finish work until one or two in the morning, but to include an infant and a dog, certainly calls for an exceptionally good friendship. I thank Joanne, Mike and the girls for such a friendship.

And most of all, Deborah, my thanks for making it all worthwhile.

This research has been supported for the past three years by the National Aeronautics and Space Administration through their Graduate Researchers Fellowship Grant #33-015-802. Additional support has been most generously provided by the Marine Sciences Research Center.

CHAPTER 1

INTRODUCTION

'Technology often plays a vital role in the emergence of new sciences by allowing access to facts not available to the casual observer or present techniques' (Kuhn, 1970). Recent advances in remote sensing technologies, notably satellite-borne sensing systems, have provided means never before possible with which we can study the oceans. Satellite derived measurements of sea surface temperatures, ocean currents, low-level wind fields and ocean color can now be made over vast areas of the ocean on a regular, and most importantly, repetitive basis. The synoptic perspective available through the use of these new observational techniques, when complemented with the appropriate surface measurements, allow us to address more effectively questions concerning the interrelations between climate, the oceans, and their biology.

For the highly productive regions of the world's oceans, it is the pattern of physical processes that to a large extent determines the character and richness of the ecosystem. While much progress has been made in elucidating the mechanisms relating changes in winds, ocean circulation, and the vertical distribution of density and nutrients to the patterns of enhanced biological production, our understanding of the temporal and spatial scales

of these processes and of the resulting variability in the distribution and abundances of biological production, specifically primary production, remains limited. This is particularly significant when one considers that marine primary production is estimated to be about equal to that occurring on land (Global Ocean Flux Study, 1984). The changes in ocean color that can be measured from space are related to the concentration of near-surface phytoplankton pigments (Esaias, 1980). In addition to providing information about the distribution and abundances of phytoplankton, one of the most important features of these measurements lies in their role as a link between the major physical and chemical processes that take place in the ocean with the first step in the system of biological production.

It is the principal goal of this investigation to assess the degree to which satellite ocean color observations can be used to improve our understanding of the patterns of biological production in the eastern equatorial Pacific Ocean. Specifically, observations from the Nimbus-7 Coastal Zone Color Scanner (CZCS) are used to quantify the variability of phytoplankton abundance over a wide range of time and space scales.

The eastern equatorial Pacific, specifically the region from 5°N to 15°S and from 95°W to the coast of South America, is of interest for several reasons. One of the most productive regions of the world's ocean is the coastal upwelling zone off Peru. At its peak, the fishery for the Peruvian

anchoveta (Engraulis ringens) caught nearly 11 million metric tons in a single year (Paulik, 1971). The islands along the Peru coast from which sea bird deposits of guano provided much of the world's supply of natural fertilizer is another indicator of the high biological productivity of this region. Aside from its biological importance, this region is of special interest because it is where coastal and equatorial processes overlap (Lukas, 1981). Located at the eastern end of the equatorial 'waveguide', it is not only subject to perturbations in local physical forcing, but also to disturbances generated in the central and western Pacific. The large scale, low frequency, interannual event known as El Nino is the most powerful example of such an oceanic and atmospheric disturbance. There is evidence, however, that significant interannual variability exists even under supposedly non-perturbed conditions. This variability is one aspect of a ten year international research program (Tropical Oceans and Global Atmosphere, TOGA) which is designed to improve the understanding of events in the tropical oceans and global atmosphere that significantly influence the predictablility of seasonal to interannual variations.

The investigation presented here has components which relate directly to the objectives of the TOGA program, notably the description of the biological variability associated with large scale processes of the annual cycle, interannual variability, and the effects of the El Nino-Southern Oscillation phenomenon.

1.1. OBJECTIVES OF THIS INVESTIGATION

As stated above, the primary goal of this investigation is to assess the degree to which satellite ocean color observations can be used to improve our understanding of the patterns of primary production in the eastern equatorial Pacific. To accomplish this goal, several specific objectives are addressed. The primary objective is to use the satellite data to quantify the variability of phytoplankton biomass at different time and space scales. The temporal coverage provided by the CZCS allows for the short-term variability on the daily to weekly scale to be assessed as well as providing the capability for monitoring the changes occurring over the longer-term (monthly to seasonal to interannual) periods.

The spatial resolution of the CZCS permits a variety of spatial scales to be addressed as well. Phytoplankton variability at different spatial scales can often be related to a variety of physical and biological processes (Campbell & Esaias, 1985). Significant meso-scale variability (10-100km) often associated with water-mass boundaries, frontal regions, upwelling plumes, or island wakes can be identified in the CZCS imagery. On the larger scale (100-500km), the variability of the Galapagos Archipelago as a whole and of the upwelling region along the Peruvian coast are assessed. The largest spatial scale addressed in this study was set by the scan width of the CZCS (~1500km) and the limitations

which were imposed by the processing and display capabilities available at the time. This large-scale region, which for the purpose of nomenclature is referred to as the basin-wide scale, includes the region from 5°N to 15°S and 95°W to the coast of South America (~75°W). The general distribution of phytoplankton at this scale is probably related to large-scale energy exchange and circulation patterns. The large-scale, interannual variability of phytoplankton on the basin-wide scale is addressed through the use of seasonal composites. The methods used and the utility of this technique are described later. In addition, the satellite images are used to identify the major features of phytoplankton distributions in the region. The persistance of these features and their relationships to the physical environment are assessed.

The second objective of this investigation is to determine the extent to which coastal and island induced processes (e.g. tidal mixing, topographically and wind-induced upwelling, etc.) enhance the biological productivity of the surrounding waters. The concept of the productive habitat is discussed and the variability in its areal extent assessed. In addition, the CZCS-derived chlorophyll concentrations are used to estimate the total primary production of the region, which is then compared with that estimated from shipboard measurements.

The productivity of the upwelling regions along the coast of South America and of the highly productive waters around the

Galapagos Islands are not only subject to variability in local forcing, but to a combination of local and remote effects. The most powerful source of oceanic and atmospheric disturbances that affect these regions are those associated the the El Nino-Southern Oscillation (ENSO) phenomenon (Rasmusson & Wallace, 1983). These disturbances are often generated in the central or western Pacific and propagate eastward along the equatorial wavequide and then poleward along the coastal boundaries of North and South America. The El Nino event of 1982-83 has been the most extensively documented event of its kind to date, particularly its effects on the climate (e.g. Rasmusson & Wallace, 1983), the oceanography (e.g. Halpern et al., 1983) and the biology (e.g. Barber & Chavez, 1983) of the equatorial Pacific.

In this investigation, I utilize for the first time the synoptic coverage provided by satellite ocean color observations to document the effect of the 1982-83 El Nino on the distributions and abundances of phytoplankton biomass throughout this region. To assess the impact of El Nino, several specific questions are addressed. Was there an overall decrease in phytoplankton biomass associated with El Nino or merely a geographic redistribution? Were some regions within the study area affected differently than others (ie. a reduction along the coast vs. a redistribution around the Galapagos Islands) ? How did El Nino affect phytoplankton abundance at the three spatial scales under consideration in this study ? How does the

variability observed during El Nino compare with that observed in the historical CZCS data ? And finally, what are the ecological consequences of the results ?

1.2. LIMITATIONS IMPOSED UPON THIS STUDY

It is not the intention of this investigation to advance remote sensing technology or science per se in terms of algorithm development or refinement. The methodologies that have been developed and refined by others to relate the satellite-derived ocean color measurements to the abundance of phytoplankton in the ocean are taken as a starting point for this study. The approach of this study is to utilize remotely sensed data as a tool in furthering our understanding of how oceanic processes affect the distribution and abundances of life in the oceans. Specific examples of how the satellite ocean color data are used include the production of basin-wide, seasonal composites which enable the interannual variability of phytoplankton abundances to be assessed over a very large region that is generally poorly sampled by ships. In addition, a rather simple theoretical approach is used to estimate regional primary production from the satellite data. Measurements from satellites do not take the place of shipboard observations. Instead, they offer a complementary data set which permits the highly detailed surface measurements to be placed into a broader perspective.

The original intention was to document the temporal and spatial variability of phytoplankton biomass for one intensively sampled period in time for which concurrent CZCS coverage had been scheduled. This period began in early September 1982 and coincided with the major oceanographic sampling program that was part of NOAA's EPOCS (Equatorial Pacific Ocean Climate Study) program in the equatorial Pacific. It was hoped that by establishing the patterns of phytoplankton variability under what were believed at that time to be non-perturbed conditions and by correlating those patterns with the physical oceanographic description of the region provided by the extensive surface observations, we would be in a better position to assess the biological impact of changes in the physical system the next time a major perturbation (El Nino) occurred. The 1982-83 El Nino, which soon proved to be the major event to date of the century, struck the South American coast the week the CZCS data began to be collected.

While a data set was now available which showed what conditions were like under the most perturbed conditions, what was missing was a data set documenting the patterns of phytoplankton distribution and abundances during which conditions were 'normal' or at least less perturbed. Although intensive CZCS coverage of this region was not scheduled for the period prior to El Nino, sufficient historical data (since November 1978) had been acquired with which it was possible to piece together a picture of this

region under non-El Nino conditions. One of the problems that was faced, however, with this historical data was the lack of extensive or coincident surface observations. Although a number of oceanographic and meteorological observations were made during the November 1978 through November 1981 period, from which the historical data set was derived, there are large gaps which were not adequately covered either by the CZCS or by surface measurements. Because of this, I exercised caution in trying to infer causal mechanisms for the patterns observed in the satellite images. In addition, the temporal patchiness of the available CZCS data often limited what could be said about the representativeness of a particular image.

In Chapter 2, the satellite data and surface observations used in this study are described. Chapter 3 deals with considerations regarding the use and interpretation of satellite ocean color data and the validity of the algorithms used to process the images presented. The remaining chapters contain the actual data analysis and discussion. Chapter 4 describes the patterns of phytoplankton production around the Galapagos Islands and deals primarily with the mesoscale variability of phytoplankton biomass around the islands and with the influence of changing oceanographic conditions on the patterns of phytoplankton distribution. Chapter 5 examines the structure and variability of one of the major coastal upwelling regions along the Peruvian coast. The patterns of pigment distributions revealed in the

satellite images are compared with the idealized version of a classical upwelling center as derived from shipboard observations. Also, the short-term variability of this system and its relation to changes in atmospheric forcing is described. In Chapter 6, the discussion focuses on the concept of the productive habitat as it relates to the coastal upwelling zone off Peru and Ecuador. The spatial and temporal variability of phytoplankton distributions along the coast is examined through a series of individual CZCS images. Regional composites are used to quantify the large-scale, interannual variability of both the spatial extent of productive habitat and of the estimated total primary production. The final chapter summarizes the major findings of this study, points to some as yet unanswered questions discusses some possibilities for future research.

CHAPTER 2

DATA DESCRIPTION

Of the nearly 125 Nimbus-7 Coastal Zone Color Scanner orbits of the eastern equatorial Pacific that were examined, a much smaller number (~66) were actually processed to produce the quantitative pigment distribution maps that are presented. This chapter briefly describes the sources of data and the criteria used to select scenes for inclusion in this study.

2.1. DATA SELECTION AND QUALITY CONTROL

The digital data that are acquired by the CZCS are transmitted to earth in real time or recorded onboard the spacecraft for later transmission. A sample of the daily coverage provided by the CZCS is given in Figure 2.1 where the orbital tracks for one day are shown (light lines) along with the specfic regions for which data were collected (shaded boxes). These raw data are used to produce a quick look Laserfax image from which scenes are selected for further processing. Regions which are heavily contaminated with clouds or contain only land are normally not selected for further processing. Those scenes which pass the initial screening criteria are then processed into Level-1 Calibrated Radiance Tapes (CRT's) and black and white film

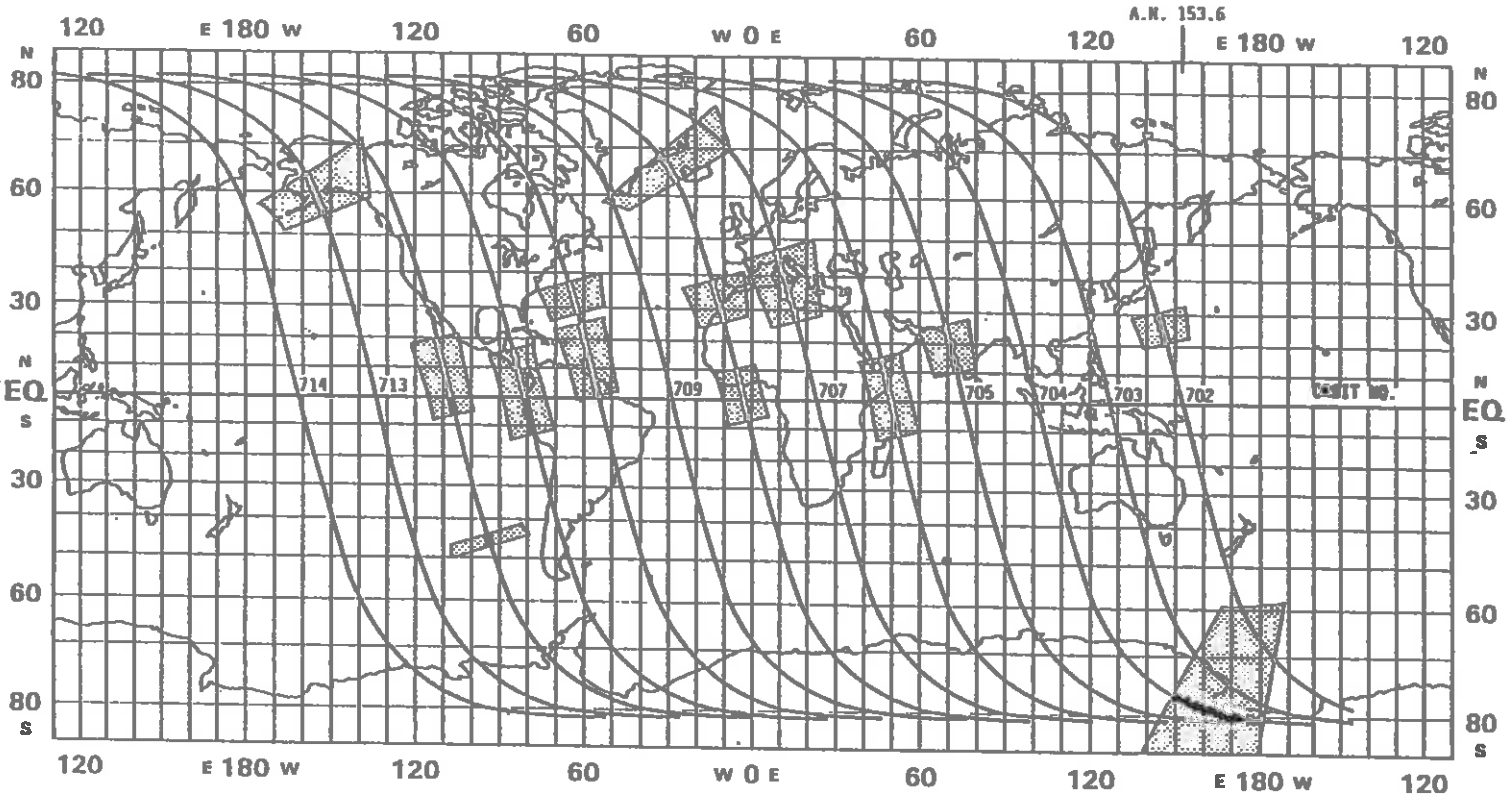

Figure 2.1. Map showing an example of the daily coverage provided by the Coastal Zone Color Scanner (CZCS) on the Nimbus-7 satellite. The orbital tracks are indicated (light lines) as are the specific regions for which data were collected (shaded boxes) on 14 December 1978.

products. A complete description of the CZCS, its history, characteristics, data collection and processing is given by Hovis (1981).

The first step in selecting the satellite scenes to be used required the examination of the Nimbus-7 CZCS Data Catalogs and scheduling records. From these it was possible to identify the orbits and times for which data of the eastern equatorial Pacific had been acquired and to determine which had passed the preliminary selection criteria for processing. What was immediately apparent was that the eastern equatorial Pacific is generally a very cloudy place and that much of the useful data that had been collected by the CZCS had not been processed to Level-1 because of excessive cloudiness. In addition, the Galapagos Islands are very difficult to pick out in the quick look Laserfax images and accordingly, several scenes in which they appeared were not processed because of the cloud cover along the coast. It was necessary, therefore, to reexamine all the Laserfax images of the eastern equatorial Pacific and select scenes which had been passed over in the initial screening for processing to Level-1. The digital data as well as the film products of all the scenes thus identified were then examined once again to select those images that would be used in this investigation.

The scenes that were selected for detailed discussion and inclusion as color plates in this study had to meet a number of specific criteria. The overall quality of the image was of prime

concern as was its significance in being able to demonstrate the usefulness of satellite ocean color observations. To do this the region of interest contained in each scene had to be relatively cloud-free. Scenes that covered the entire study region from the Galapagos to the coast and in which both regions were generally clear were particularly difficult to find. It was rare when a single scene could be used in the statistical analysis for all three spatial scales. However, scenes which may have been questionable with regard to clouds obscuring a portion of the image but which contained specific features of interest (e.g. sharp fronts, island wakes, upwelling plumes) were selected. Images taken at times for which concurrent surface observations were available were given special attention, particulary if the region in which the surface measurements were taken was not obscured by clouds. Also, the representativeness of a particular scene in which recurrent patterns appear was taken into account as a basis for selection. Finally, there were a few scenes which were included because they were clearly unusual in comparison with the majority of images examined. While not every scene processed met all of the above mentioned criteria, most were of sufficient quality to be included in the statistical analyses. Table 2.1 lists the orbits, dates, processing parameters and geographic coverage of the CZCS data used in this study. The orbits for which no processing information is given were those for which the images, although of interest, were of such questionable quality

Table 2.1. Orbit numbers, dates, processing parameters and geographic coverage of the Coastal Zone Color Scanner data used in this study. Those orbits for which no processing parameters are given were those for which the images, although of interest, were of such questionable quality that they were not used in the analyses.

ORBIT	DATE	TILT	GAIN	C.LOW	ANG. EXP.			EPSILONS			NOTES
642	12-09-78	+12	1	1.2	-.16	-.1	-.13	1.07	1.03	1.03	a,b,c
711	12-14-78	+20	1	0.97	-.13	-.12	-.14	1.05	1.03	1.03	b,c
739	12-16-78	+20	1	0.81	-.24	-.37	-.17	1.10	1.10	1.03	a,c
808	12-21-78	+20	1	1.4	-.19	-.28	-.11	1.08	1.07	1.02	a,b,c
1209	1-19-79	+20	1	1.02	-.34	-.37	-.32	1.15	1.10	1.06	b,c
1375	1-31-79	+20	1	1.19	-.48	-.50	-.46	1.22	1.14	1.10	b,c
1638	2-19-79	+20	1	0.88	-.17	-.23	-.11	1.07	1.06	1.02	a
2605	4-03-79	0	2	0.99	-.71	-.77	-.66	1.34	1.21	1.14	d
2619	5-01-79	-20	1	0.91	-.37	-.44	-.30	1.17	1.12	1.06	b,c
2854	5-18-79	-20	1	0.81	-.19	-.23	-.16	1.08	1.06	1.03	b,c
2868	5-19-79	-20	1	1.09	-.17	-.19	-.16	1.07	1.05	1.03	a
3324	6-21-79	-20	1	1.6	-.17	-.18	-.17	1.07	1.05	1.03	a
3352	6-23-79	-20	1	1.6	-.17	-.18	-.17	1.07	1.05	1.03	a,h
3476	7-02-79	-20	1	1.09	-.18	-.21	-.15	1.08	1.05	1.03	a
4388	9-06-79	+20	1	1.18	-.26	-.32	-.19	1.11	1.09	1.04	a
4678	9-27-79	-20	1								e
5369	11-16-79	+20	1	1.00	-.65	-.58	-.72	1.31	1.16	1.15	c,f
5480	11-24-79	+20	1	1.01	-.38	-.53	-.24	1.17	1.14	1.05	a
5673	12-08-79	+20	1								f
5922	12-26-79	+20	1	1.22	-.24	-.36	-.13	1.11	1.09	1.03	b,c
6212	1-16-80	+20	1	1.28	-.28	-.44	-.12	1.13	1.12	1.02	b,c,f
6226	1-17-80	+20	1	1.09	-.23	-.29	-.16	1.10	1.08	1.03	a,b,c
6378	1-28-80	+20	1								f,g
6585	2-12-80	+20	1	1.46	-.44	-.64	-.23	1.20	1.18	1.05	c,f
6613	2-14-80	+20	1	1.01	-.24	-.31	-.18	1.11	1.08	1.04	b,c,f
6876	3-04-80	+20	1	1.07	-.26	-.39	-.14	1.11	1.10	1.03	h
7124	3-22-80	+20	1								f,g
7235	3-30-80	+20	1	1.34	-.41	-.54	-.28	1.19	1.15	1.06	h
7442	4-14-80	+20	1	1.46	-.33	-.35	-.32	1.15	1.09	1.06	f
7566	4-23-80	-06	2								d,i
7608	4-26-80	-20	1	0.85	-.26	-.38	-.13	1.11	1.10	1.03	a
8935	7-31-80	-20	1								h
9211	8-20-80	-20	1	0.98	-.28	-.43	-.13	1.12	1.11	1.03	a
9570	9-15-80	+20	1	0.98	-.14	-.15	-.13	1.06	1.04	1.03	b
10786	12-12-80	+20	1	1.10	-.31	-.35	-.28	1.14	1.09	1.06	c,d
12210	3-25-81	-20	1								f
12306	4-01-81	-20	1	1.52	-.32	-.30	-.34	1.14	1.10	1.07	d
12334	4-03-81	-20	1	1.08	-.27	-.40	-.14	1.12	1.11	1.03	b,c,d,f
12624	4-24-81	-20	1	0.90	-.16	-.17	-.15	1.07	1.04	1.03	b,c,d
13288	6-11-81	-18	1	1.20	-.21	-.25	-.17	1.09	1.07	1.03	a
13398	6-19-81	0	1	1.26	-.72	-.70	-.75	1.35	1.19	1.16	d
15610	11-26-81	+20	1	3.30	-.37	-.43	-.31	1.17	1.12	1.06	a

ORBIT	DATE	TILT	GAIN	C.LOW	ANG. EXP.			EPSILONS			NOTES
19829	9-27-82	+20	1								h
19868	9-30-82	+20	1	0.82	-.34	-.47	-.21	1.15	1.13	1.04	h
20323	11-02-82	+20	1								j
20337	11-03-82	+20	1	0.92	-.28	-.43	-.12	1.12	1.11	1.02	a
20378	11-06-82	+20	1								j
20406	11-08-82	+20	1	1.21	-.16	-.20	-.12	1.07	1.05	1.02	a
20461	11-12-82	+20	1								f,g
20682	11-28-82	+20	1								e,g
20696	11-29-82	+20	1	1.07	-.33	-.47	-.20	1.15	1.13	1.04	b,c,d
20724	12-01-82	+20	1	0.82	-.30	-.46	-.13	1.13	1.12	1.03	a,b,c
21429	1-21-83	+20	1								f
21567	1-31-83	+20	1	1.01	-.26	-.40	-.12	1.11	1.10	1.02	a,c
21581	2-01-83	+20	1	1.45	-.30	-.48	-.11	1.13	1.12	1.02	a
21622	2-04-83	+20	1								c,e
21636	2-05-83	+20	1								a
21691	2-09-83	+20	1	1.11	-.28	-.32	-.23	1.12	1.08	1.05	b
21705	2-10-83	+20	1	1.52	-.21	-.31	-.11	1.09	1.08	1.02	b
21733	2-12-83	+20	1	0.95	-.24	-.36	-.13	1.11	1.10	1.03	a
21774	2-15-83	+20	1	0.83	-.31	-.40	-.23	1.14	1.11	1.05	b,c
22023	3-05-83	+20	1								j
22037	3-06-83	+20	1								a,x
22134	3-13-83	+20	1								a,x
22341	3-28-83	+20	1	1.46	-.25	-.35	-.16	1.11	1.09	1.03	a,c
23129	5-24-83	-20	1	1.03	-.35	-.52	-.18	1.16	1.14	1.04	a,c

NOTES: a - Galapagos Islands
b - Coastal Upwelling Region (2x2 reduction)
c - Eastern Equatorial Pacific (4x4 reduction)
d - Pisco Upwelling Center
e - Pisco Upwelling Center (partially obscurred)
f - Galapagos Islands (partially obscurred)
g - Coastal Upwelling Region (partially obscurred)
h - Open Ocean Region West of Galapagos Islands
i - Northern Chile
j - not processable (glint)
x - processed with Univ. of Miami software on NOAA/NESDIS system

that they were not used in the analyses.

There were a number of images that were inspected but which for several reasons were not included in the discussion or in the statistical analysis of this study. These included scenes in which there were difficulties in the processing procedures and consequently the accuracy of the resulting pigment concentrations and distributions were questionable. Sun glint was one problem that reduced the number of useful images. The CZCS has a mirror which can be tilted +/- 20^0 from nadir to look either in front of, or behind, the spacecraft's line of flight to avoid sun glint. In ocean color work, sun glint obscures any scattering from below the surface and thus makes derivation of in-water constituents impossible for the affected regions. Because of the time required to change the tilt angle of the mirror, the mirror was often set to a position that would reduce glint in the northern hemisphere while passing over the study area of this investigation. As a result, sun glint significantly affected some otherwise important images.

Clouds posed problems in both a direct and indirect way. If the region of interest was obscured by clouds, then that scene was excluded from the analysis. The problem of cloud ringing, in which clearly erroneous values are observed to the east of clouds or land, needed to be addressed as well. Cloud ringing is a result of the finite period of time required for the CZCS sensor to regain sensitivity after passing over a relatively 'bright'

object such as a cloud, during which time the sensor was saturated. The chief difficulty with cloud ringing was its intermittent nature. In some scenes, although clouds were present, there was no indication of the ringing effect. In other scenes, however, the effect could be seen to extend across the entire scan line. Where possible, regions that were obviously affected by cloud ringing were excluded from the statistical analyses. The final reason for exclusion of a scene had to do with the 'limb effect'. When the region of interest was on the edge of the scene, the algorithms currently in use often gave results that were highly questionable. This effect was generally indicated by a band of exceptionally high pigment concentrations along the western edge of the scene. However, regions within these scenes, particulaly those near the center of the image, produced valid results and were used in the analysis.

2.2. SURFACE OBSERVATIONS

Although satellite ocean color data provide the material for most of the discussion in this study, a large number of surface observations (i.e. ship and buoy-derived measurements) were used as well. The surface measurements of various physical (sea surface temperature, ocean currents, sea level, winds), chemical (nutrient concentrations) and biological (chlorophyll) variables were useful in the interpretation of the patterns observed in the

satellite images. The discussion of these data along with their sources is given in the text.

CHAPTER 3

PROCESSING PROCEDURES AND CONSIDERATIONS

This chapter addresses the question of what the Coastal Zone Color Scanner measures, how it measures it, and what those measurements mean. Also, some of the basic assumptions that need to be made for the interpretation of satellite ocean color images are discussed.

3.1. SATELLITE OCEAN COLOR MEASUREMENTS: ALGORITHMS

The Coastal Zone Color Scanner (CZCS) on NASA's Nimbus-7 satellite, launched in October 1978, was designed to provide quantitative estimates of near-surface phytoplankton pigment concentrations by measuring the spectral radiances backscattered from the ocean (Hovis et al., 1980). These radiances are not merely reflected from the sea surface, but are derived from sunlight that has entered the ocean, been selectively absorbed, scattered and reflected by phytoplankton and other suspended material in the upper layers, and then backscattered through the surface. Phytoplankton, through scattering and by the presence of their photosynthetically active pigments (primarily chlorophyll a) are a major determinant of ocean color for most of the

world's ocean. The four visible spectral bands on the CZCS have been optimized so as to quantify these changes in ocean color. The narrow (20 nm) bands centered about 443 and 670 nm are in regions of the spectrum where chlorophyll a absorption is strong. The two bands at 520 and 550 nm are located at wavelengths where upwelled radiance variations due to changes in chlorophyll concentation are small. The band at 670 nm is strongly affected by absorption by water. Because of this, it is assumed that most of the radiance detected by the CZCS in this band, particularly in regions of very low phytoplankton concentrations, can be attributed to the atmosphere. This assumption forms the basis of the 'clear water' ('black ocean') radiance concept for atmospheric correction of the CZCS imagery (Gordon & Clark, 1981). This correction is by no means a trivial consideration since roughly 80-90 percent of the total radiance received by the CZCS is due to backscattering from the atmosphere.

The goal of the atmospheric correction procedures as summarized by Gordon & Morel (1983) and more recently by Smith (1984) are to accurately determine the water-leaving radiances on a pixel by pixel basis throughout the image. To do this, the atmospheric contribution to the total radiance must be removed. The component due to scattering from the air (Rayleigh scattering) can be estimated quite accurately from theory (Viollier et al., 1980). Determining the scattering caused by the microscopic particles in the air (aerosol scattering) is somewhat more complex

and two approaches are generally used. The first is the 'clear-water' radiance concept where the aerosol path radiance is determined for portion of the spectrum where the water leaving radiance is assumed to be zero. Gordon & Clark (1981) showed that for oceanic, Case 1 waters (those waters in which phytoplankton and their covarying degredation products are the main determinants of ocean color) with pigment concentrations < 0.25mg/m3, this assumption is true for the CZCS band at 670 nm. However, if the region under investigation does not contain waters for which the 'clear-water' method can be applied (e.g. pigment concentrations >0.25mg/m3, or with significant amounts of suspended sediment or dissolved organic matter), then the approach developed by Smith & Wilson (1981) in which an iterative procedure utilizing a bio-optical model linking pigment concentration and water-leaving radiance is used.

A number of algorithms (again summarized by Gordon & Morel, 1983; and Smith, 1984) have been developed to relate the retrieved spectral radiances to the concentration of near-surface phytoplankton pigments. Most of these are empirical models based upon regressions between 'optically weighted' pigment concentrations (Smith & Baker, 1978) as determined from shipboard observations and upwelled radiance ratios using the 443, 520, and 550 nm CZCS bands. There is general agreement that these algorithms can be used to estimate near-surface pigment concentrations to within 30-40 percent for 'Case I' waters. For

regions in which inorganic and/or resuspended material play a major role in determining the optical properties of the ocean, referred to as 'Case 2' waters by Morel & Prieur (1977), estimates to within a factor of two can be expected.

3.2. SATELLITE OCEAN COLOR MEASUREMENTS: MEANING

Once these various algorithms have been applied and the resulting quantitative estimate of near-surface phytoplankton pigment concentration has been produced, the question still remains as to exactly what do these values mean and how well do they represent both the horizontal and vertical distribution of phytoplankton in the ocean. The satellite-derived concentrations represent the sum of the photosynthetically active phytoplankton pigment chlorophyll _a_ and phaeopigment _a_, its primary degredation product, which because of the limitations in spectral resolution available with the bands available on the CZCS, cannot be separated. Although the phaeopigments comprise a variable and sometimes significant proportion of the estimated total pigment concentration, they are typically less than 10 percent of the chlorophyll _a_ concentration (Smith & Baker, 1978).

The depth to which these measurements apply is inversely related to the concentration of phytoplankton and suspended material in the water column. Studies have shown that approximately 90 percent of the water-leaving signal detected by

the CZCS originates from within the first optical attenuation length (Clark, 1981) the depth of which varies from approximately 1.6 to 17 m over the pigment concentration range of 0.1 to 10.0mg/m3, respectively (Smith & Baker, 1978). The CZCS-derived values, therefore, represent the average pigment concentration in the upper 22 percent of the euphotic zone and are derived from the layer in which 63 percent of the surface irradiance has been attenuated (Smith & Baker, 1978).

It has been shown that there may be significant correlation between surface chlorophyll (e.g. from ships) or near-surface concentrations (e.g. from satellite) and chlorophyll integrated through the water column (Lorenzen, 1970; Smith & Baker, 1978; Hayward & Venrick, 1982; Platt & Herman, 1983). In addition, near-surface chlorophyll is also strongly correlated with total euphotic zone primary production (Hayward & Venrick, 1982; Eppley et al., 1985), particularly in regions such as the California Current where strong gradients and a wide range of chlorophyll concentrations are found. However, such correlations do not appear to exist for regions in which surface values do not adequately reflect the subsurface chlorophyll distribution. Such a situation was observed in the central North Pacific gyre (Hayward & Venrick, 1982) where the presence of a deep chlorophyll maximum significantly affected the integrated values but was not reflected in the surface measurements. Hayward & Venrick do point out, however, that on the global scale in which a large range of

ecosystems are considered, a positive relation between the surface and water-column values will exist. This is particularly significant in that it supports the validity of ocean-wide, or global assessments of oceanic production using satellite ocean color observations.

It is beyond the scope of this investigation to address in detail the complex relationships among chlorophyll, phytoplankton biomass and primary production. A review of the subject by Cullen (1982) discussed the variability in these relationships as well as the various physical processes that determine the vertical distribution of these properties. He showed that although the concentration of chlorophyll is still the best, and most readily measurable, indicator of phytoplankton biomass in natural populations, the carbon to chlorophyll ratios can vary by more than an order of magnitude. One source of this variability is due to the diel variation in the chlorophyll content per cell which varies by about a factor of 2 depending upon time of day. The consequences of this variability are reduced in the CZCS observations since the orbital configuration provides for coverage of the same geographic area at roughly the same time each day. The variability in the chlorophyll:productivity ratio is also very large and is discussed in Chapter 6 where the CZCS data is used to estimate regional primary production.

3.3. SATELLITE/SHIP INTERCOMPARISON

Quantitative comparisons between ship measured and satellite derived chlorophyll concentrations were carried out to determine the accuracy of the satellite values and the reliability of the algorithms and processing procedures used in this study. While most other studies have relied upon surface pigments measured continuously along a ship track, no such data were available for this region during the period of this study. However, coincident shipboard measurements of near-surface chlorophyll concentrations from individual sampling stations and CZCS-derived pigment values were available for six days during the study period. To be included in the comparison, the surface observations had to have been taken within 12 hours of the satellite overpass. In addition, the location from which the satellite value was obtained had to have been sufficiently cloud-free to minimize any possible cloud-ringing effects.

The CZCS values used in this comparison were 7 x 7 pixel averages centered around the geographical location of the ship measurement (pixel stands for picture element, the smallest geographic area resolved by the sensor which for the CZCS is 0.825km^2 at nadir). This was done for several reasons. The first was because time differences between the satellite and ship observation, and the strength of the currents in this region made

a one to one correspondence between pixel location and ship position somewhat difficult and questionable. The second reason involved the accuracy with which any given point in the CZCS images could be geographically located. The procedure used to navigate the CZCS images involved superimposing a geometrically correct coastal outline on the remapped satellite image. Then, by applying time and spacecraft attitude correction factors, those areas of the coastline seen in the satellite image could be made to coincide with the coastal outline. The accuracy of this technique decreases as you get further away from clearly identifiable coastal features. Because many of the ship/satellite values came from open ocean stations, it did not seem that it was possible to navigate the satellite images to anything better than a 3 pixel accuracy.

The comparison between the shipboard station measurements and satellite estimates presented in Figure 3.1 suggests that for this region and for the time periods from which the data were available, the procedures and algorithms used to process the CZCS data were at least as accurate as those applied elsewhere (Smith et al., 1982; Gordon et al., 1983; Brown et al., 1985). Satellite estimates were generally within 30 percent of the ship measurements in this study. This also included the nearshore station when pigment concentrations of ~5 mg/m3 were recorded during El Nino. In addition to the nearly coincident ship/satellite values presented in Figure 3.1, a less rigorous

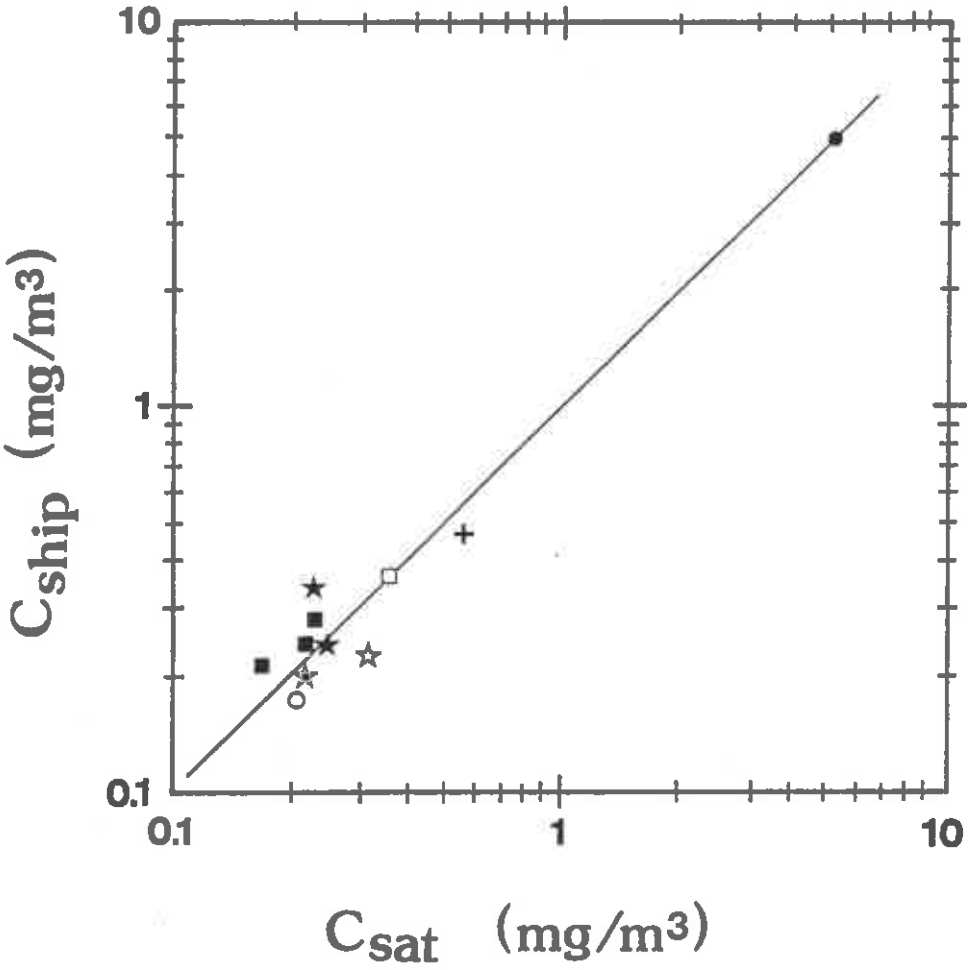

Figure 3.1. A comparison between shipboard station measurements of surface chlorophyll and satellite-derived estimates of near-surface pigment concentrations (mg/m3) from the same location taken within six hours of each other on:
○ 6/11/81; ■ 11/3/82; ★ 11/8/82 (NOAA Ship Researcher);
□ 11/8/82 (Academy Bay); ☆ 1/31/83; ● 2/9/83; + 3/28/83.

comparison between ship measured and satellite derived chlorophyll concentrations throughout the region showed a general agreement between the two data sets. The absence of any systematic bias, particularly in the El Nino data, supports the accuracy of the correction factors used to compensate for the reduction in radiometric sensitvity of the CZCS with time (Gordon et al., 1983a).

CHAPTER 4

PATTERNS OF PRODUCTION AROUND THE GALAPAGOS ISLANDS

4.1. INTRODUCTION

"The currents about these islands are very remarkable..."

Fitz-Roy (1839)

It has long been recognized that the ocean waters around islands are inherently more productive than waters far removed from land (Gilmartin & Revelante, 1974; Barber & Chavez, 1983). This increased productivity, which is often referred to in the literature as the Island Mass Effect (Doty & Oguri, 1956), depends primarily on the supply of nutrients to the euphotic zone brought about by enhanced vertical mixing around islands. Localized upwelling on the downstream sides of islands (LaFond & LaFond, 1971), topographically induced upwelling (Houvenaghel, 1978), the formation of island wakes (White, 1973), wind driven coastal or equatorial upwelling and tidal mixing (Kogelschatz et al., 1985) are some of the mechanisms that can produce vertical mixing around islands. Although the mechanisms may differ, the end result is often the same; an increase in the vertical transport of nutrients to the surface waters supporting enhanced levels of primary

production and phytoplankton biomass.

Straddling the equator approximately 900 km to the west of the South American mainland, the Galapagos Islands (Figures 4.1 & 4.2) lie within the heart of the equatorial current system. Rising from the sea floor, the volcanic islands of the Galapagos are set on top of a distinctive platform. The main portion of the Galapagos Platform is relatively flat and less than 1000m in depth. The steepest slopes are found along the western and southern flanks of the platform with a gradual slope toward the east.

Numerous submarine banks and topographic features interrupt the flow of two of the major ocean currents of this region. The surface circulation around the Galapagos Islands is dominated by the generally westward flows of the South Equatorial Current (SEC). The strength and direction of flows associated with the SEC normally have a strong annual cycle which is related to the intensity of the Southeast Trade Winds (Halpern, 1988); westward surface flows associated with maximum westward winds (July through December) and eastward near-surface currents correlated with minimum westward wind or weak easterlies (March and April). The thickness of the SEC is minimal at the equator (20 to 50m) deepening to the north and south (Houvenaghel, 1984). Below this shallow westward-flowing surface layer are the waters of the Equatorial Undercurrent (EUC), also called the Cromwell Current, which is a subsurface, eastward flowing current approximately 200m

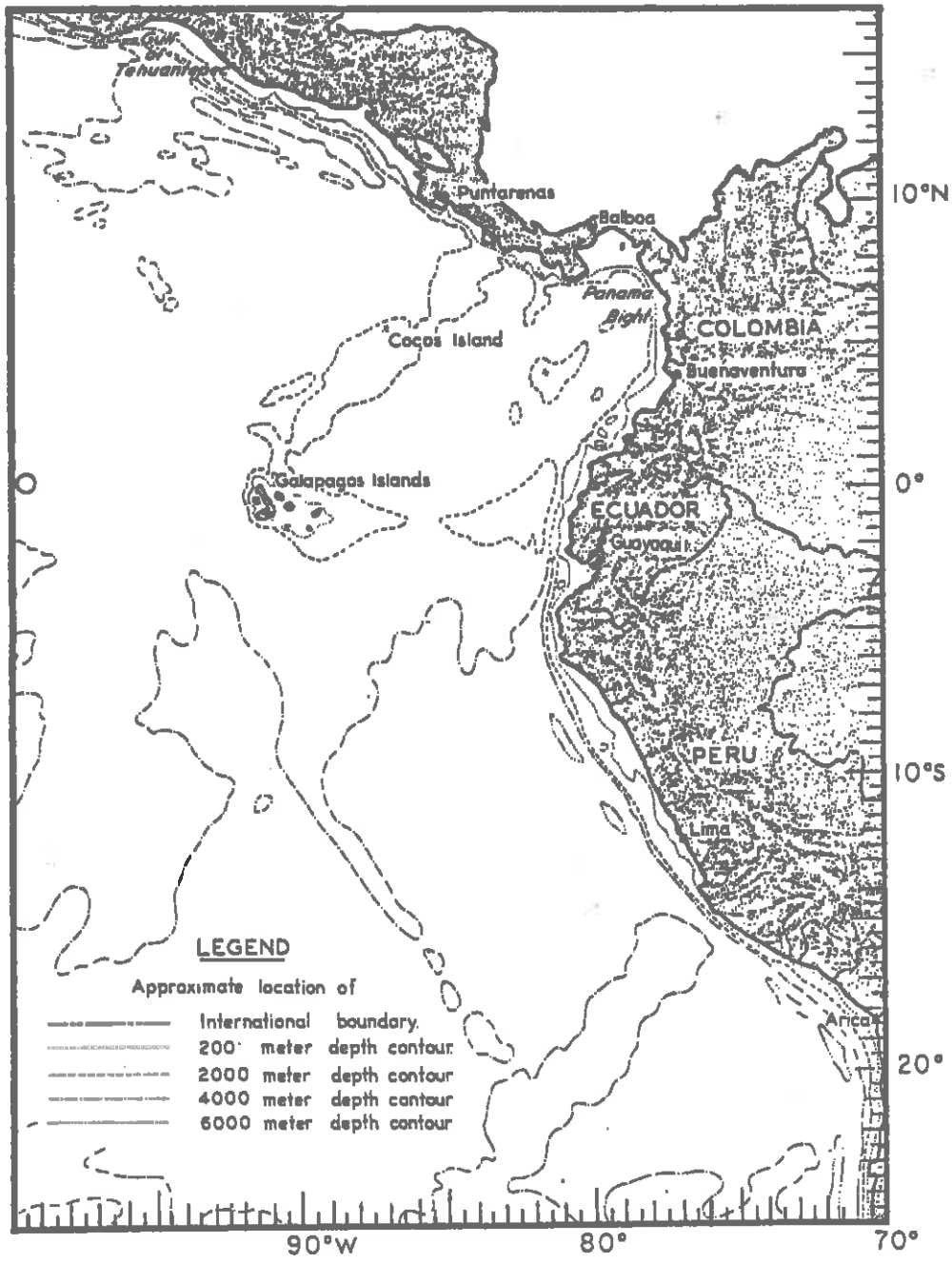

Figure 4.1. Map of the eastern equatorial Pacific Ocean showing the major features of the submarine bathymetry. Open circle at 0°, 110°W shows the location of the current meter from which the data presented in Figure 4.6 were derived.

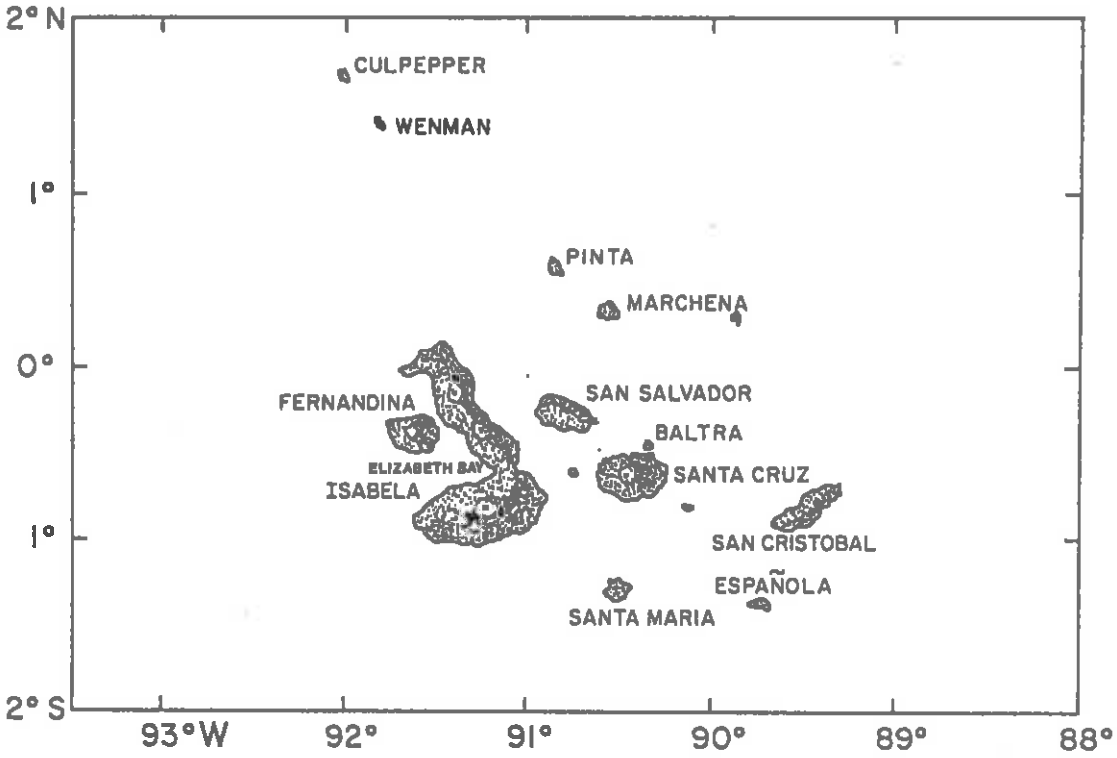

Figure 4.2. Chart of the Galapagos Islands in which the major islands of the archipelago are shown.

thick with its high velocity core normally found at ~75m. The influence of these two opposing flow regimes makes the circulation patterns around these islands remarkably complex. The logs written by captains of 18th and 19th century sailing vessels are filled with references to the bewildering currents and winds they encountered as they explored, provisioned their vessels, or hunted the whales that were abundant in the waters around the Galapagos Islands.

There has been much recent work dealing with the influence of tides and tidal mixing around islands (Simpson & Tett, 1985). Unfortunately, little is known and even less is written about the tides of the Galapagos Islands. What is known, however, is that the tides are predominantly semidiurnal, having two nearly equal high and low waters each day. The tidal range (~1.5 to 2.5m) varies from one location to another throughout the archipelgo, and since tidal currents in a particular area are often proportional to the range of the tide, it can be assumed that tidal currents also vary throughout the islands. Beebe (1926) wrote that

> "The captain discovered the fact that at the surface at least there is a tidal current. On the lowering tide the current sets strongly north, and on the rising tide it turns and sets as strongly southward along the coast, at least ten miles out"

Houvenaghel (1978) found that tidal mixing played a role in reducing water column stratification, while Kogelschatz et al. (1985) believed that the strongly periodic surface enrichment of nutrients they observed at their Academy Bay time-series site may

have been caused by tidal destratification. Clearly, more work needs to be done in order to fully assess the role of tidal mixing around the Galapagos Islands.

What all the descriptive and scientific evidence points to is that this region is exceptionally dynamic and that many mixing processes are at work, any one of which could provide the vertical transport of nutrients necessary to support enhanced phytoplankton production. Not only do phytoplankton represent the first link in the oceanic food chain, but their patterns of distribution in time and space may indicate changes in the physical environment (Steele, 1978) and provide clues as to how oceanographic processes regulate primary production (Yentsch, 1983). Until recently, the limitations imposed by traditional sampling techniques and strategies have made it difficult to assess the variability of the biological response to changes in the physical environment. The development of satellite sensing systems has provided the synoptic perspective, the quantitative areal data and the temporal coverage required for an accurate description of this region.

It is not the purpose of this chapter to describe the mixing processes associated with these islands, but rather to show how mixing processes affect the distribution and abundance of phytoplankton in the surrounding waters. Satellite ocean color observations are used to describe the patterns of distribution and the degree of temporal and spatial variability of phytoplankton biomass around the Galapagos Islands. The relationship between

temperature (where colder temperatures at the surface often indicate the injection of newly upwelled, or recently mixed waters rich in nutrients) and the distributions and abundances of phytoplankton are described using sea surface temperature and ocean color imagery.

In addition, it is shown that changes in the speed and direction of flows (winds and currents) past the islands produce significant variations in the patterns of phytoplankton distribution in the region and that these patterns are correlated with the seasonal cycle evident in the meteorological and oceanographic data. Finally, the satellite data are used to determine the spatial extent of the area of enhanced biological production, referred to here as the productive habitat, associated with the Galapagos Islands.

4.2. MAJOR FEATURES OF PHYTOPLANKTON DISTRIBUTION AROUND THE GALAPAGOS ISLANDS

Twenty Coastal Zone Color Scanner (CZCS) images of the Galapagos Islands covering the period from December 1978 through March 1983 were processed according to the procedures described by Gordon et al. (1983). The color-encoded maps of pigment concentrations presented in this section are representative of the patterns and variability in phytoplankton distribution observed in most of the analyzed data. The colors represent the

satellite-derived pigment concentrations (Plate 4.1) and in each case the islands are black and the clouds are white.

CZCS data of the Galapagos Islands from Nimbus-7 orbit 739 taken on 16 December 1978 were processed to produce simultaneous, co-registered images of sea surface temperature (Plate 4.2) and derived pigment concentrations (Plate 4.3). These images are discussed in detail to describe the relationship between upwelling and enhanced phytoplankton production. Two additional ocean color images of the Galapagos Islands acquired during December 1978 are presented to show the degree of variability in phytoplankton distributions during this period. Although direct observations of the oceanographic conditions around the islands are not available for December 1978, data gathered during the November 1978 cruise in the vicinity of the Galapagos by the research vessel Orion of the Oceanographic Institute of Ecuador (Arcos, 1981; Jimenez, 1981) provide surface information useful in the interpretation of the satellite images. The time difference between the ship survey and the satellite overpass makes direct comparisons difficult, however, a general agreement of the large-scale features does exist.

The satellite-derived sea surface temperature distributions (Plate 4.2) show that warm waters (yellow) were found predominantly in the northern and southern regions of the archipelago. The warm, tropical surface waters to the north are separated from the generally cooler waters (blue) of the south by

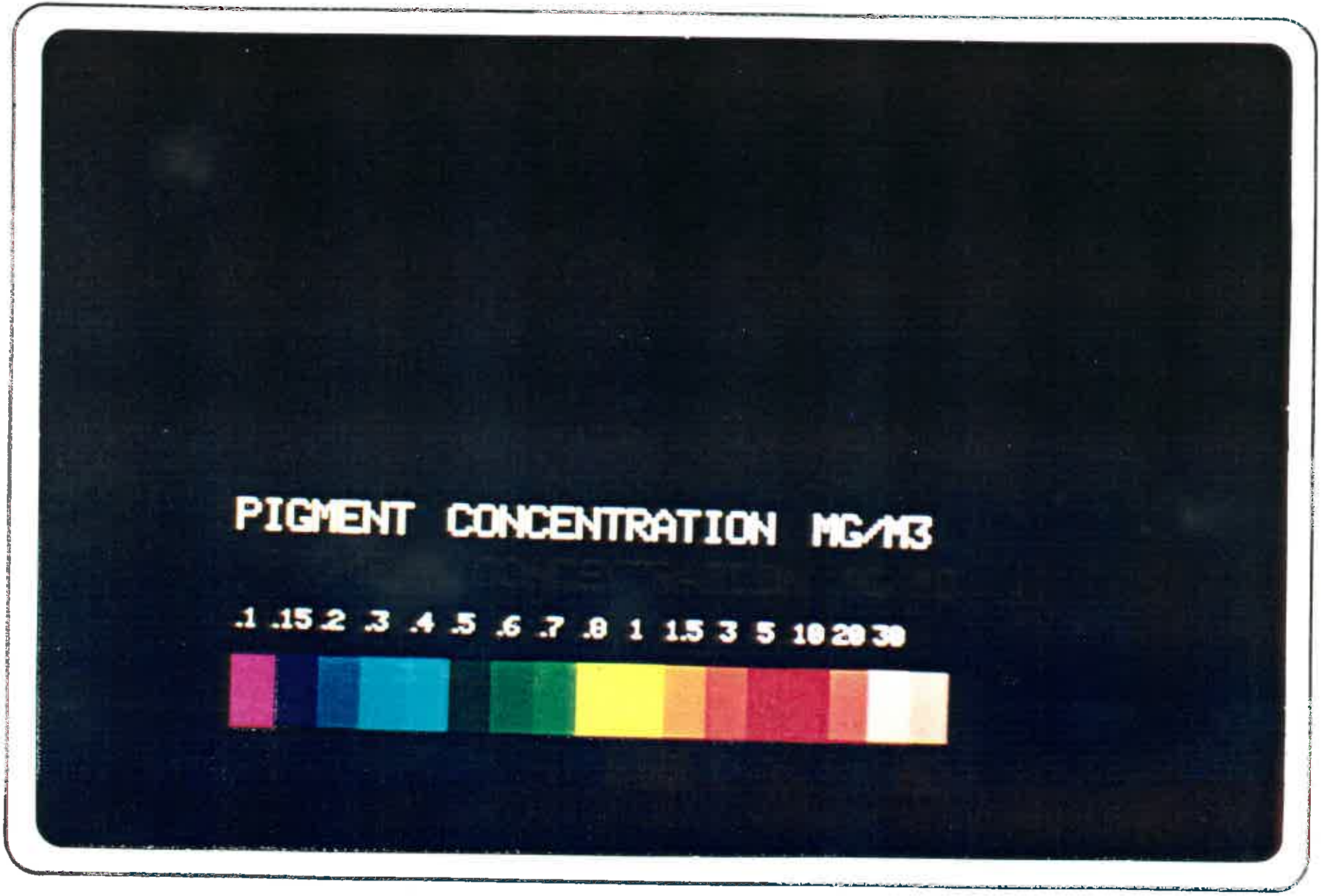
PIGMENT CONCENTRATION MG/M3
.1 .15 .2 .3 .4 .5 .6 .7 .8 1 1.5 3 5 10 20 30

Plate 4.2. Satellite-derived sea surface temperature distributions around the Galapagos Islands acquired on 16 December 1978 (Nimbus-7 orbit 739). Regions of warm waters (above 21°C) are yellow and red: intermediate temperatures (20 to 21°C) are light blue; coolest temperatures (less than 20°C) associated with the upwelling of the equatorial Undercurrent are deep blue. Major islands are gray and clouds white.

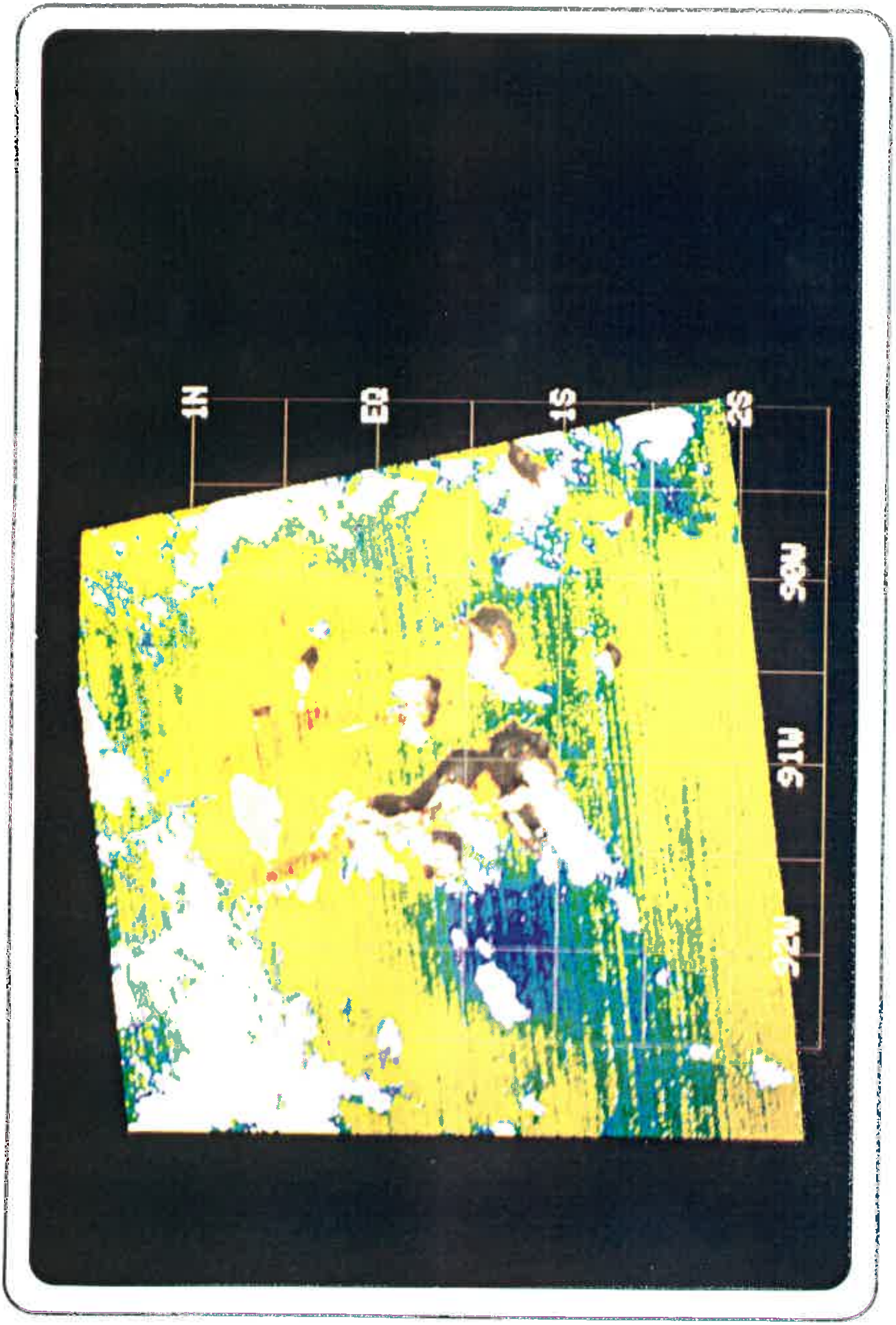
1N
EQ
1S
2S
98W
91W
84W

Plate 4.3. Satellite ocean color image showing the distribution of phytoplankton pigments around the Galapagos Islands acquired on 16 December 1978 (Nimbus-7 orbit 739). Major islands are black and clouds white. The dotted line across the sharp color front located to the west of Isabela Island represents the trackline from which the data presented in Figures 4.3. and 4.4. were derived.

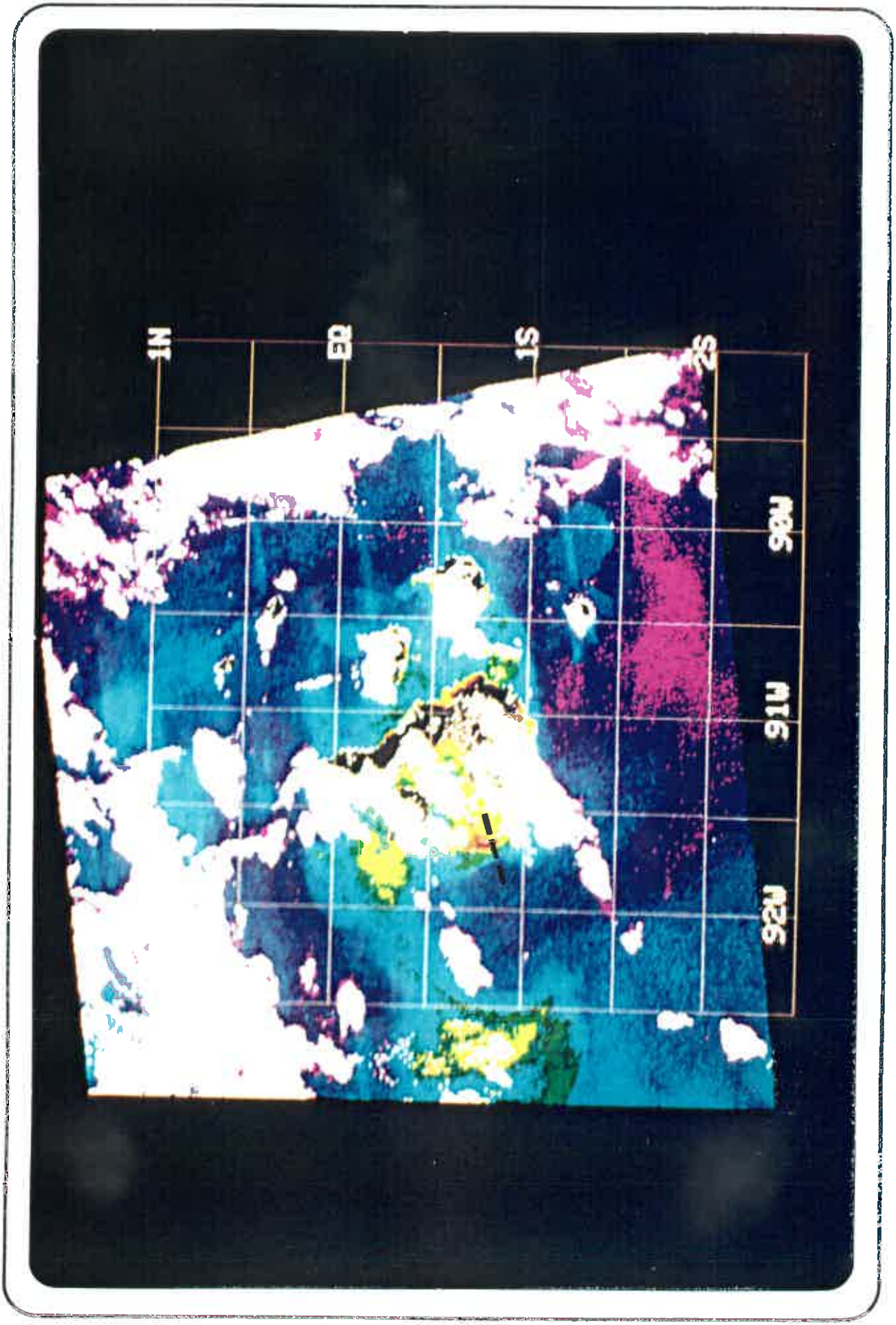
1N
EQ
1S
2S
98W
94W
91W
92W

the Equatorial Front which extends zonally, and generally crosses the equator in the vicinity of the Galapagos Islands (Hayes, 1985). The Equatorial Front, sometimes referred to as the Galapagos Front in the vicinity of the islands, was very strong on the western side of the archipelago in November 1978 and was located just off the northwestern tip of Isabela.

One striking feature evident in the temperature image is the patch of relatively cold water (~19°C) located to the west of Isabela Island between the equator and 1.5°S. Jimenez (1981) reported that during November 1978 the axis of the eastward flowing subsurface Equatorial Undercurrent (EUC) was displaced slightly to the south of the equator; other studies (Bubnov and Egorikhin, 1981; Lukas, 1981) have given some indication of the behavior and the extent and period of the meandering of the axis of the EUC. Measurements have shown that subsurface waters belonging to the EUC (Houvenaghel, 1978) upwell in the Galapagos area and influence the hydrology and productivity of the entire archipelago. Both Houvenaghel and Jimenez report the existence of a large patch of cold (19°) water to the west of Isabela Island. This patch, representing the topographically induced surfacing of the EUC, is clearly seen in Plate 4.2. The satellite-derived temperature distributions seem to indicate that at the time of the satellite overpass, the EUC flowed primarily through the southern portion of the archipelago although its signature is not nearly as distinct as it is to the west. These

data support the observations reported by others (Stevenson & Taft, 1971; Lukas, 1981; Hayes, 1984) that the EUC flows southward through the islands.

The CZCS-derived pigment concentrations for this period (Plate 4.3) show that phytoplankton biomass was by no means uniformly distributed around the archipelago. Pigment concentrations were highest on the western side of Isabela, particularly in Elizabeth Bay, while a small (~25km) patch of relatively phytoplankton-rich water was found just to the north of Fernandina. Jimenez (1981) reported that diatoms were the most abundant phytoplankton group encountered during November 1978. The lowest concentrations are associated with the warm waters to the south of the islands and with the regions to the north of the reported position of the Equatorial Front. The region of relatively low pigment water located to the west of Isabela corresponds with the center of the EUC upwelling water as seen in the sea surface temperature image. It has long been recognized that newly upwelled water, although generally high in nutrients is usually low in phytoplankton biomass (Barber & Ryther, 1969). Jimenez's (1981) findings and the satellite data support this idea. Both show a sharp decrease in pigment concentrations where the EUC core upwells; however, the waters surrounding the upwelling center have some of the highest pigment concentrations in the region.

A particularly sharp and nearly coincident temperature and

color front can be seen on the eastern edge of the EUC upwelling center. The bathymetry of the region (Figure 4.1) indicates that this front is located in waters with depths greater than 1000m. Sea surface temperatures and pigment concentrations across this front (Figure 4.3) extracted from the CZCS imagery along the trackline shown in Plate 4.3 show the sharpest gradient across the color front (0.4 - 6.1 mg/m3) occurs between pixels 22 to 26 (a distance of approximately 3 km). Mean pigment concentrations on the east side of the front (0.95 mg/m3) extending into Elizabeth Bay are significantly higher than those to the west (0.28 mg/m3), which are generally within the newly upwelled EUC waters. The temperature data shows a marked, although less dramatic difference across the front. Temperatures are cooler (~18.8°C) in the western region, increasing across the front and averaging 19.6°C on the eastern side. A closer analysis of the data along the portion of the transect to the east of the front (pixels 30-50) reveals four, approximately equally spaced, peaks in both pigment concentrations and sea surface temperatures. The peaks are approximately 5 pixels (4km) apart with the temperature maxima displaced nearly 1km to the west of the maximum pigment concentration. Phytoplankton variability at this scale could result from a number of physical or biological processes (Haury et al., 1978), but the apparent correspondence between the temperature and pigment fields and the relatively uniform spacing between peaks suggests that physical processes may be the dominant

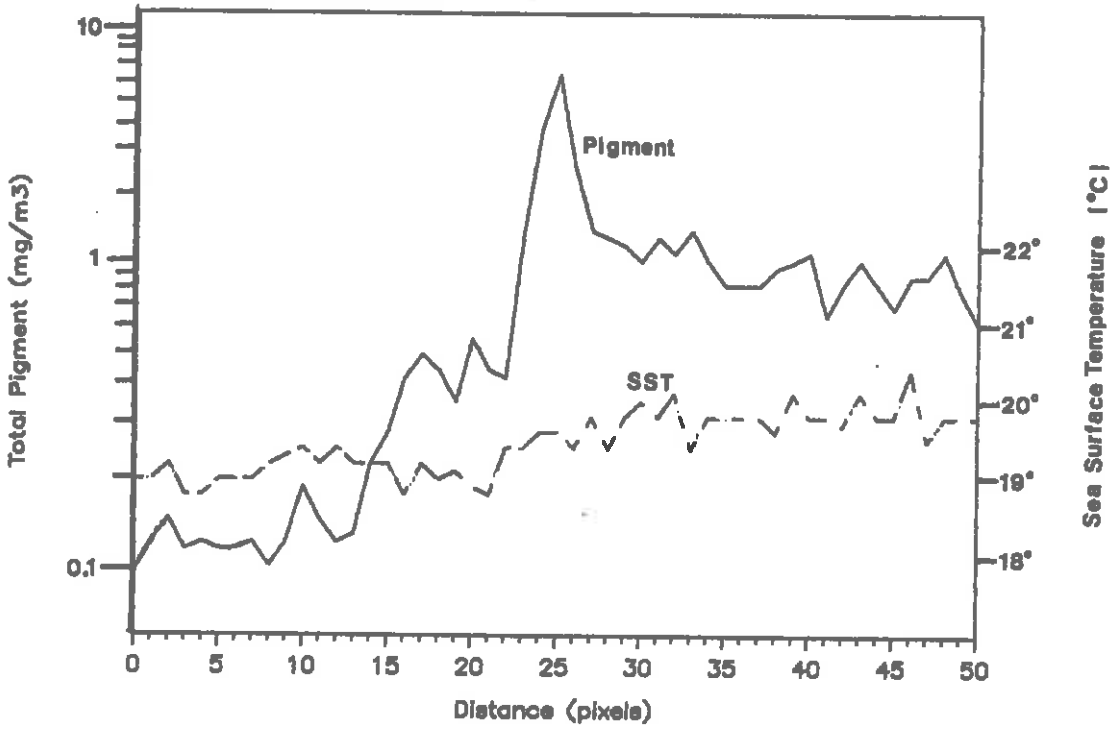

Figure 4.3. Satellite-derived sea surface temperatures (°C, dashed line) and phytoplankton pigment concentrations (mg/m3, solid line) versus distance (1 pixel = .825 meters) along the trackline depicted in Plate 4.3. extracted from the Coastal Zone Color Scanner data acquired on 16 December 1978 (Nimbus-7 orbit 739).

factor.

An example of subsurface temperature distributions along the approximate position of the trackline in Plate 4.3 is given in Figure 4.4. This data is from Houvenaghel (1978) in which the the results of a number of bathythermograph sections throughout the Galapagos Archipelago were used to describe the oceanographic setting of the islands and to investigate the role of upwelling and vertical mixing. The location of the sharp color front observed in the satellite images corresponds roughly to the position where the 20°C isotherm breaks the surface. The isotherm spreading that is evident as one progresses along the transect into Elizabeth Bay is an indication of enhanced vertical mixing, caused either by the EUC impinging on the islands or by tidal mixing in the nearshore zone.

The short-term variability in phytoplankton distributions can be seen by comparing the three CZCS images of this period. Mean pigment concentrations for the entire archipelago were 0.36mg/m3 (SD = 0.23mg/m3) on 9 December (Plate 4.4), 0.26mg/m3 (SD = 0.1mg/m3) on 16 December (Plate 4.3), and 0.41mg/m3 (SD = 0.29mg/m3) on 21 December 1978 (Plate 4.5). The major change occurred in the western half of the archipelago where two major phytoplankton blooms were observed at the beginning and end of this period. The southernmost edge of the zonally oriented ocean color front seen in the 9 December image migrated approximately 100km to the north by 21 December. The significance of the

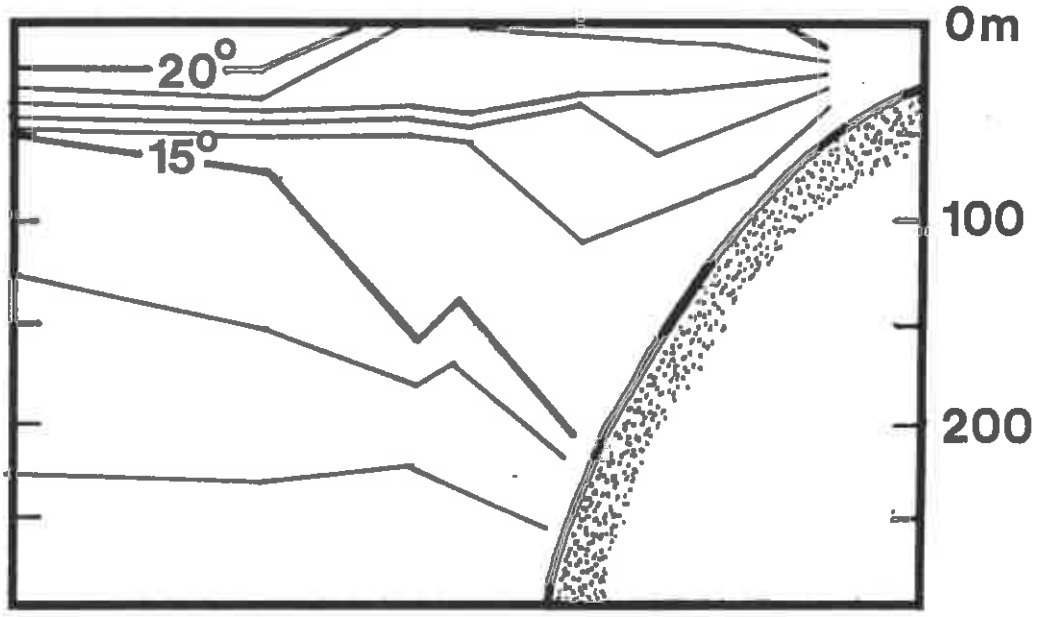

Figure 4.4. Subsurface temperature (°C) distributions along the approximate location of the trackline depicted in Plate 4.3., derived from a number of bathythermograph sections around the Galapagos Islands (after Houvenaghel, 1978).

Plate 4.4. Satellite ocean color image showing the distribution of phytoplankton pigments around the Galapagos Islands acquired on 9 December 1978 (Nimbus-7 orbit 642). The highest pigment concentrations (greater than 5.0 mg/3) can be seen in Elizabeth Bay, between Fernandina and Isabela Islands.

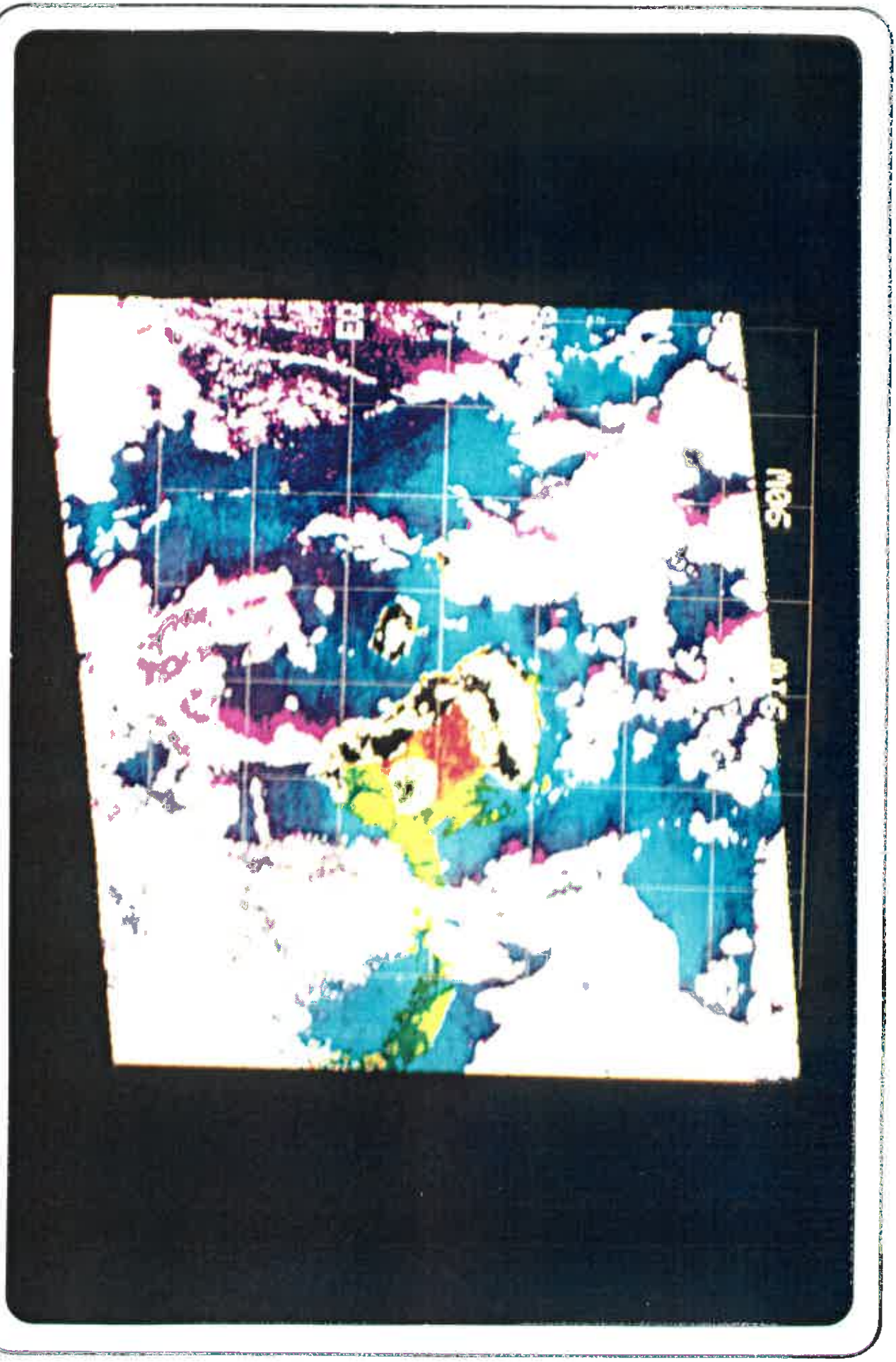
NOAA

Plate 4.5. Satellite ocean color image showing the distribution of phytoplankton pigments around the Galapagos Islands acquired on 21 December 1978 (Nimbus-7 orbit 808). Note the northward displacement of the zonally oriented ocean color front seen clearly in this, and in the preceeding image.

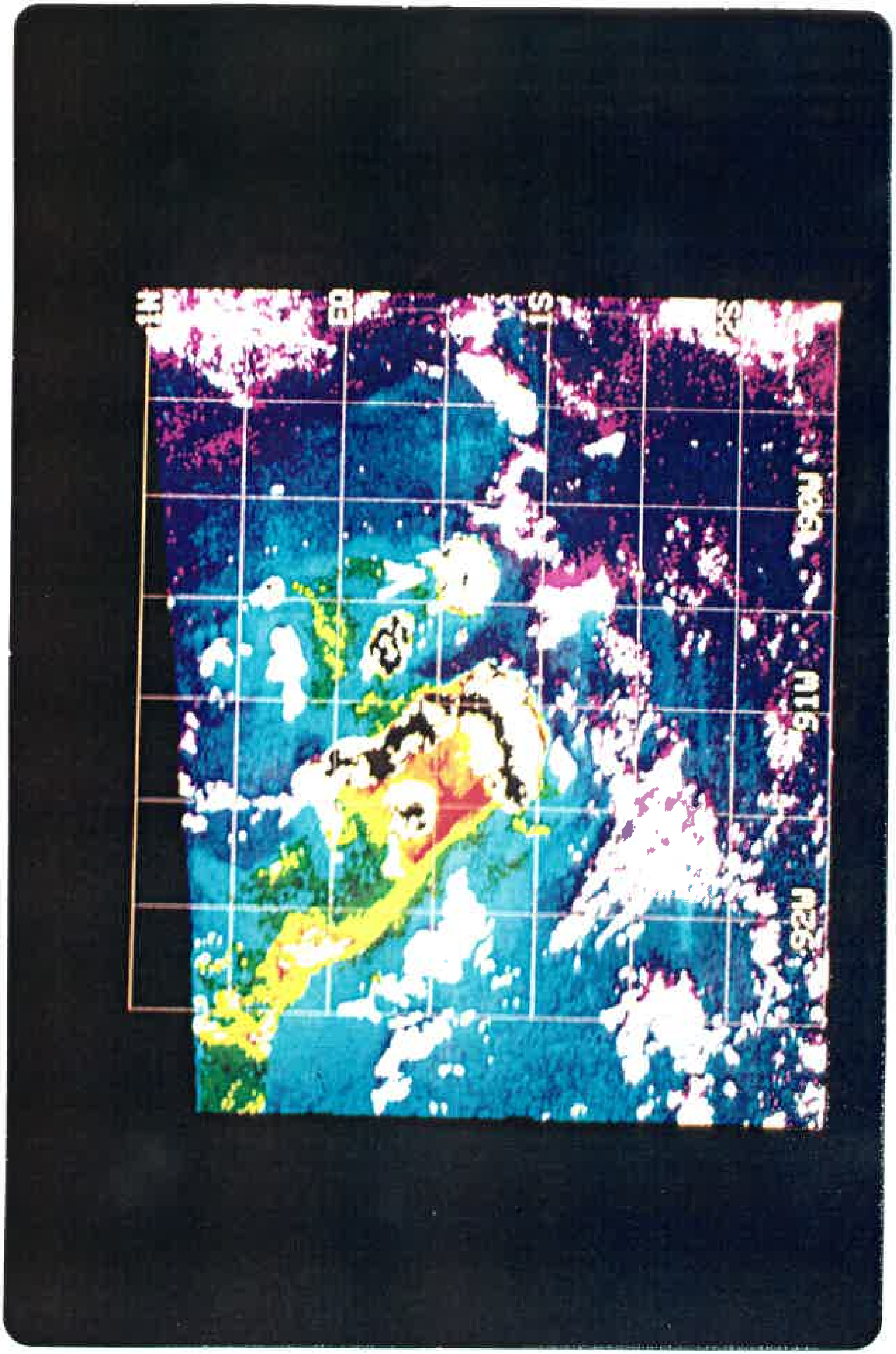

variability in frontal location will be discussed later in this chapter.

Pigment distributions on 11 June 1981 (Orbit 13288, Plate 4.6) show that although different in some respects to the patterns observed during December 1978, several features are clearly similar. Once again, the highest pigment concentrations are found on the western side of Isabela in Elizabeth Bay. The sharp color front seen in December 1978 also appears in the June 1981 image, although its position is displaced approximately 20km to the east. A small patch of pigment-rich water is again found off the northern tip of Fernandina Island. The most notable differences between the December 1978 and June 1981 images are (1) the appearance of phytoplankton-rich plumes extending to the northwest from most of the islands in June 1981 and (2) an overall increase in pigment concentrations in the waters around the archipelago. The overall mean pigment concentration for the entire region covered by the CZCS image increased from 0.26 mg/m3 16 December 1978 to 0.42 mg/m3 in June 1981. This increase is particularly evident in the offshore waters, indicating the possibility of either a large-scale seasonal or interannual effect. The seasonal influence will be addressed later in this chapter, whereas the interannual variability in phytoplankton biomass and production experienced by this region will be discussed in Chapter 6.

Oceanographic measurements of the large-scale circulation patterns which are available for the June 1981 period, proved

Plate 4.6. Satellite ocean color image showing the distribution of phytoplankton pigments around the Galapagos Islands acquired on 11 June 1981 (Nimbus-7 orbit 13288).

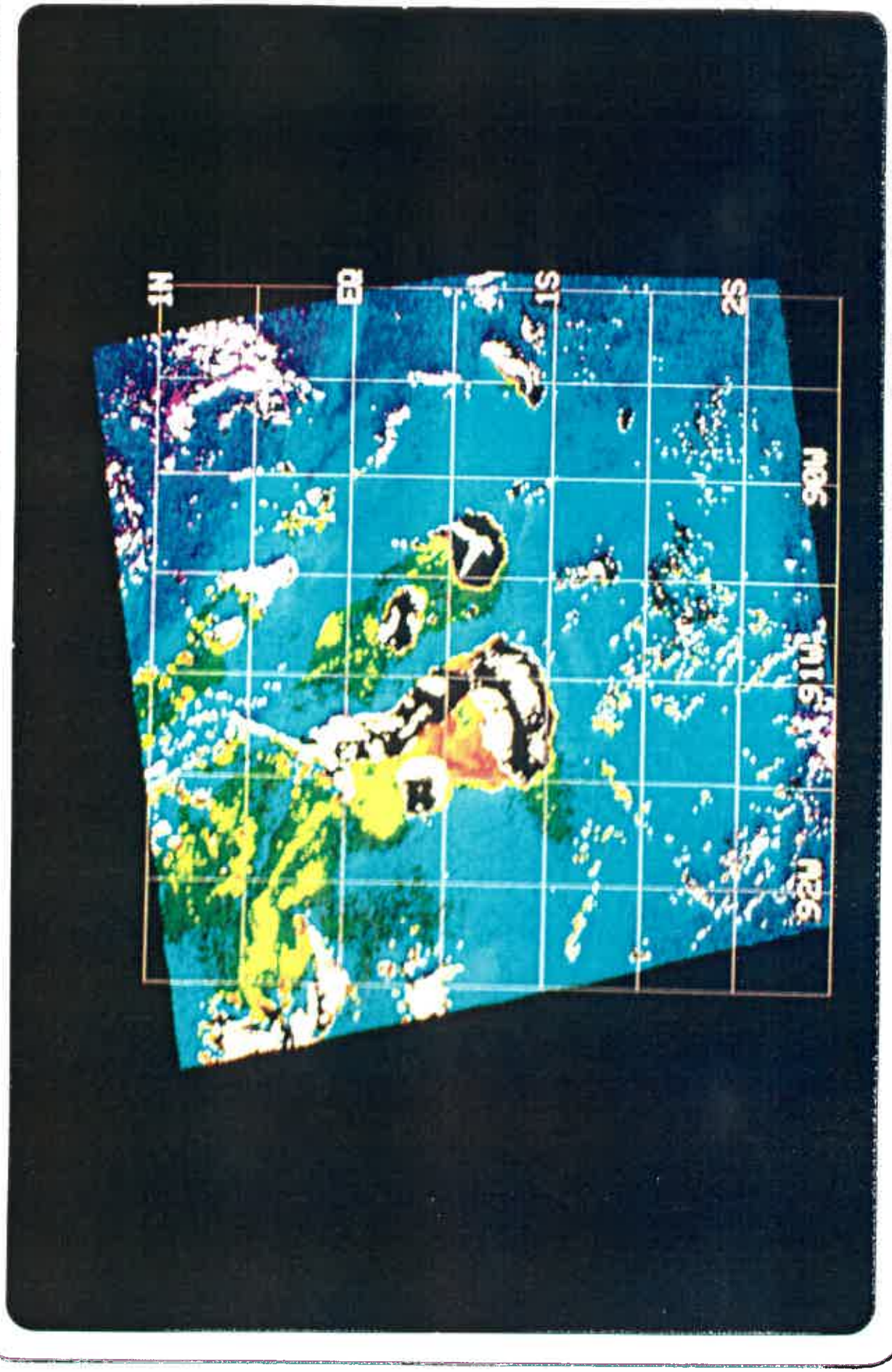
4N
2S
90W
95W

useful in interpreting the patterns seen in the satellite image. The trajectories of four satellite-tracked driting buoys deployed to the east of the Galapagos Islands (Pazos & Paul, 1984) during the latter half of June 1981 are presented in Figure 4.5; the tic-marks along the trajectories represent successive ten day intervals. The horizontal displacements of the buoys have been interpreted as providing a measure of the velocity and direction of water movement in the upper layer (~50m) of the ocean (Hansen & Paul, 1984). The trajectories show that the surface waters to the north of the equator around the Galapagos Islands were moving in a generally west-northwest direction, and in a west-southwest direction for the waters to the south. The plumes of pigment-rich water seen in the satellite image are, therefore, forming on the downstream sides of the islands.

Simpson et al. (1982) and Simpson & Tett (1985) described the mixing processes associated with flows around islands. It was noted that at times when significant non-tidal residual flows were present (4-20cm/sec was reported by Simpson et al. for the waters around the Scilly Isles), mixed water would be swept away from the island and produce a plume downstream. Houvenaghel (1978) reported that around the Galapagos, newly upwelled waters of the EUC were mixed with and carried along by the flows of the South Equatorial Current. The appearance of distinctive island wakes in most of the ocean color images of the Galapagos clearly indicates the presence and significance of the mean surface flows in

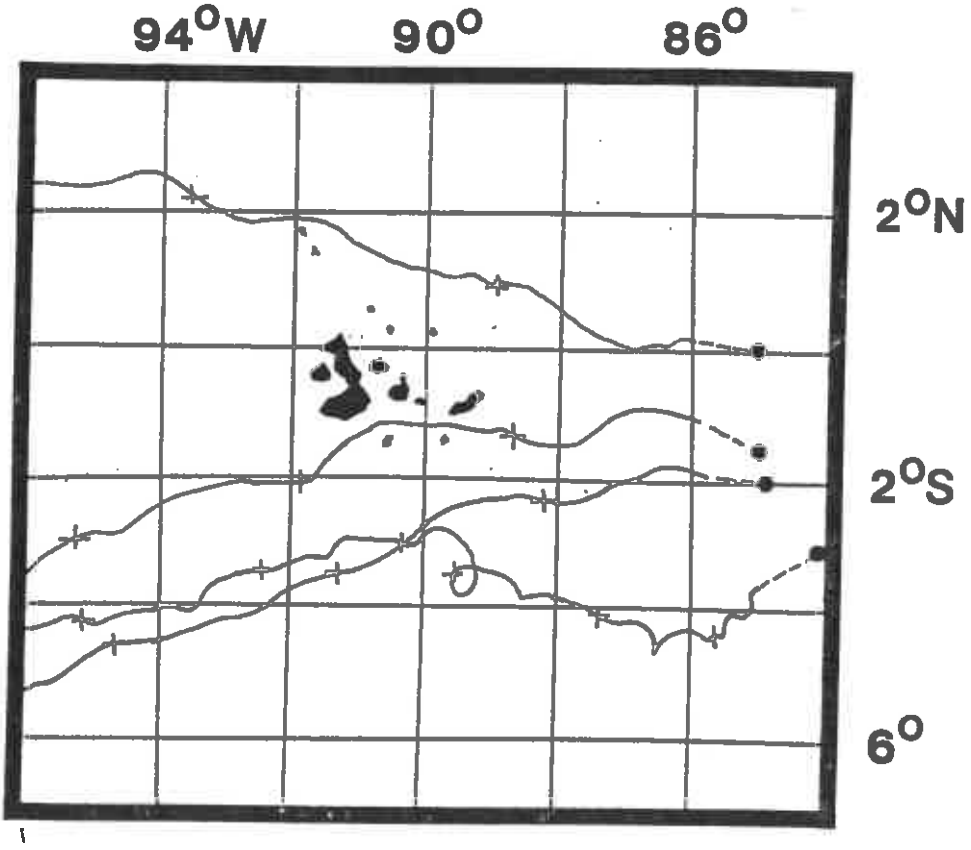

Figure 4.5. The trajectories of four satellite-tracked drifting buoys deployed to the east of the Galapagos Islands during the third week of June 1981. The deployment locations are indicated (closed circles) and the tic-marks along the trajectories represent subsequent ten-day intervals (after Pazos and Paul, 1984).

determining the patterns of phytoplankton distribution around the islands.

The trajectories given in Figure 4.5 indicate that the buoy to the north of the islands traveled further during the same period of time than did the buoy to the south. For the second ten-day interval, the period when the buoys were closest to the islands, the northern buoy covered approximately 54Km/day (~63cm/sec) while the southern buoy averaged only 35Km/day (~41cm/sec). The slower westward movement of this southern buoy may possibly be due to the influence of the eastward flows of the EUC, particularly if, as is indicated in Plate 4.2, the major portion of the EUC flows were through the southern part of the archipelago.

The distributions of phytoplankton pigments observed on 26 April 1980 (Orbit 7608, Plate 4.7) are dramatically different from those found in the previously described scenes. Although the mean pigment concentration for the entire region is only slightly lower in April 1980 than during June 1981 (0.37 vs. 0.42mg/m3), the greatest difference is seen in the patterns of phytoplankton distribution around the islands. The regions of highest phytoplankton biomass are no longer located on the western side of Isabela, but rather are found to the south and east. Mean pigment concentrations for the waters around Elizabeth Bay were only 0.35mg/m3 (SD = 0.61mg/m3) while those between Isabela, San Salvador and Santa Cruz were 0.74mg/m3 (SD = 1.5mg/m3).

Plate 4.7. Satellite ocean color image showing the distribution of phytoplankton pigments around the Galapagos Islands acquired on 26 April 1980 (Nimbus-7 orbit 7608). Note that phytoplankton pigment concentrations are greatest in the waters to the east of Isabela Island and that relatively low phytoplankton abundances (pigment concentrations less than 0.4 mg/m3) are observed in Elizabeth Bay.

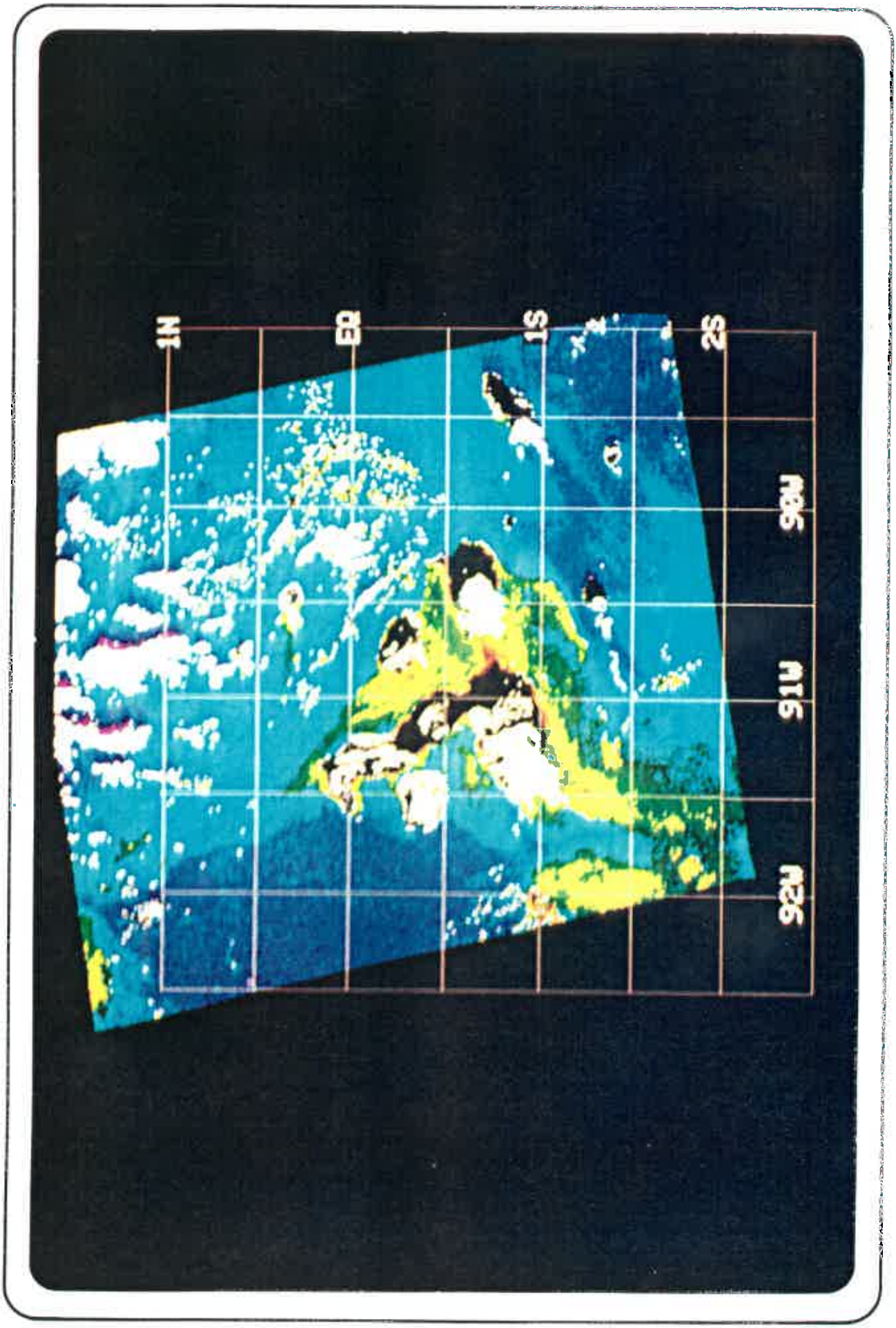
1N
EQ
1S
2S
96W
91W
86W

A question that can be asked is what differing oceanographic conditions existed during these periods that could possibly explain the contrasting patterns of phytoplankton distributions observed in the satellite images. One possiblility is the altered circulation patterns observed during April 1980. Near-surface (15m) current meter measurements taken at 0°, 110°W for the period February 1980 through September 1981 are presented in Figure 4.6a (Halpern, personal communication, 1984). Although these observations were made nearly 2100Km to the west of the Galapagos Islands, they document the dominant oceanic circulation features of the region. Coincident sea level records from the Galapagos Islands are presented in Figure 4.6b (Hayes, personal communication, 1984). A recent study (Hayes & Halpern, 1984) has shown that for the period March 1980 to July 1981 sea level at the Galapagos was highly correlated with the currents measured at 0°, 110°W. Specifically, they found that eastward flows, expressed as vertically averaged zonal velocities, resulted in rising sea level at the Galapagos.

Enhanced eastward surface flows and elevated sea levels are clearly seen during the March through May periods of each year. By the latter part of April 1980, sea level at the Galapagos had been rising rapidly and strong eastward flows had been recorded throughout the preceeding month. This is in sharp contrast to the conditions that were observed during June 1981 at which time sea level was low, and the surface flows although variable, were in a

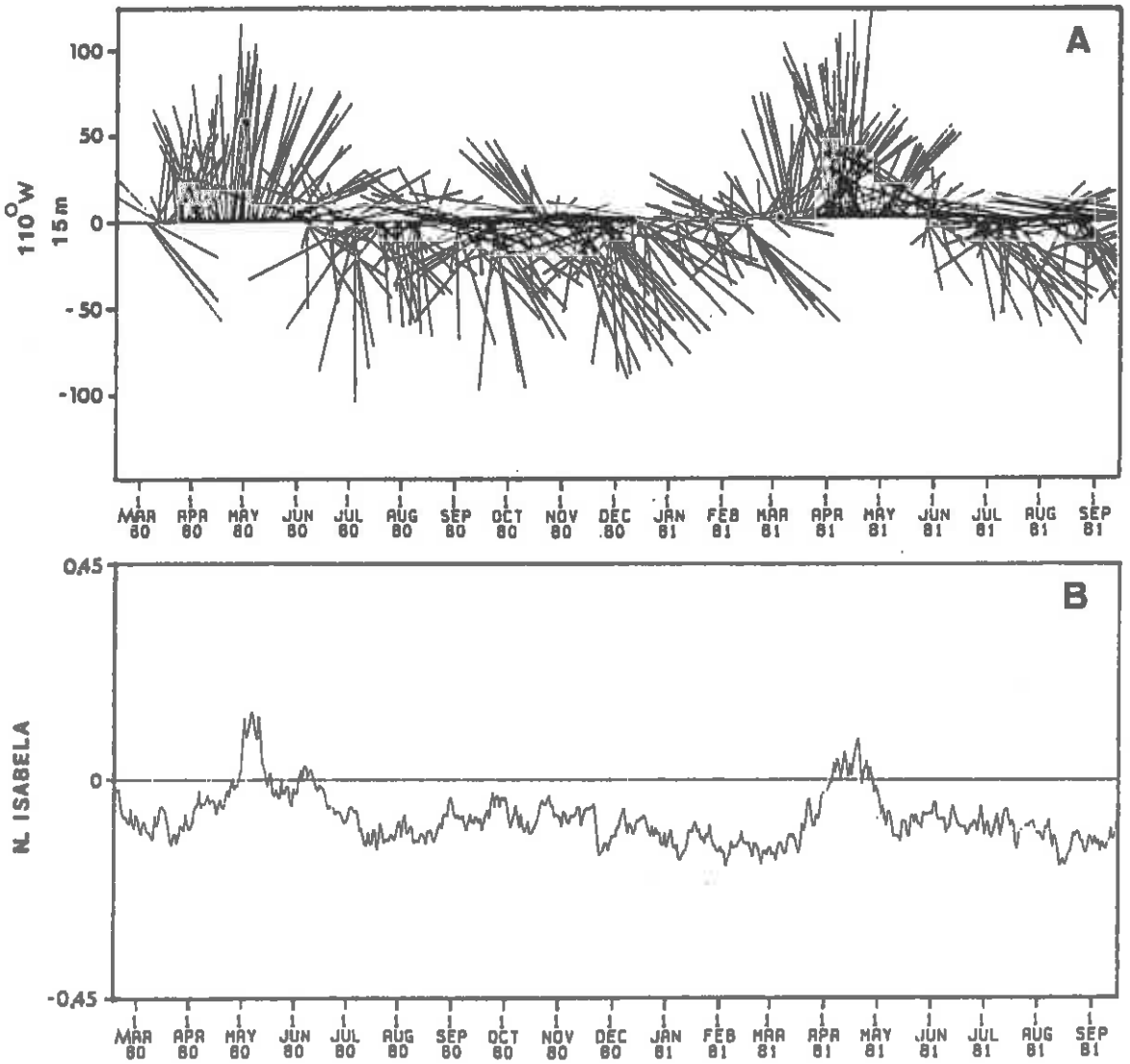

Figure 4.6. A) Daily vector-averaged current meter records showing speed and direction at a depth of 15 meters measured at 0°, 110°W (Halpern, personal communication, 1984). Eastward direction is upward. B) Low pass filtered and detided sea level record from the Galapagos Islands (recorded at the northern tip of Isabela Island) for the same period covered by the current meter data (Hayes, personal communication, 1984).

generally westward direction.

The position of clouds associated with oceanic islands may provide useful clues as to the direction of the prevailing winds. As one approaches many of the high islands in the trade wind regions, one often sees clouds piled against the windward sides of the islands. These clouds form when the warm, moist air of the trades are deflected upward upon striking the often very steep flanks of these islands. The Galapagos Islands are volcanic, with steep peaks (between 1000 to 1500 meters on Isabela) near the centers of most of the islands in the archipelago. In the June 1981 CZCS image (Plate 4.6) clouds are clearly seen along the eastern flanks of Fernandina, Santa Cruz, Isabela, and down the center of San Cristobal. Wind data (Halpern, personal communication, 1984) indicates that the southeast Trades were quite strong (~7m/sec) during this time. The cloud patterns in the April 1980 image (Plate 4.7), however, are quite different. At this time, large clouds can be seen along the western flanks of most of the islands. Unfortunately, wind records are not available for this period, but as will be discussed, a weakening of the southeast trades often occurs at this time. While inferring wind direction from cloud positions is somewhat speculative, it appears to offer at least some qualitative information about relative wind direction for places such as the Galapagos where accurate wind records are often difficult to obtain.

The position of the Galapagos Islands near the eastern end of the equatorial waveguide, subjects them not only to perturbations in local forcing, but also to disturbances generated in the central and western Pacific (Kogelschatz et al., 1985). These propagating disturbances, the most dramatic of which are associated with El Nino, have been shown to have profound effects on the biota of these islands. A recent investigation utilizing satellite ocean color observations and complemented with coincident oceanographic measurements demonstrated the tight coupling that exists between the distribution of phytoplankton biomass around the Galapagos Islands and the oceanographic and atmospheric conditions observed during the 1982-83 El Nino (Feldman et al., 1984).

The CZCS data presented in Plate 4.8 were acquired on 8 November 1982 (Orbit 20406) during the onset phase of El Nino. When the overall mean pigment concentration for the entire archipelago was computed in the same manner as the other CZCS scenes presented in this paper, an interesting fact emerged; the mean pigment concentration calculated for the November 1982 scene (0.23mg/m3) was not significantly lower than was calculated for December 1978 (0.26mg/m3), which supposedly represents non-Nino conditions. In fact, the sharp color front and highest pigment concentrations were once again found outside of Elizabeth Bay. What is particularly striking about this scene, however, is the large region to the north of the islands where waters with

Plate 4.8. Satellite ocean color image showing the distribution of phytoplankton pigments around the Galapagos Islands acquired on 8 November 1982 (Nimbus-7 orbit 20406) during the onset of the 1982-83 El Nino. Note the sharp boundary between waters very low in phytoplankton abundances (pigment concentrations less than 0.1 mg/m3) in the northern portion of the image and the generally richer waters to the south.

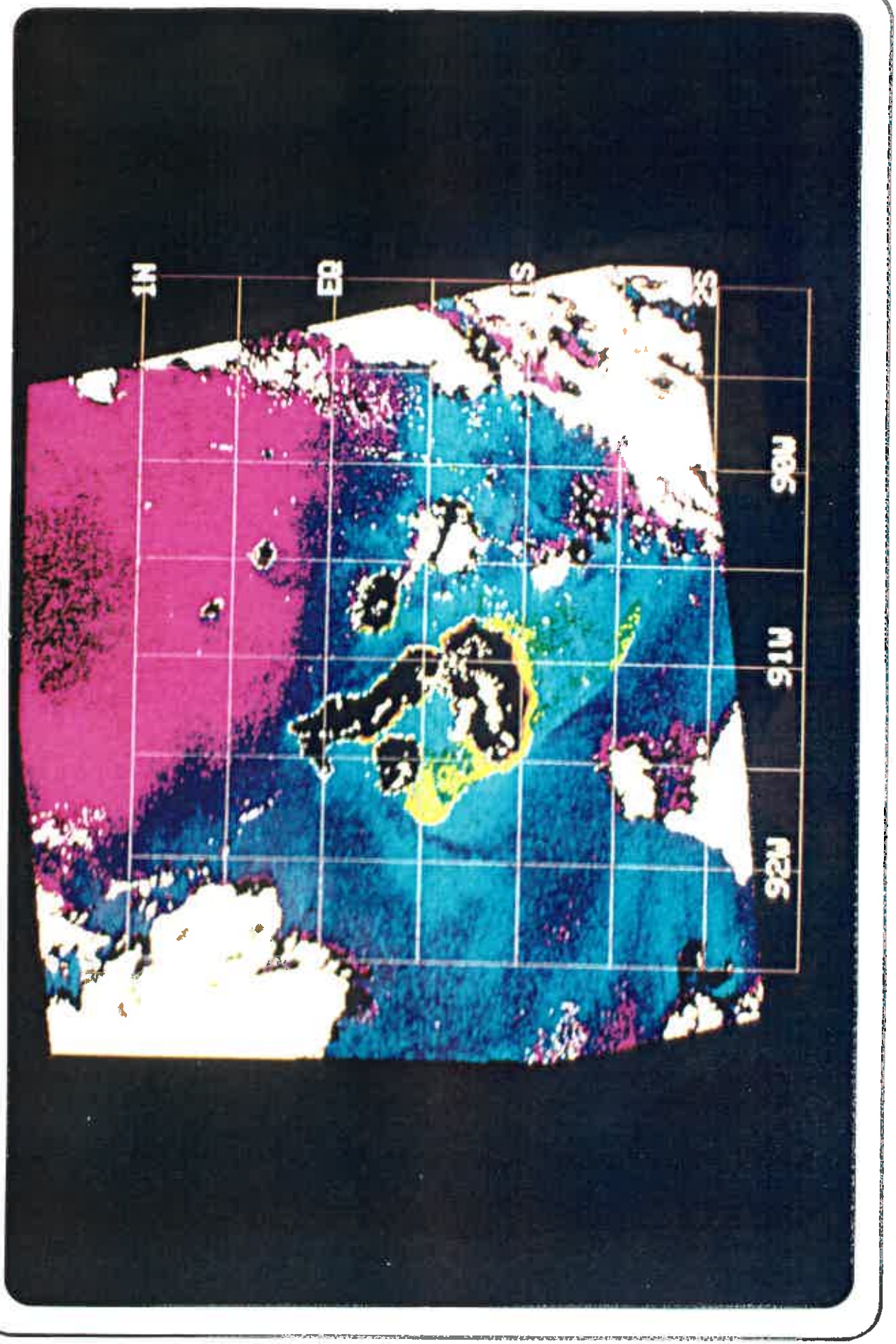
4N
8N
12N
16N
92W
88W
84W
80W

exceptionally low pigment concentrations were observed. In the satellite-derived sea surface temperature distributions of the eastern equatorial Pacific on 8 November 1982 presented in Philander et al. (1985) two features appear which are also observable in the CZCS image of that day. The equatorial Front was in a position very close to that observed in the CZCS image as the boundary between the low pigment waters to the north and the richer waters to the south. The front is displaced to the south during El Nino (Barber & Chavez, 1983; Hayes, 1985) and it appears as if the 8 November CZCS image caught the front just as it reached the Galapagos. The sea surface temperature data also indicates a plume of relatively cool water extending to the south of Isabela. A similar plume of pigment-rich water can be seen in the CZCS image. It is not known whether the plumes were generated locally or swept around the island from the west as a result of the changing oceanographic and meteorological conditions at the time. Although locally high levels of phytoplankton biomass were observed around the Galpagos Islands during El Nino (Feldman et al., 1984; Kogelschatz et al., 1985), the productivity of the offshore waters was reduced significantly (Barber & Chavez, 1983).

4.3. PATTERNS OF PRODUCTION AND THE SEASONAL CYCLE

The satellite ocean color images presented in this chapter demonstrate the degree of spatial and temporal variability of phytoplankton biomass around the Galapagos Islands. One of the first things evident from the satellite images is that some areas around the Galapagos appear richer than others. To quantify this observation, the archipelago was divided into nine mesoscale sampling regions (Figure 4.7). The criteria that were used to select the number, location and size of each sampling region were somewhat subjective. The size of the sampling region was set at approximately 50 x 50 Km so that most of the mesoscale variability in phytoplankton distributions associated with a particular island could be determined. In addition, the choice of sampling region size and location roughly coincides with the maximum feeding range and nesting location of many of the species of seabirds that are abundant throughout the Galapagos, and are the subject of much ecological investigation (R. Rickleffs, personal communication, 1984). Since, as has been previously noted, all the images are remapped to the same spatial co-ordinates, the geographic area covered by each sampling region is the same in each image. The mean pigment concentration for each sampling region along with the variability about the mean could then be calculated.

Several additional kinds of information can be obtained through this approach. First, by comparing the individual regions

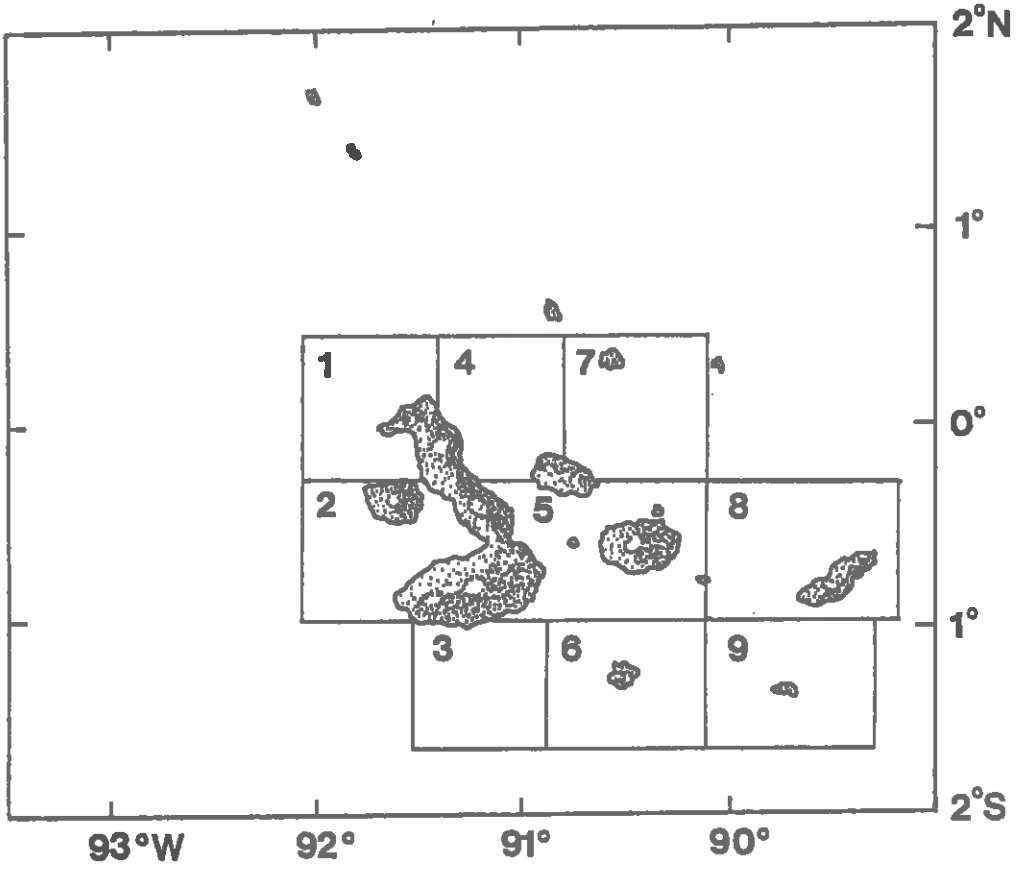

Figure 4.7. Chart of the Galapagos Islands showing the location of the nine mesoscale sampling regions used to assess the spatial and temporal variability of phytoplankton biomass around the archipelago.

within a single scene, the spatial variability in phytoplankton biomass around the islands can be determined. Second, a given sampling region or group of regions can be compared from one image to the next, giving an indication of the temporal variability. Third, the distribution of phytoplankton within a given sampling region can be determined both by a visual inspection of the CZCS images as well as through a relatively simple statistical analysis of the data.

Since it is well known that phytoplankton often exhibit non-random or patchy horizontal (Cassie, 1959) and vertical distributions (Platt & Herman, 1983), it is possible to estimate whether the distribution over a given spatial domain (i.e. a sampling region in this case) is patchy (over-dispersed), randomly distributed, or uniform (under-dispersed) by comparing the mean (M) with the variability about the mean. This technique usually compares the mean number of organisms with the variance, but since the numbers in this case are concentration units, using the variance would result in a ratio that contains the units mg/m3. Using the standard deviation (SD) rather than the variance, however, produces a dimensionless ratio commonly referred to as the coefficient of variation. This ratio is an indicator of how the plankton are distributed within a given sampling region, such that as the ratio becomes larger, the distribution is considered to be more patchy. These values will also be referred to as dispersion coefficients for this study. A similar technique was

applied by Wirick (1981) in which the mean squared plus the variance was used to define a habitat's value to a forager requiring food above some minimum concentration.

The final way in which this data can be treated involves the compositing of images to develop an overall as well as seasonal mean. Twelve CZCS images of the Galapagos Islands spanning the period from December 1978 through November 1981 (orbits 642, 739, 808, 1638, 2868, 3324, 3352, 3476, 5480, 7608, 13288, 15610) were composited to produce the data presented in Table 4.1, in which the overall mean pigment concentration for each sampling region, along with the minimum and maximum values are given.

The range of mean pigment concentrations for each of the sampling regions indicates that the greatest variability was found in the maximum values. The minimum values for all nine regions prior to El Nino were surprisingly similar (0.12-0.21mg/m3) whereas the maximum values ranged from 0.25-2.05mg/m3. Individually, sampling regions 6, 8, and 9 had the lowest overall mean concentrations and the smallest ranges. The dispersion coefficients calculated for each sampling region from seven individual CZCS orbits indicate a similar pattern (Table 4.2). The regions characterized by the highest pigment concentrations and dispersion coefficients generally greater than one (i.e. regions 1 & 2) are those in which the large plumes and sharp frontal zones are most often found. The sampling regions in the eastern portion of the archipelago appear more oceanic in

	SAMPLING REGION								
	1	2	3	4	5	6	7	8	9
MEAN	0.41	0.83	0.29	0.26	0.38	0.21	0.25	0.23	0.18
MAX.	0.95	2.05	0.50	0.43	0.74	0.31	0.48	0.35	0.25
MIN	0.16	0.16	0.15	0.15	0.21	0.13	0.14	0.17	0.12

Table 4.1. Overall mean phytoplankton pigment concentrations (mg/m3) for each of the nine mesoscale sampling regions derived by compositing twelve Coastal Zone Color Scanner images of the Galapagos Islands for the period December 1978 through November 1981. The maximum and minimum mean pigment concentration for each region is also given.

SAMPLING REGION	12/9/78 C_{SAT} (d)	12/16/78 C_{SAT} (d)	12/21/78 C_{SAT} (d)	7/2/79 C_{SAT} (d)	4/26/80 C_{SAT} (d)	6/11/81 C_{SAT} (d)	11/8/82 C_{SAT} (d)
1	0.30 (1.6)	0.26 (1.1)	0.44 (1.6)	0.46 (1.9)	0.30 (1.1)	0.57 (1.0)	0.19 (1.4)
2	1.38 (1.6)	0.78 (2.5)	1.48 (1.6)	0.58 (1.7)	0.35 (1.7)	0.86 (1.5)	0.41 (1.6)
3	0.23 (0.7)	0.15 (1.5)	0.20 (2.3)	0.20 (0.5)	0.50 (1.1)	0.38 (1.7)	0.33 (0.8)
4	0.16 (0.7)	0.22 (0.5)	0.36 (0.9)	0.16 (1.8)	0.43 (2.0)	0.41 (0.7)	0.13 (1.3)
5	0.30 (1.8)	0.38 (2.5)	0.31 (2.5)	0.24 (2.1)	0.74 (2.0)	0.44 (1.7)	0.32 (2.3)
6	clouds	0.14 (0.4)	0.13 (0.4)	0.15 (0.3)	0.27 (0.7)	0.31 (1.1)	0.23 (0.7)
7	0.16 (0.6)	0.16 (0.3)	0.23 (0.6)	0.14 (0.3)	0.40 (1.6)	0.31 (1.0)	0.10 (1.2)
8	0.21 (0.4)	0.17 (0.5)	0.17 (1.5)	0.19 (1.2)	0.30 (0.8)	0.28 (1.1)	0.22 (0.7)
9	0.19 (0.4)	0.12 (0.4)	0.12 (0.3)	0.14 (0.4)	0.22 (0.7)	0.25 (0.6)	clouds

Table 4.2. Mean phytoplankton pigment concentrations (C_{SAT} in mg/m3) and 'dispersion coefficients' (d, see text for definition) calculated for each of the nine mesoscale sampling regions derived from seven Coastal Zone Color Scanner images of the Galapagos Islands.

character, with low, and relatively uniform pigment concentrations. The description of the western regions of the archipelago as being the most productive (e.g. Maxwell, 1974; Jimenez, 1981) is confirmed by the satellite data, particularly when seasonal influences are not considered as is the case in the composited data just described. The seasonal influence on the distributions and abundances of phytoplankton around the Galapagos, however, appear to be significant.

Seasonal variability in the oceanic and atmospheric parameters affecting the Galapagos Islands has been described by many authors; however, the transition periods from one season to the next are often poorly defined and to a large extent based upon the data set being described. Palmer & Pyle (1966) noted a distinct annual variation between a wet season from January to April and a dry season during the rest of the year. The wet season is characterized by increased air and sea temperatures and a weakening of the southeast trade winds which, during this season, are often replaced by calms or periods of westerly winds. The wet season, also referred to as the warm season by some authors, is the time when heavy rains fall on the typically arid Galapagos. The dry season is characterized by cooler air and sea temperatures, strong southeast trade winds and less frequent periods of rainfall. Distinct annual variations in the intensity and duration of both seasons have also been noted. Houvenaghel (1978) places the warm season from February till April, Hayes

(1985) from February to May while others (Maxwell,1974; Kogelschatz et al.,1985) extend it from January through May.

The oceanographic conditions around the Galapagos, in particular the two main current systems which influence this region, also exhibit pronounced seasonality. The strength of the Equatorial Undercurrent varies annually (Wyrtki,1974; Lukas,1981; Leetma & Molinari,1984) and is generally stronger during the early part of the year. Halpern (1983) found that the near-surface flows of the South Equatorial Current have a strong annual cycle with predominant westward flows from July-December, eastward flows during March-May (Figure 4.6), with February and June being transition periods between the two.

Although there are reports of the interannual variability in phytoplankton biomass and productivity around the Galapagos Islands (Barber & Chavez, 1983; Kogelschatz et al., 1985), the identification of a distinct seasonal cycle has been hampered by the difficulty in making synoptic measurements of this highly dynamic region using traditional ship sampling techniques. Maxwell (1974) reported that seasonal differences in productivity were evident in Galapagos waters with the cold season (June-December) being more productive than the warm season (February-May). Hovenaghel (1978), however, found that no distinct seasonal cycle in either phytoplankton biomass or productivity could be deduced.

The satellite data presented here provide both the synoptic

perspective and the temporal coverage required to address more effectively the question of whether or not a seasonal cycle in phytoplankton abundance does exist, and if so, to what factors may it be related. The mean pigment concentrations for each of the nine sampling regions for the twelve CZCS images (December 1978-November 1981) were grouped according to season and the seasonal mean concentration for each region was calculated. These values are presented in Figure 4.8.

The first conclusion that can be drawn from the data is that there appears not to be a statistically significant difference in pigment concentrations between seasons for the archipelago as a whole. The mean concentration for the June through December period (0.34mg/m3) was just slightly greater than that for the February through May period (0.31mg/m3). The major difference between the two seasons, however, is the dramatic and definitely significant decrease in pigment concentrations in the western half of the archipelago (regions 1 & 2) from the June through December to the February through May period. The mean concentration in region 2 decreased nearly 4-fold while the mean concentration in region 1 during February through May was less than half of that recorded during June through December. Also seen in Figure 4.8 along with the decrease in pigment concentrations to the west of the archipelago during February through May, is a corresponding increase in concentrations for all regions to the east.

It is this seasonal redistribution or, more specifically, a

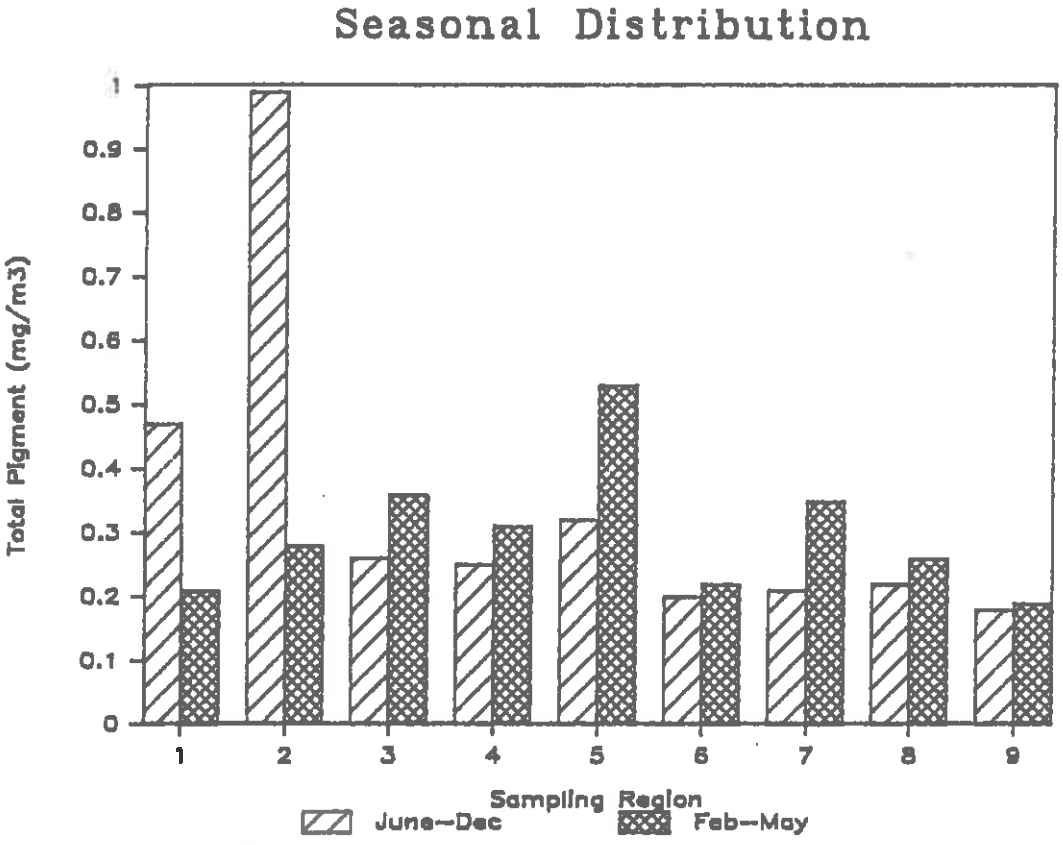

Figure 4.8. Seasonal mean phytoplankton pigment concentrations (mg/m3) for each of the nine mesoscale sampling regions based upon a seasonal grouping of twelve Coastal Zone Color Scanner images of the Galapagos Islands for the period December 1978 through November 1981.

shift in the areas of increased production, that the satellite images have allowed us to identify. From the data presented, it appears that the patterns of phytoplankton distributions revealed in the satellite ocean color observations reflect features of, and changes in, the large-scale oceanic and atmospheric circulation systems. Although to draw conclusions based upon twelve CZCS images spanning 2.5 years may be tenuous, it appears as if interannual variability is seen predominantly by an increase or decrease in pigment concentrations over the region as a whole, while seasonal variability more specifically affects the distribution of phytoplankton around the islands. Obviously, increasing the number of images from which these kinds of analyses are based will greatly improve our understanding of these relationships. Also, the increasing amount of meteorological and oceanographic data that will be gathered as part of the ten year observational and modeling program designed to study the interelationships between the tropical oceans and the atmosphere (TOGA) will vastly expand our knowledge of the physical environment.

4.4. THE PRODUCTIVE HABITAT OF THE GALAPAGOS ARCHIPELAGO

Investigations that have tried to assess the impact of the Galapagos Islands on the surrounding waters have focused primarily upon the role that the islands play in altering the 'downstream'

circulation patterns. White (1971, 1973) discussed the theoretical and observational evidence for an oceanic wake in the equatorial Undercurrent downstream (to the east) of the Galapagos. More recently, Rowlands (1982) presented a linear theory to describe the flow of equatorial Kelvin waves and of the equatorial Undercurrent around these islands. Unfortunately, very few investigations have looked at the area to the west of the Galapagos, and those that have focused primarily upon the role of equatorial upwelling (Sorokin et al., 1975). This region is downstream from the islands with regard to the predominant westward surface flows of the South Equatorial Current. Robinson (1972), in sailing westward from the Galapagos to Tahiti noted that although the islands were quite a distance away, their influence was still felt. They attributed the large rips and powerful eddies they observed to the disturbance to the surface flow caused by the islands. It can be assumed that these strong physical processes would have some biological consequences.

The question that will be addressed in this section is to what extent do the Galapagos Islands enhance the production of the surrounding waters? Making use of both the qualitative and quantitative information contained in the CZCS data, it is possible to determine the spatial extent of the area of enhanced biological production, referred to here as the productive habitat, associated with the islands. The relationships among biomass, growth, and production are complex. Yentsch (1984) has argued

that the pigment distributions observed by the CZCS reflect the net growth processes of phytoplankton and not merely the redistribution of abundance. He hypothesizes that it is vertical mixing, resulting in the periodic injection of nutrients into the surface waters, that is responsible for the growth and, therefore, the abundance of phytoplankton evident in the satellite images. The colder, subsurface waters around the Galapagos are generally rich in nutrients; thus the appearance of cold water at the surface is, in this case, an indicator of nutrient rich water. Traganza et al. (1981) found a similar correlation between regions of newly upwelled water, elevated nutrient concentrations, and enhanced phytoplankton production. The relationship between temperature and the distribution and abundance of phytoplankton presented here (i.e. the newly upwelled water seen in Plate 4.2 and Figure 4.3) support Yentsch's hypothesis. In general, it is fair to say that the areas of increased phytoplankton biomass seen in the satellite ocean color images reflect a period of net increased phytoplankton production.

If the open ocean phytoplankton concentrations observed in areas not influenced by islands represent nutrient-limited conditions (Simpson et al., 1982), then the increased nutrient supply generated by mixing processes around the Galapagos should produce regions of enhanced phytoplankton production. Such regions are evident in all the CZCS images, but in particular, the twin plumes extending nearly 600km downstream from the islands in

the 20 August 1980 scene (Plate 4.9), the single plume seen on 24 November 1979 (Plate 4.10), and the large (~200 x 50km) eddy-like feature seen to the north of the islands on 19 February 1979 (Plate 4.11) are particularly impressive. To calculate the area of enhancement associated with the Galapagos, it was assumed that the regions in the CZCS images where pigment concentrations were less than 0.4 mg/m3 (blue) represented open ocean, unenhanced conditions. The next step was to select a pigment concentration value which delineated most clearly the boundary separating the enhanced conditions (productive habitat) from the open ocean region. The actual plumes appeared to be very well defined by the yellow (>0.7mg/m3) contour. However, aside from the plumes themselves, there appeared to be somewhat less distinct regions of enhanced phytoplankton abundances obviously associated with the islands, perhaps representing the diffusing outer edges of the plumes. These regions were best delineated by the 0.4mg/m3 contour and are colored green in the images. The area of the productive habitat calculated from five large-scale CZCS images of the Galapagos Islands are given in Table 4.3. What is particularly striking about these findings are the size and variability of the region influenced by the Galapagos and the ability to assess it with the satellite ocean color data.

It is perhaps more meaningful to compare the actual areal extent of the productive habitats, rather than their percentage of the total because the cloud-free surface area varied considerably

Date	Area ($10^3 km^2$) >0.4	Area ($10^3 km^2$) >0.7	Total Cloud Free Area ($10^3 km^2$)	Overall Mean Pigment Conc. (SD)
2-19-79	55 (21%)	9 (3%)	267	0.30 (0.29)
11-24-79	110 (57%)	18 (10%)	192	0.45 (0.36)
4-26-80	46 (14%)	9 (3%)	318	0.29 (0.43)
8-20-80	80 (26%)	25 (8%)	313	0.37 (0.69)
6-11-81	31 (10%)	6 (2%)	317	0.28 (0.44)

Table 4.3. Total cloud-free surface area ($10^3 km^2$), and the areas of ocean surface containing phytoplankton pigment concentrations greater than 0.4 mg/m3 (wake) and 0.7 mg/m3 (plume), and the overall mean pigment concentration (mg/m3) and Standard Deviation (SD) computed from five large-scale Coastal Zone Color Scanner images of the Galapagos Islands. The numbers in parentheses are the percentage of total surface area represented by each value.

between images. A visual inspection of the images reveals, for instance, that the areal extent of the plume (>0.7mg/m3) in the August 1980 image (Plate 4.9) may have been underestimated by at least 12,000km² because of cloud cover. The largest plumes and consequently, the largest productive habitats (November 1979, August 1980) appear to be associated with times of maximum trade wind strength and strong westward flows of the South Equatorial Current. Buoy displacements (Pazos & Paul, 1984) indicate that surface flows of approximately 50cm/sec were found in the vicinity of the northern plume during the August 1980 period. This would mean that a water parcel brought to the surface at the Galapagos, would take between 10-15 days to reach the westernmost tip of the plume. Similar buoy trajectories for November 1979 (Hansen & Paul, personal communication, 1984) indicate that horizontal displacements were smaller (~35cm/sec) during this time. The northward displacement of the western tip of the November 1979 plume is mirrored in the buoy trajectories.

It is interesting to speculate as to whether or not a steady state system exists, with nutrients being supplied by mixing processes at the Galapagos supporting enhanced phytoplankton production along the axis of the plume. The horizontal (downstream) extent of the plume may be limited by several factors including (1) rate of nutrient supply (2) advective and diffusive losses (3) nutrient depletion resulting from phytoplankton uptake (4) grazing by zooplankton or (5) sinking losses. There is also

Plate 4.9. Satellite ocean color image showing the distribution of phytoplankton pigments around the Galapagos Islands acquired on 20 August 1980 (Nimbus-7 orbit 9211). This image is presented at full swath resolution (approximately 1500 kilometers wide) so that the spatial extent of the area of enhanced phytoplankton production associated with the Galapagos Islands can be assessed.

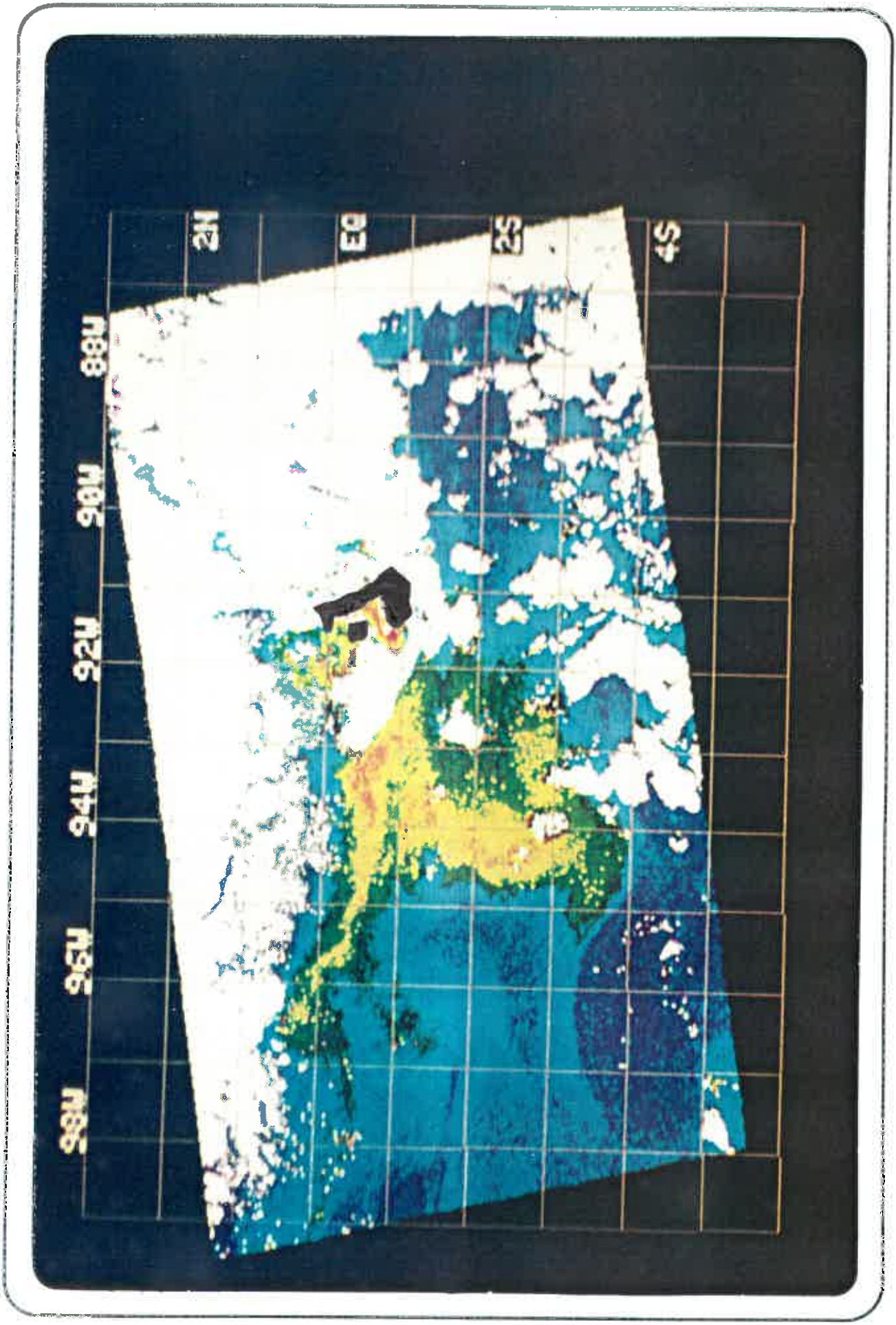
2N
EQ
2S
4S
88W
90W
92W
94W
96W
98W

Plate 4.10. Satellite ocean color image showing the distribution of phytoplankton pigments around the Galapagos Islands acquired on 24 November 1979 (Nimbus-7 orbit 5480). As in the previous scene, the locations of Fernandina and Isabela have been masked in black.

5S
10S
15S
20S
25S
30S
35S
40S
45S
50S
55S
60S
65S
70S
75S
80S
85S
90S
95S
100S
105S
110S
115S
120S
125S
130S
135S
140S
145S
150S
155S
160S
165S
170S
175S
180
175N
170N
165N
160N
155N
150N
145N
140N
135N
130N
125N
120N
115N
110N
105N
100N
95N
90N
85N
80N
75N
70N
65N
60N
55N
50N
45N
40N
35N
30N
25N
20N
15N
10N
5N
EQ

Plate 4.11. Satellite ocean color image showing the distribution of phytoplankton pigments around the Galapagos Islands acquired on 19 February 1979 (Nimbus-7 orbit 1638). The locations of Fernandina and Isabela Islands have been masked in black. Note the large, phytoplankton-rich (pigment concentrations greater than 1.0 mg/m3), eddy-like structure to the north of the archipelago.

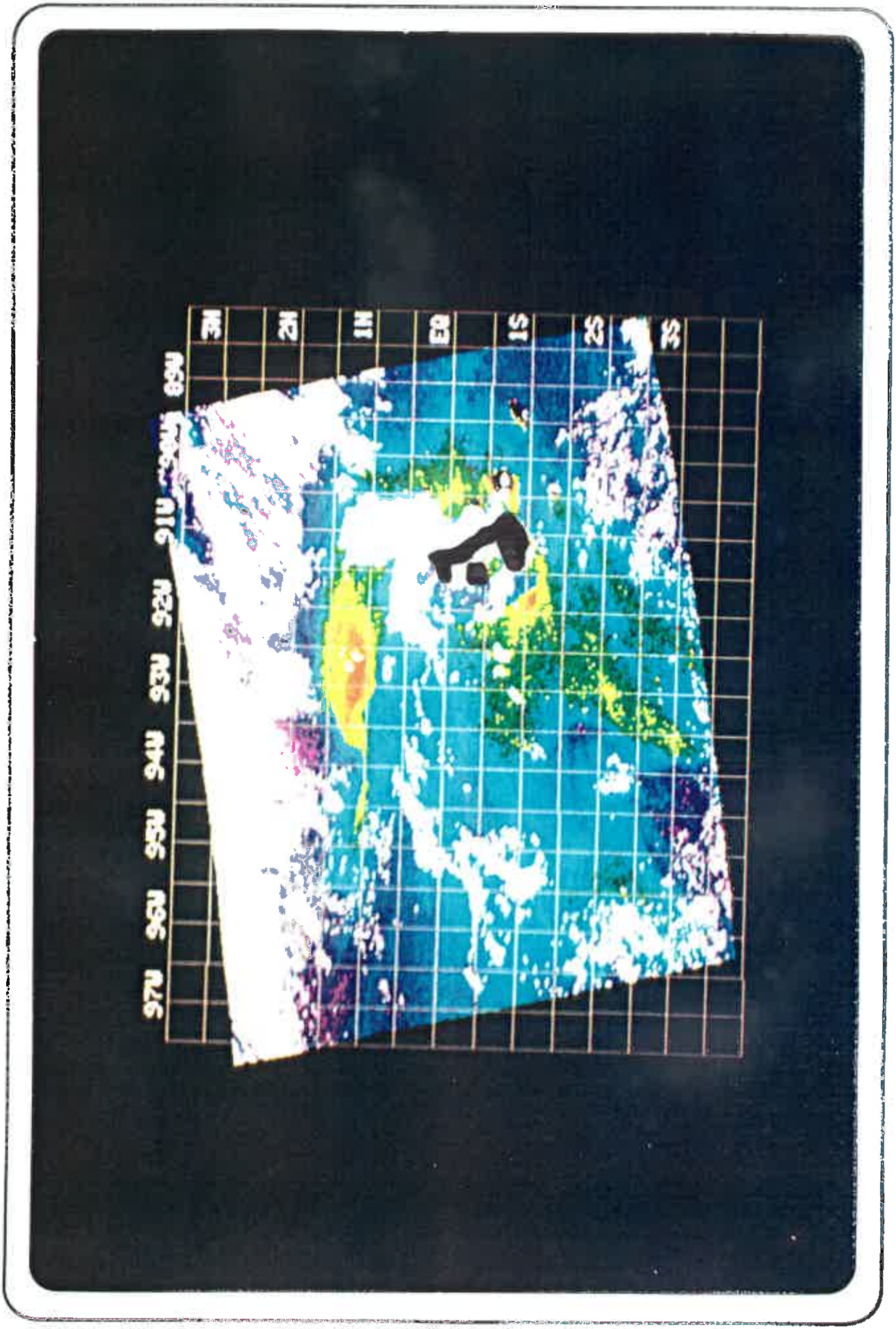

the possibility that the residence time in the plume may be longer than estimated because of the complex circulation patterns and numerous trapping mechanisms, including eddies that form on the downstream sides of islands (Hamner & Hauri, 1981; Wolanski et al., 1982). The topic of island plumes and wakes is of considerable interest both from a physical and biological perspective and deserves further study. An island plume model (Okubo, personal communication, 1985) is being developed which will make use of the satellite data to study the processes associated with plume formation and decay and to more fully assess the impact of islands and island groups on the productivity of the surrounding waters.

4.5. ECOLOGICAL IMPLICATIONS

The conditions for, and the unique character of, life on the Galapagos Islands are related to the oceanographic setting and the biological productivity of the surrounding waters. Variations in ocean conditions have profound effects on the biota of these islands, particularly during times of El Nino (e.g. Boersma, 1978). The results presented here and those of a recent investigation in which satellite ocean color observations combined with coincident oceanographic measurements demonstrated the tight coupling that exists between the distributions of phytoplankton populations around the Galapagos Islands and the oceanographic

conditions observed during the 1982-83 El Nino (Feldman et al., 1984). The reversal of winds and ocean currents during February-March 1983 was associated with a major redistribution of food resources around the archipelago. The mean pigment concentrations of the nine mesoscale sampling regions presented in Figure 4.9 clearly document this change. The dramatic increase in pigment concentrations in the eastern half of the archipelago (regions 4,5,7,8) that were observed on 28 March 1983 were accompanied by a significant decrease in pigment concentrations to the west of Isabela (regions 1 & 2). This redistribution, combined with a decrease in primary productivity of the region (Barber & Chavez, 1983), might explain the observed reproductive failure of seabirds and marine mammals on the Galapagos Islands during this El Nino.

The evidence of the dramatic effect El Nino has on the distribution of phytoplankton, and the close correlation found between the prevailing oceanographic and meteorological conditions and the patterns of plankton distribution observed under non-perturbed conditions as well, raises some interesting ecological questions. The satellite images not only provide information about the magnitude of biological production taking place in the waters around the Galapagos, but also provide a means to study the persistance and spatial variabilty of this production. It has been shown that for the marine life in the Galapagos, the patterns of upwelling are instrumental in

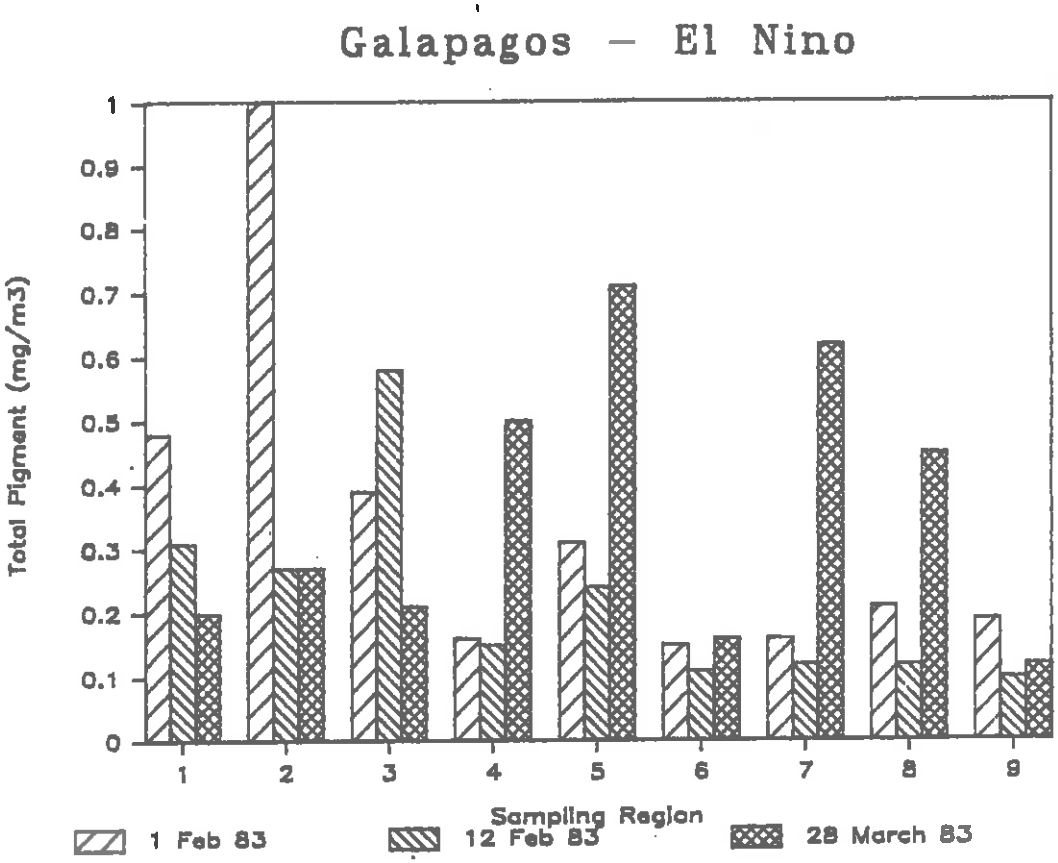

Figure 4.9. Mean phytoplankton pigment concentrations (mg/m3) for each of the nine mesoscale sampling regions computed from three Coastal Zone Color Scanner images of the Galapagos Islands acquired during the 1982-83 El Nino. Note the changes that occurred between the western (region 2) and eastern (regions 5 and 7) regions during this phase of El Nino.

maintaining the lower trophic levels which in turn supply the higher carnivores (e.g. seabirds and marine mammals) with food (Maxwell, 1974). How organisms can adapt to an environment in which food resources are extremely variable in both time and space is the subject of much ecological research. The results presented here may provide some previously unavailable information about the variability of those resources.

It is important to keep in mind that satellite-derived pigment concentrations are an indicator of phytoplankton biomass, and not necessarily a direct indicator of the abundance of organisms at higher trophic levels. What is evident in the satellite images is that the regions of enhanced primary production are often separated from the generally less productive oceanic waters by sharp frontal zones. It has been shown that frontal regions play a significant role in the ecology of many marine organisms. Frontal regions and eddies are areas where zooplankton, squid, and fish often congregate (Owen, 1981). In fact, many seabirds feed effectively only when their prey have been concentrated, as is the case along frontal zones (Ashmole, 1971). More recently, Schneider (1982), using concurrent bird and oceanographic data, presented quantitative evidence of seabird aggregations along fronts.

Perhaps it is the persistence of regions of high primary production, rather than the absolute magnitude, that is important to the higher trophic levels. The short-term (days-weeks) spatial

variability evident in the satellite-derived pigment distributions is probably caused by changes in winds and tides and small fluctuations in the strength and direction of current flows. While a region of high production may move about some central position in response to physical processes, its mean location remains relatively stable over longer time scales (weeks-months). The short-term variability observed in the three December 1978 CZCS images of the Galapagos Islands is an excellent example of this variability. However, when significant changes in the patterns of production take place over a relatively short period (as described in Feldman et al., 1984), one could expect to see significant effects on organisms at higher trophic levels.

The catastrophic failure of seabirds and marine mammals during El Nino has been well documented (Schreiber & Schreiber, 1983; Limberger et al., 1983); researchers pointed toward a disruption in the normal food web and the disappearance of the small fish and squid which were the usual prey for these species as the prime cause. Short-term growth fluctuations for several species of seabirds on the Galapagos Islands have been related to the availability of food resources (Rickleffs, personal communication, 1983). During the breeding season the foraging range of many species of seabirds is very limited, leaving the birds susceptible to any major redistribution of food. Breeding strategies, particularly the location of nesting colonies and the season in which breeding occurs, have been optimized over many

generations through natural selection (Boersma, 1978); therefore, the long-term environmental conditions at a particular location will determine the suitability of that site. When environmental conditions change dramatically, as during the 1982-83 El Nino, populations that are tied to specific locations and are unable to adjust to short-term geographic redistribution of food resources may suffer reproductive failures.

A recent investigation (Papastavrou, personal communication, 1985) in which the distribution, abundances, and behavior of sperm whales around the Galapagos Islands were studied, surprisingly suggests that the distribution of whales in this region may in some way be correlated with the patterns of phytoplankton distribution observed in the satellite images. Sperm whales appeared to be concentrated in the waters to the west of Isabela and Ferandina and moved in a generally north and south direction. The historical whaling records generally confirm these findings and often reported that the largest concentrations of whales were found off the northwest tip of Isabela. One example is given by Melville (1856) in which he states that

> "...large fleets of whalemen cruised for spermaceti upon what some seaman call the Enchanted Ground... off the great outer isle of Albemarle (Isabela).."

The northwest tip of Isabela is the location of what appears to be the sharpest and most persistant feature of this region, the

Galapagos Front (Hayes, 1985). What is particularly interesting is the fact that the whales very rarely went much beyond the northern or southern flanks of the island and appeared to restrict their movements to within a region very similar to the plankton-rich zone west of Isabela as seen in the December 1978 and November 1979 CZCS images. This observation is at first somewhat surprising because sperm whales are subsurface feeders, often diving to depths of several hundred meters to feed on squid. It seems unlikely, at first consideration, to think that the near-surface plankton distributions would influence the distributions of such subsurface creatures as squid and eventually whales. But as has been shown by Bowman et al. (1982), dense aggregations of euphausids (krill) often occur in regions of enhanced phytoplankton production, particularly where sharp frontal zones are found. These swarms of krill and other small fish feeding at the same trophic level are a major food source for such creatures as tuna (Sette, 1955) and squid. There is evidence (Papastavrou, personal communication, 1985) of such dense aggregations of either euphausids or possibly myctophids in the regions around the Galapagos where the whales were most abundant. It may be possible to demonstrate more clearly the relationship between CZCS-derived phytoplankton distributions and the distributions and abundances of sperm whales around the Galapagos when more recent CZCS data, coinciding with the whale survey are analyzed.

CHAPTER 5

THE STRUCTURE AND VARIABILITY OF THE PISCO UPWELLING

In this chapter the processes and variability of coastal upwelling are discussed using satellite-derived ocean color and sea surface temperature images as well as wind records for the Pisco upwelling region. The patterns of phytoplankton distribution observed in the satellite images are compared with past observations and the applicability of coastal upwelling theory are discussed in light of the satellite findings. The ability of the CZCS to quantify the short term variability of a coastal upwelling sysytem will be demonstrated. In particular, a major wind reversal in which upwelling favorable conditions were replaced by onshore flows drastically altering the near-surface phytoplankton pigment concentrations.

5.1. THE STUDY AREA

One of the most extensively studied regions of intensified upwelling, and the one from which most of our knowledge about the structure and dynamics of a coastal upwelling system was derived, is located at approximately 15°S along the Peru coast (Figure 5.1). This region was the focus of the Coastal Upwelling Ecosystem Analysis JOINT II expeditions which conducted intensive

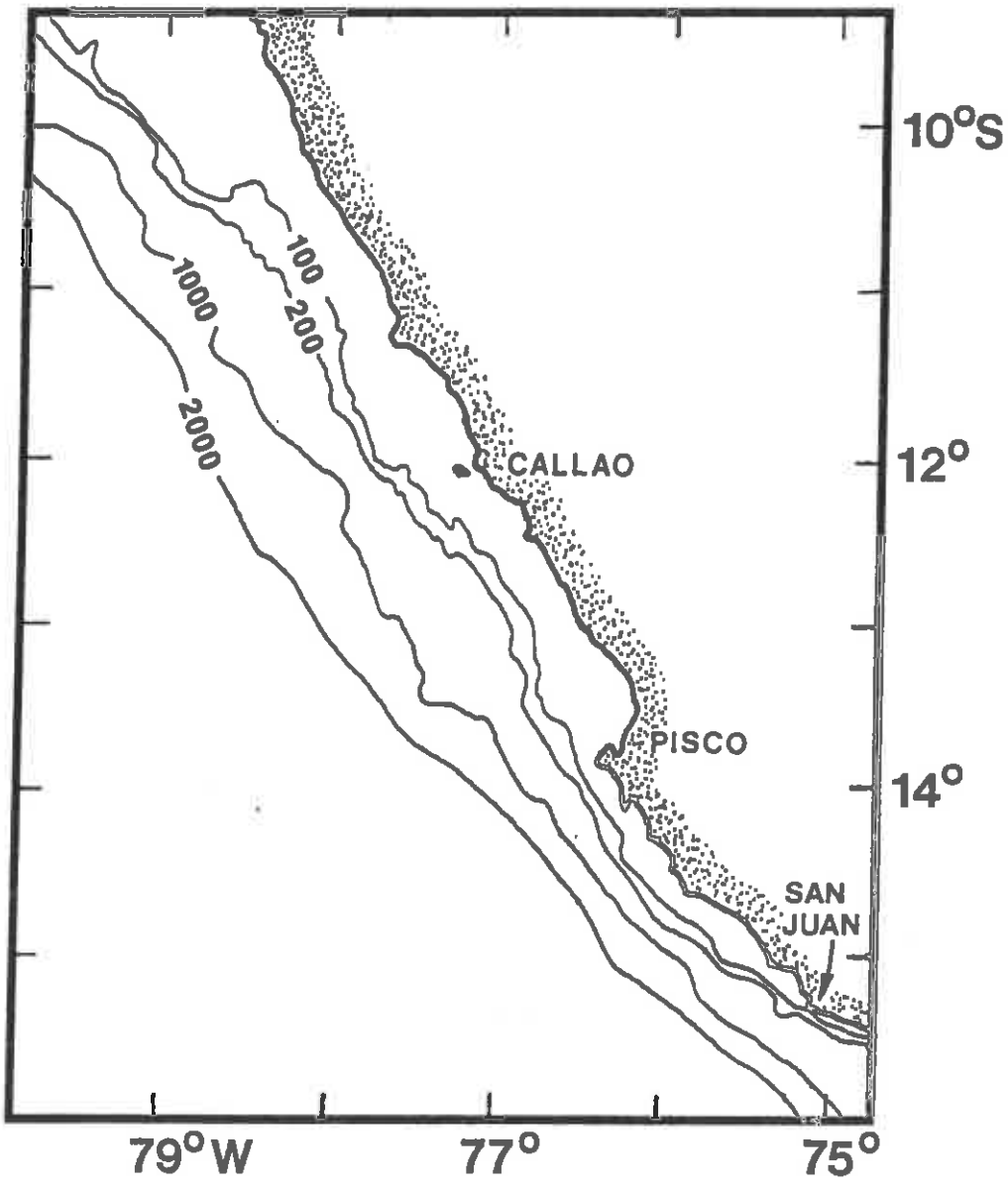

Figure 5.1. Map of the southern Peruvian coastal region. The 100-, 200-, 1000-, and 2000 fathom (183-, 366-, 1830-, and 3660 meter) isobaths are shown. Note the change in coastal orientation that occurs around Pisco.

physical (Brink et al., 1981), chemical (Codespoti, 1983), and biological (Barber et al., 1978) sampling between 1976 and 1977. Although aircraft mapping of sea surface temperature distributions was a part of the JOINT II sampling program, these observations as well as those that were obtained during the intensive ship surveys were generally restricted to within 100 km of the coast. The satellite images presented in this chapter are, therefore, the first large-scale synoptic picture of this region and provide observations with which the results and conclusions derived from the JOINT II expeditions may be compared.

Coastal upwelling (Barber & Smith, 1981) is the process in which surface waters are transported offshore by oceanic and atmospheric forcing mechanisms and are replaced by cold, generally nutrient-rich subsurface waters. The combination of enhanced nutrient supply and favorable light regime for phytoplankton growth in the stabilized surface divergent flow often results in high levels of phytoplankton production. This enhanced primary production supports large populations of organisms at higher trophic levels (fish, birds) and is responsible for the legendary biological richness of coastal upwelling regions. There is ample evidence to support the hypothesis that the intensity and location of coastal upwelling is controlled predominantly by topography and surface wind stress. While broad bands of meridionally oriented upwelling may occur, it is more common to find isolated regions of intense upwelling, or upwelling centers. These centers of

intensified upwelling often are associated with coastal irregularities (Jones et al., 1983). It is well known that topographic features such as headlands or capes exhibit regions of intensified upwelling on their equatorward sides. Submarine topography also plays an important role in determining the location of upwelling (McClain et al., 1984) and upwelling centers as demonstrated by the results of both numerical (Preller & O'Brien, 1980) and experimental models (Maxworthy et al., 1985).

Alongshore variations in wind strength also are important in producing regions of enhanced upwelling. Not only is the strength of the wind significant, but the direction of the wind relative to the coastal orientation is of particular importance (Wooster & Sievers, 1970) since the offshore Ekman transport is a function of the wind stress component parallel to the coastal boundary. The orientation of the South American coast changes significantly between 14° to 16°S. To the north of this region the coastline runs approximately 328° while to the south its orientation is approximately 300°. Although several small capes (e.g. Cabo Nazca) are found along the coast between 15° to 18°S, the most prominent feature of this region occurs at 14°S where the coastline changes direction. It seems possible that this change in coastal orientation plays a significant role in determining the patterns of phytoplankton distribution observed in the satellite images.

5.2. DESCRIPTION OF AN ACTIVE UPWELLING EVENT

The wind speed and direction values (presented as wind vectors) recorded every six hours at Callao (12°S) for the first week in April 1979 (Figure 5.2, Enfield, personal communication, 1985) show that upwelling favorable winds were prevalent throughout this period. In addition, winds increased in strength from approximately 3 m/sec to nearly 6 m/sec during the 36 hours prior to the satellite overpass (approximately 1200hr.). Using oceanographic and meteorological observations to describe the various features of the mesoscale (weather event time scale) response of a coastal region over the continental shelf to variable wind forcing, Halpern (1976) found that the onset of strong, upwelling favorable winds off Oregon induced the vertical advection of cold, nutrient rich water along the coast with a time lag of 1 to 3 days. Similarly, Ikeda & Emery (1984) described the appearance of cold, newly upwelled water along the west coast of Vancouver Island within a day after the initial wind increase. During such an upwelling event, the region of coldest water propagated offshore at a speed of ~5-10 km/day. The increase in wind strength observed in Figure 4.2 would therefore be expected to intensify the offshore Ekman flow, driving the system into a state of active upwelling.

The CZCS-derived phytoplankton pigment distributions of the Pisco to Callao region acquired on 3 April 1979 are presented in

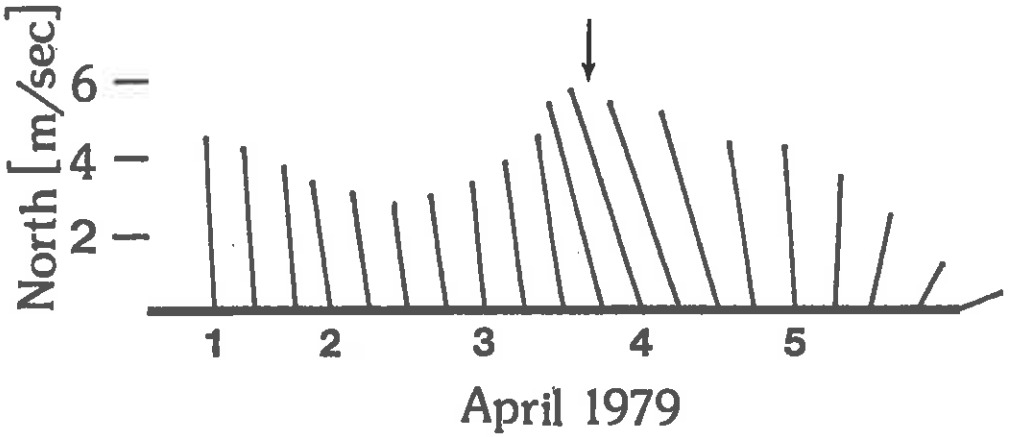

Figure 5.2. Wind speed and direction values recorded every six hours (0100, 0700, 1300, 1900 hrs.) at Callao (12°S) during the first week in April, 1979. North is upward and the ordinate provides a scale against which vector length may be related to wind speed. The arrow indicates the time of the 3 April 1979 satellite overpass.

Plate 5.1. Satellite ocean color image showing the distribution of phytoplankton pigments along the southern Peruvian coast from Coastal Zone Color Scanner data acquired on 3 April 1979 (Nimbus-7 orbit 2605). The coastline is masked in white along the right side of the image.

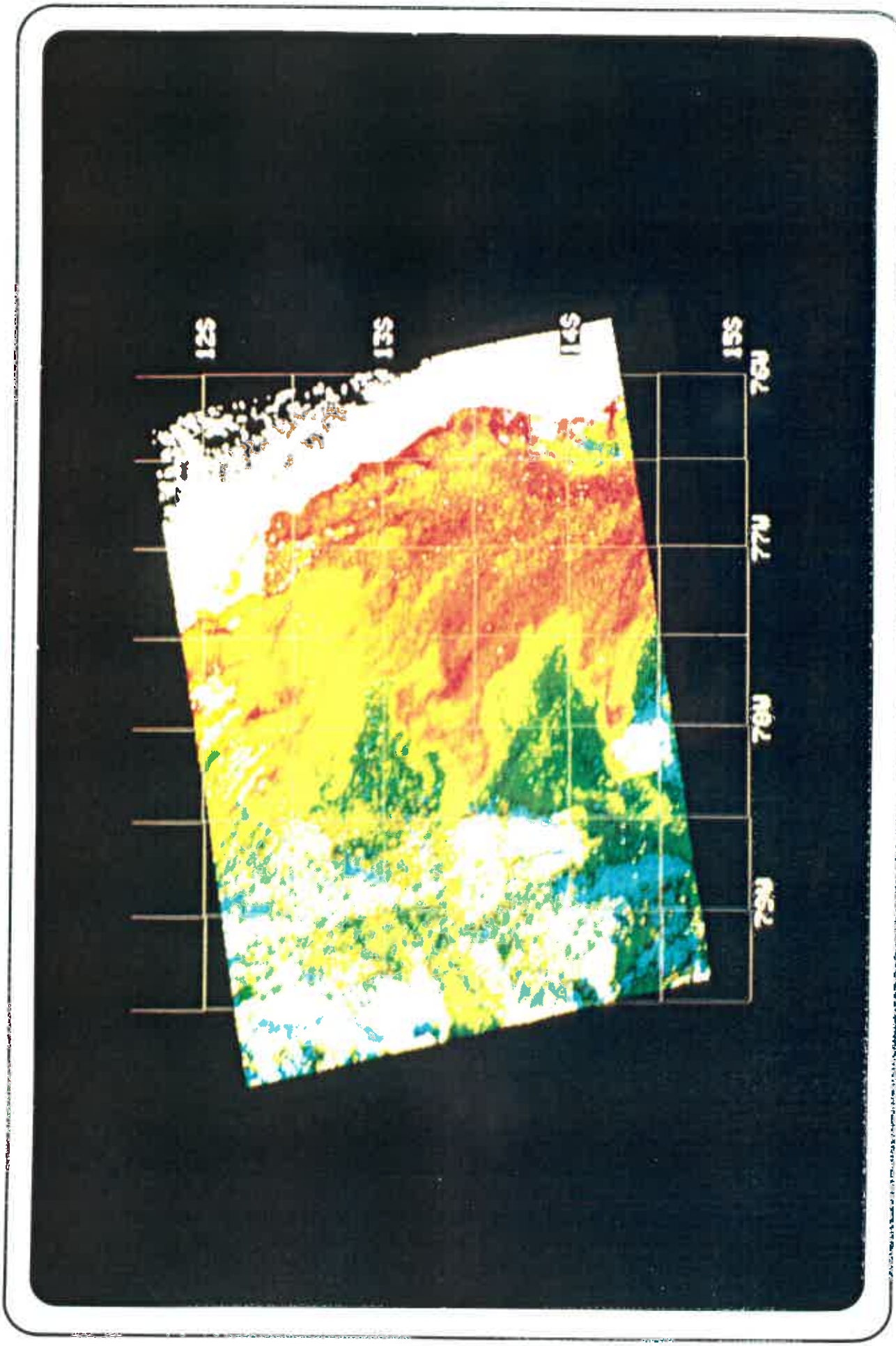
12S
15S
18S
21S
72W
74W
76W
78W

Plate 5.1. This image is presented at full resolution so that each image element (pixel) in the approximately 400 km x 300 km study area is displayed. By presenting the image in this way, with no filtering or subsampling of the data, many of the small scale features are resolved. The frequency distribution of pigment concentration vs. percent total cloud-free area derived from the CZCS image is given in Figure 5.3. The mean pigment concentration for the region covered by this image was 1.24 mg/m3 (SD = 1.64 mg/m3). The frequency distribution appears to be bimodal with the 1.0 mg/m3 separating the two lobes. Waters with concentrations greater than 1.0 mg/m3 covered nearly 40% (~25,000 km^2) of the total cloud-free surface area. The bimodal appearance of the frequency distribution may be a function of the way the data are presented (i.e. pigment concentration displayed on a log scale). As is discussed in the next chapter, however, the bimodality may actually represent the distinction between the low, oceanic phytoplankton concentrations and the more productive, plankton-rich coastal waters.

The satellite-derived sea surface temperature and phytoplankton pigment distributions indicate that the system was in a state of active upwelling at this time as indicated by the presence of cold (~16.9°C), newly upwelled water along the coast coinciding with a region of low pigment (~0.51 mg/m3) concentrations. This upwelling core which is seen in Plate 5.1 as a patch of light blue water, extends approximately 30 km from the

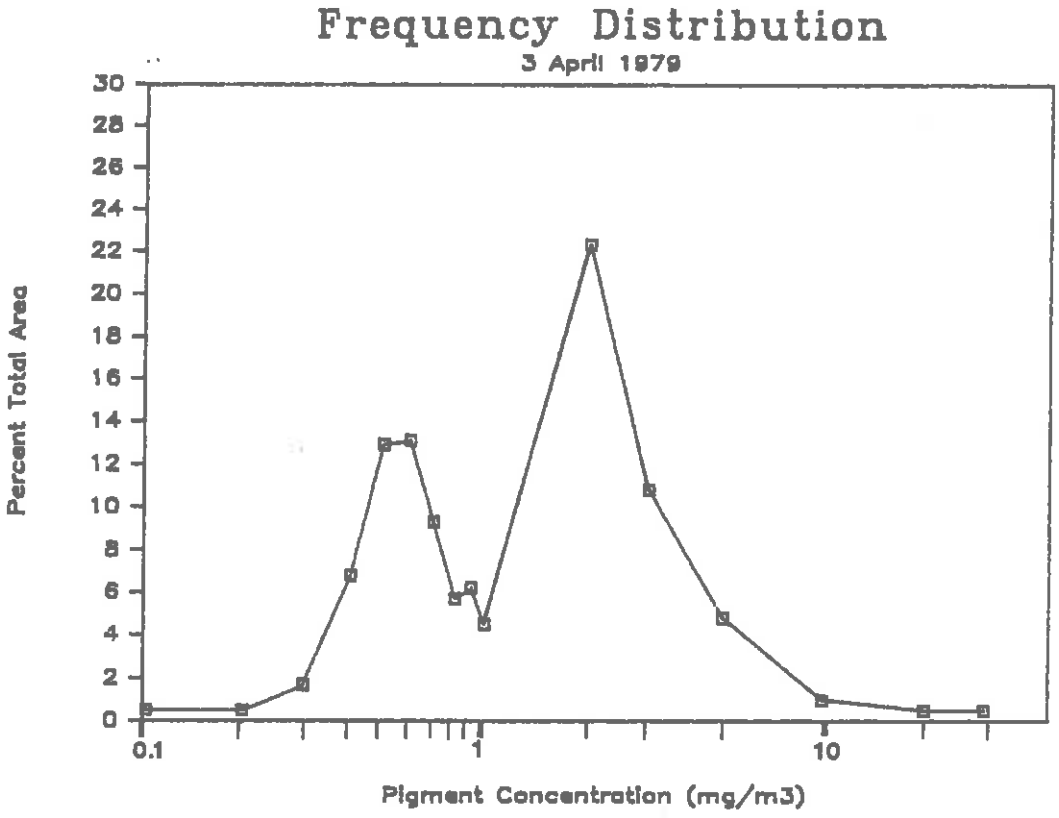

Figure 5.3. Frequency distribution of satellite-derived phytoplankton pigment concentrations (mg/m3) versus the percentage of total cloud-free surface area covered by each concentration range for the southern Peruvian coastal region seen in Plate 5.1. as observed by the Coastal Zone Color Scanner on 3 April 1979. Mean pigment concentration for the region is 1.24 mg/m3 (SD = 1.64 mg/m3).

coast and is centered at 14.25°S and 76.5°W.

Unfortunately, the CZCS data do not extend further to the south on this day and it is therefore not possible to determine the latitudinal extent of this newly upwelled water. Also evident in this image are two distinct plumes of pigment-rich water approximately 50 km in width which extend nearly 250 to 300 km from the coast. There is also an indication of a third, less clearly defined plume in the northern portion of the image. The southern edges of the plumes, particularly the southernmost plume, display sharp color fronts while the northern flanks appear scalloped, with numerous filaments of pigment-rich water intruding into less productive regions. The almost flame-like structure of these upwelling plumes is an indication that physical processes, perhaps coupled with exponential phytoplankton growth, rather than higher order biological factors such as grazing are responsible for the shape and offshore extent of the plumes. The structure of the pigment-rich streamers suggests that the middle plume may be an extension of the upwelling center described above (the region of low chlorophyll water to the south of Pisco). The southern plume may be an extension of the much studied upwelling center located at 15°S. Offshore waters containing pigment concentrations between 0.2-0.4 mg/m3 (blue) can be seen in the lower left portion of the image.

The variability in phytoplankton concentrations in the onshore/offshore direction is seen in Figure 5.4 in which the mean

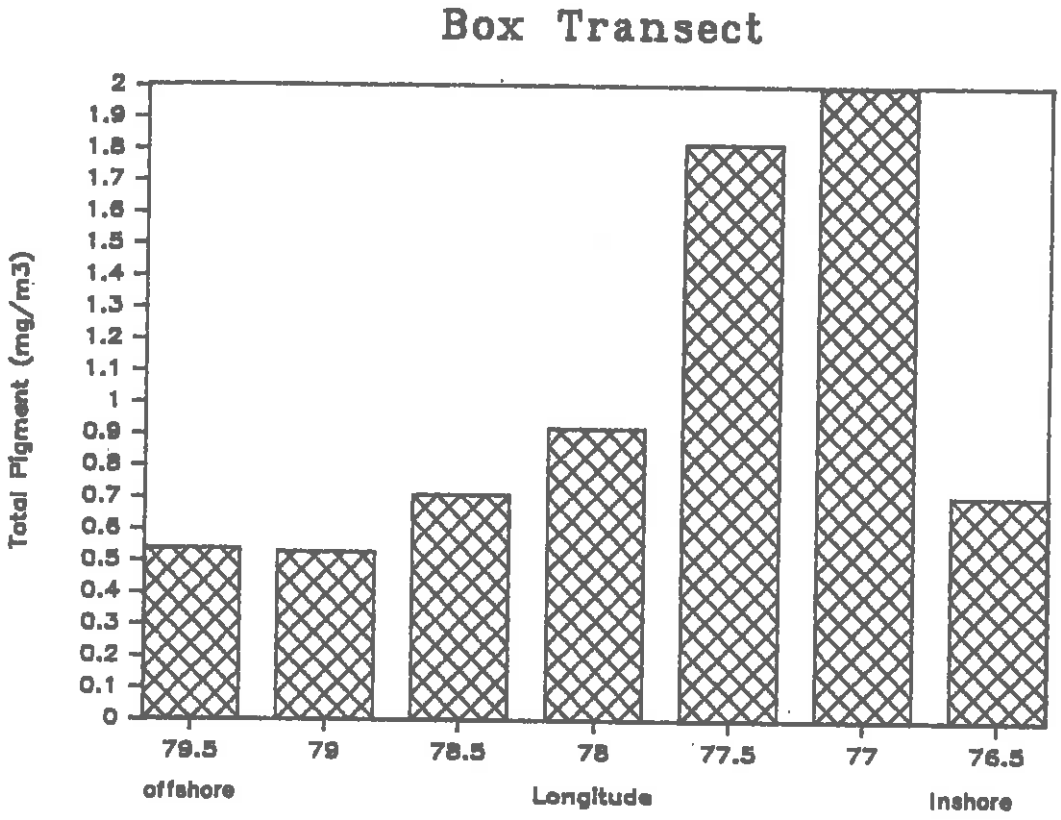

Figure 5.4. Mean phytoplankton pigment concentrations computed for 50 km x 50 km boxes along an east to west transect centered about 14.25°S derived from Coastal Zone Color Scanner data of the southern Peruvian coastal region acquired on 3 April 1979.

pigment concentration for 50 km x 50 km boxes were computed along an east to west transect centered about 14.25°S. The highest concentrations seem to occur between 50 to 150 km from the coast. The zone within 50 km of the coast in which the core of newly upwelled water is found is relatively low in phytoplankton biomass as are the waters offshore of the upwelling plume.

To examine the structure and variability of phytoplankton abundances within one of the upwelling plumes in greater detail, a transect along the major axis of the middle plume beginning at the core (14.25°S, 76.4°W) and extending to its offshore edge (13°S, 78.7°W) was performed on the CZCS image. This transect, in which pigment concentrations and sea surface temperatures (mean sea surface temperatures were computed for each 10 pixel interval along the transect) are presented as a function of distance from the center of the newly upwelled core (Figure 5.5) displays several major features. Specifically, the first 20 pixels (~17 km) of the transect are through the newly upwelled core. Pigment concentrations range between 0.4 and 1.0 mg/m3 and sea surface temperatures are generally below 17°C through this region. The second major feature is the distinct color and temperature front on the downstream edge of the core (pixels 20 to 30). An eight-fold increase in pigment concentrations occurs between pixels 20 an 24, a distance of ~3 km. This very distinct ocean color front is also seen in the patterns of sea surface temperature. The sharpest increase in sea surface temperatures

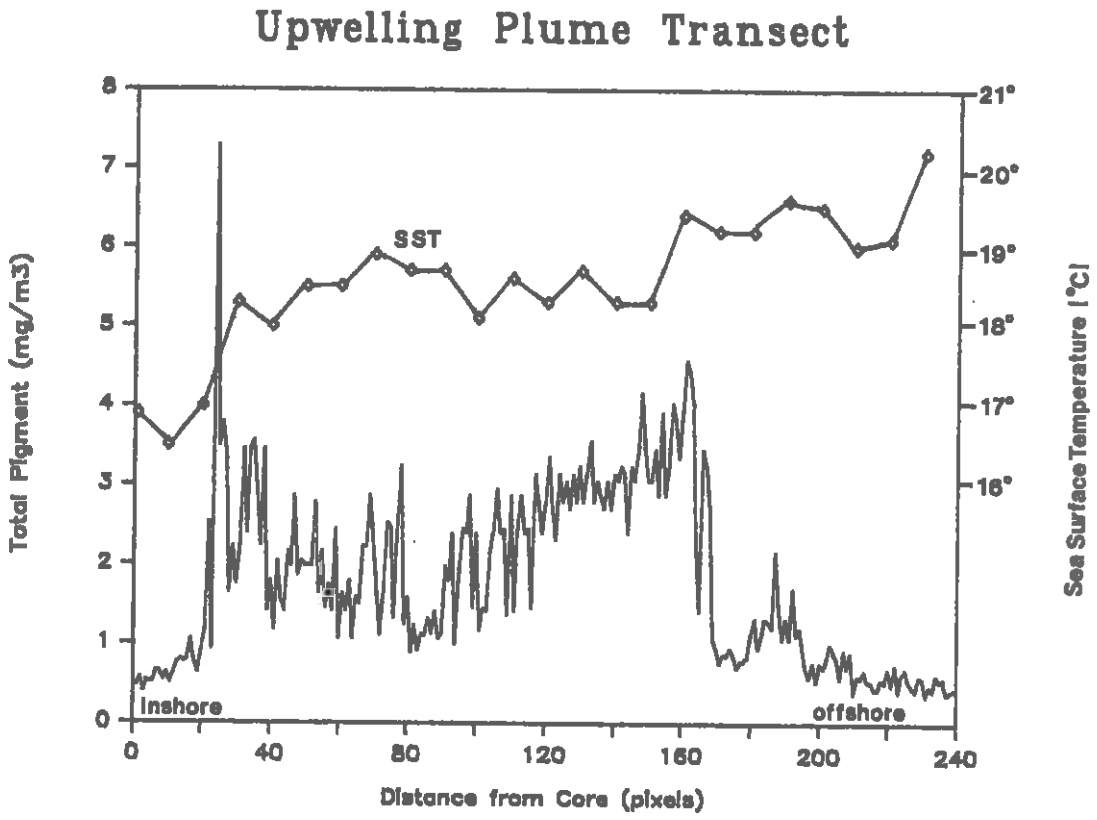

Figure 5.5. Satellite-derived phytoplankton pigment concentrations (mg/m3) and sea surface temperatures (°C) versus distance (1 pixel = .825 meters) along the major axis of the plankton-rich plume seen in the middle of Plate 5.1. beginning at the newly upwelled core (centered at 14.25°S, 76.4°W) and extending to the plume's offshore edge (approximately 13°S, 78.5°W) derived from Coastal Zone Color Scanner data of the southern Peruvian coastal region acquired on 3 April 1979.

(16.9° to 18.2°C) occurrs between pixels 20 and 30. A relatively narrow band (~20 pixels) of pigment-rich water is observed just downstream of the upwelling core. Beyond this region, pigment concentrations although variable, remained relatively high throughout the next 120 pixels (~100 km) increasing to a second peak (4.6 mg/m3) around pixel 160. Sea surface temperatures are fairly uniform along this portion of the transect (mean 18.4°C, standard deviation 0.26°C) and do not show the expected gradual increase in temperature with distance offshore. Another distinct color and temperature front occurs between pixels 160 and 170 where a sharp decrease in pigment concentrations roughly coincides with an increase in sea surface temperature (18.2 to 19.3°C). Seaward of this front and throughout the remainder of the transect, pigment concentrations are generally low and much less variable and are associated with waters warmer than 20°C.

5.3. SATELLITE IMAGE AND IDEALIZED UPWELLING CENTER: A COMPARISON

To test the extent to which the patterns of phytoplankton distribution observed in the satellite ocean color image agree with those predicted from classical upwelling theory and past observations, it is be useful to compare these patterns with the structure of an idealized upwelling center. This structure is

defined by a series of clearly defined zones in which specific changes in temperature, nutrient concentrations and phytoplankton biomass and productivity take place. The characterization of these zones, oriented along the axis of the upwelling plume are based upon the CUEA observations at 15°S is described by Jones et al. (1983) and more recently elaborated upon by MacIsaac et al. (1985) in which the physiological response of phytoplankton to changing conditions and distance along an upwelling plume had been observed. Figure 5.6 is a schematic of this idealized structure based upon Jones et al. and is the basis for the comparison with the satellite image. Zone 1 is the region of intense upwelling in which cold, nutrient rich water that is low in phytoplankton biomass is brought to the surface. In this zone of newly upwelled water, phytoplankton would be expected to be growing at below optimal rates. As the water in the shallow surface layer is carried downstream through Zone 2 away from the center of active upwelling, solar heating both warms and stabilizes it and the phytoplankton begin to adapt to the high nutrient concentations and near-surface light intensities. As a result, phytoplankton growth rates and nutrient uptake rates are increasing. As phytoplankton biomass increases, nutrient concentrations begin to decline. Zone 3 in this idealized structure is the region in which nutrients are being depleted and phytoplankton biomass is rapidly increasing to its maximum level. Further downstream is Zone 4 in which serious nutrient depletion has occurred and

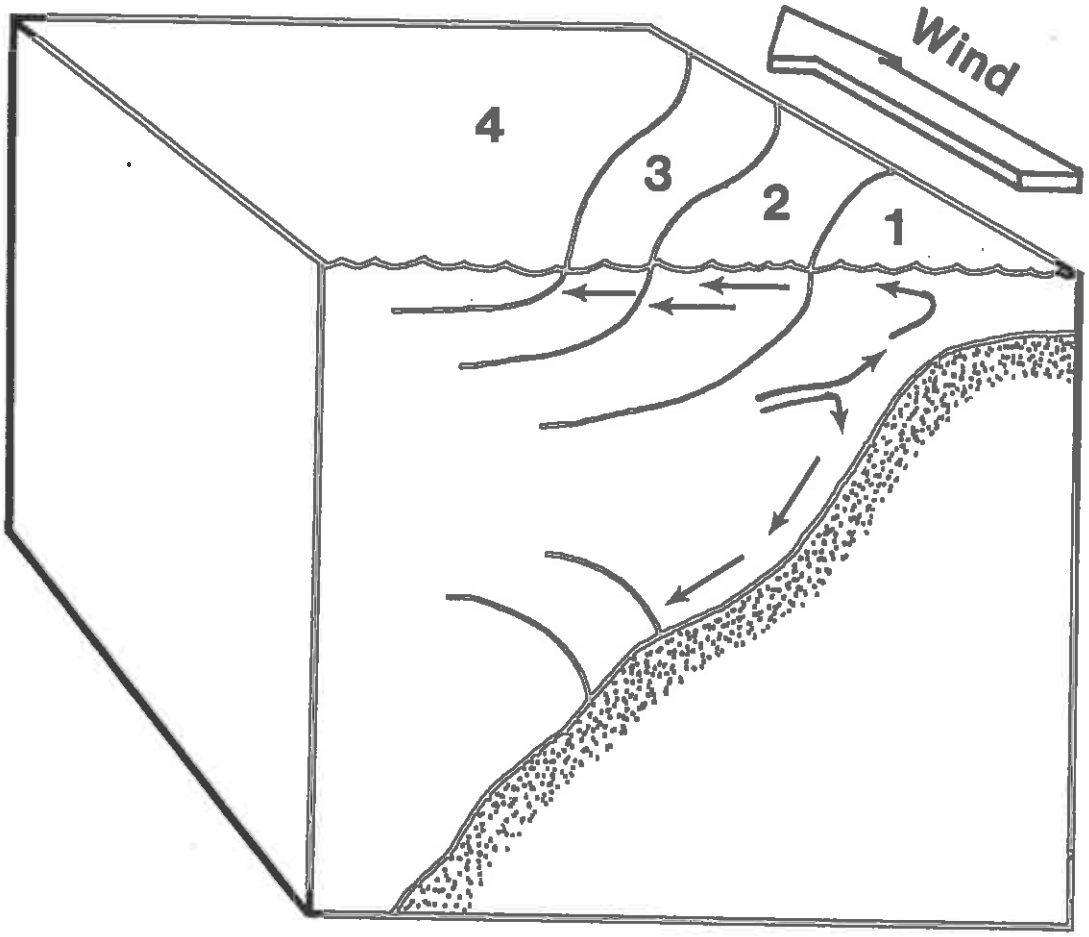

Figure 5.6. Schematic of the structure of an idealized coastal upwelling center in the southern hemisphere. The coastline is to the right and the arrows are hypothetical streamlines of the cross-shelf flow. Zones 1, 2, 3 and 4 represent the changing temperature-nutrient-phytoplankton relationships that occur during the offshore drift of the upwelled water (after Jones et al., 1983).

phytoplankton growth rates and biomass are declining relative to the preceeding zone. The change from enhanced biological productivity supported by the injection of newly upwelled nutrients to more oceanic conditions in which nutrients are supplied by primarily regenerative processes takes place in Zone 4. Because of its offshore extent, Zone 4 is the least described and most poorly sampled region but it is believed that the transition to more oceanic conditions is a gradual process (Jones et al., 1983).

How does this idealized structure of a coastal upwelling center compare with the patterns observed in the satellite ocean color image? Clearly, there are a number of features in the CZCS image which come close to those in the idealized structure. The newly upwelled core, characteristic of Zone 1, is clearly seen in both the temperature and pigment distributions. Its spatial extent and location at the 'upstream' end of the plume are consistent with both observation (e.g. MacIsaac et al., 1985) and theory (e.g. Jones et al., 1983). Zone 2, however, is less well defined although there does appear to be some evidence of a gradual increase in phytoplankton concentrations between pixels 10 to 20 (Figure 5.5). The rapid increase in phytoplankton biomass seen in the CZCS image as a band of pigment-rich water surrounding the newly upwelled core is representative of Zone 3 conditions. The offshore extent of the plumes of plankton-rich water as defined by the 1.0 mg/m3 contour, is nearly four-times that

observed during April 1977 (Walsh et al., 1980). In addition, the transition from enhanced to offshore levels of phytoplankton biomass (Zone 4) is rather sharp as opposed to the gradual transition into more oceanic conditions that are described in the idealized structure (Jones et al., 1983).

The temperature and pigment data presented in Figure 5.5 allow us to approximate the time scale of this upwelling event and to compare it with previous measurements. Observations presented by Boyd & Smith (1983) from data collected during April 1977 suggest that newly upwelled water in the ~20 m mixed layer would increase in temperature by about 0.4 C/day through solar input. The temperature rise (~1.2°C) between the core and the region defined as Zone 3 would suggest that the water at this distance offshore has been at the surface approximately 3 days. This time scale agrees well with that required to cover the distance from the core to the zone of highest pigment concentrations (~20 km) based upon the 5-10 km/day offshore propagation speed of the surface layer described by Ikeda & Emery (1984) off Vancouver Island, and observed in this region by Brink et al. (1980). Mean pigment concentrations increase by a factor of 3.8 from the core (0.69 mg/m3) to Zone 3 (2.6 mg/m3). Phytoplankton productivity measurements made within the Cabo Nazca upwelling plume (Barber et al., 1978) in which a growth rate of approximately 1.3 doublings per day was observed also support the 3 day time lag between Zone 1 (core) and Zone 3.

The plankton-rich plumes seen in the satellite image extend 200-300 km offshore. Codispoti (1981) and Boyd & Smith (1983) discussed the influence of nutrient limitation on the offshore extent of enhanced primary production. A nitrate concentration of 1.0 ug-at/l is the value often accepted as the threshold below which the effects of severe nutrient limitation become important. For the period discussed by Boyd & Smith, nutrient concentrations were above this threshold level until sea surface temperatures reached 19.5°C which occurred at about 110 km offshore. They hypothesized that above that temperature (i.e. further offshore) nutrients would be depleted and algal biomass would approach the background level of <1.0 mg/m3. Interestingly, the data presented in Figure 5.5 show a sharp decrease in phytoplankton abundance in the offshore region (~pixel 160) where the sea surface temperatures exceeded 19°C for the first time. Although the distance offshore at which this occured was nearly twice that described by Boyd & Smith, the similarities in temperature and pigment concentrations are striking.

A plot of individual sea surface temperatures versus pigment concentrations as well as mean temperatures and concentrations derived from 10 x 10 pixel boxes at nine locations in the onshore to offshore direction (Figure 5.7) reveals a pattern very similar to that described by Boyd & Smith (1982). Their results showed a maximum in chlorophyll concentrations (approximately 50 mg/m3 in their case) occurred at about 17.7°C, which is quite

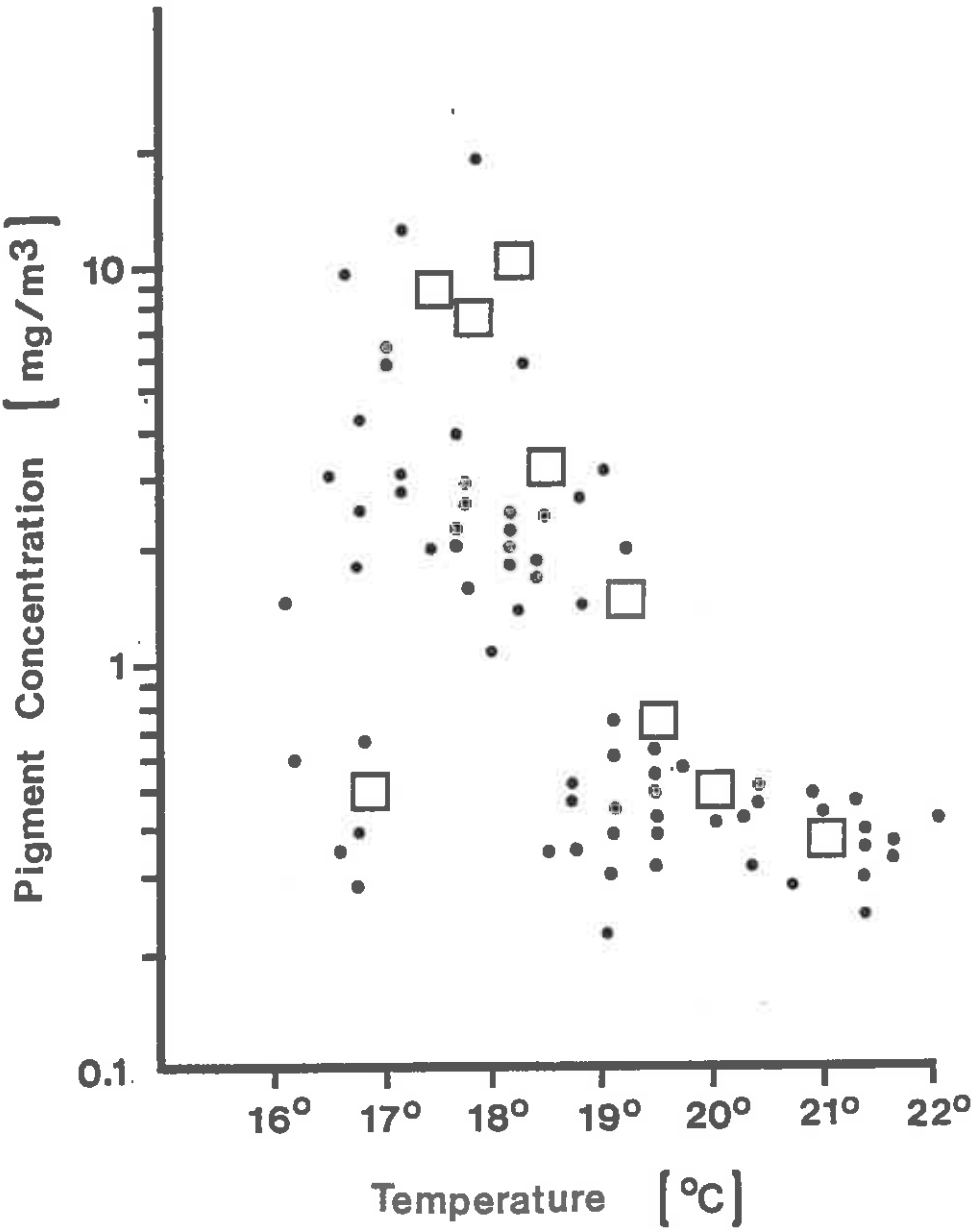

Figure 5.7. Scatter diagram of satellite-derived phytoplankton pigment concentrations (mg/m3) versus sea surface temperature (°C) from Coastal Zone Color Scanner data of the southern Peruvian coastal region acquired on 3 April 1979. The open squares represent the mean temperature and pigment values for 10 x 10 pixel boxes at nine locations throughout the region including the newly upwelled core (lowest sea surface temperature) and the offshore waters (highest sea surface temperature.

consistent with the results presented in Figure 5.7. They attributed the decrease in chlorophyll concentrations between 17.7°C and 19.5°C to increased grazing by zooplankton. As stated above, once temperatures exceeded 19.5°C they believed that nutrient limitation to phytoplankton growth became significant. What the findings described here indicate is that although there appears to be significant interannual variability in the magnitude of biological production, the pattern of phytoplankton production is remarkably constant. MacIsaac et al. (1985) reached a similar conclusion which they attributed to the physiological transformations that phytoplankton undergo as they are transported downstream in the upwelling plume.

5.4. SHORT TERM VARIABILITY OF THE PISCO UPWELLING

In the preceeding section, the structure of the Pisco upwelling region as determined from satellite ocean color data has been described. The remainder of this chapter focuses on the short-term variability of this coastal upwelling system. By comparing CZCS images of the Pisco upwelling region taken two days apart, the effect of a major wind reversal on the phytoplankton distributions and abundances is assessed.

5.5. THE WIND FIELD

Winds recorded every six hours at Callao from 20 March to 5 April 1981 (Enfield, personal communication, 1985; Figure 5.8), show the weather-event (3-5 day) variability in wind strength and direction experienced at this location. There are four distinct periods during which winds were upwelling favorable, one of which occurred during the 36 hours preceeding the satellite overpass on 1 April. However, in contrast to the intensification in wind strength which preceeded the 3 April 1979 image (from 3 to 6 m/sec) discussed in the previous section, winds were decreasing in intensity during this period (from 3 to 2 m/sec). Immediately after the 1 April satellite overpass, the winds shifted nearly 180° from an upwelling favorable (Southeast) direction to predominately onshore (Northwest). Along with this change in direction, there was an intensification in the strength of the wind so that at the time of the satellite overpass, on 3 April (~1200hr.), the wind was blowing out of the Northwest at approximately 5.5 m/sec.

5.6. THE SATELLITE IMAGES

The CZCS images acquired on 1 April (Plate 5.2) and 3 April 1981 (Plate 5.3) are presented at a different resolution from the 1979 image. These two scenes were subsampled along every other

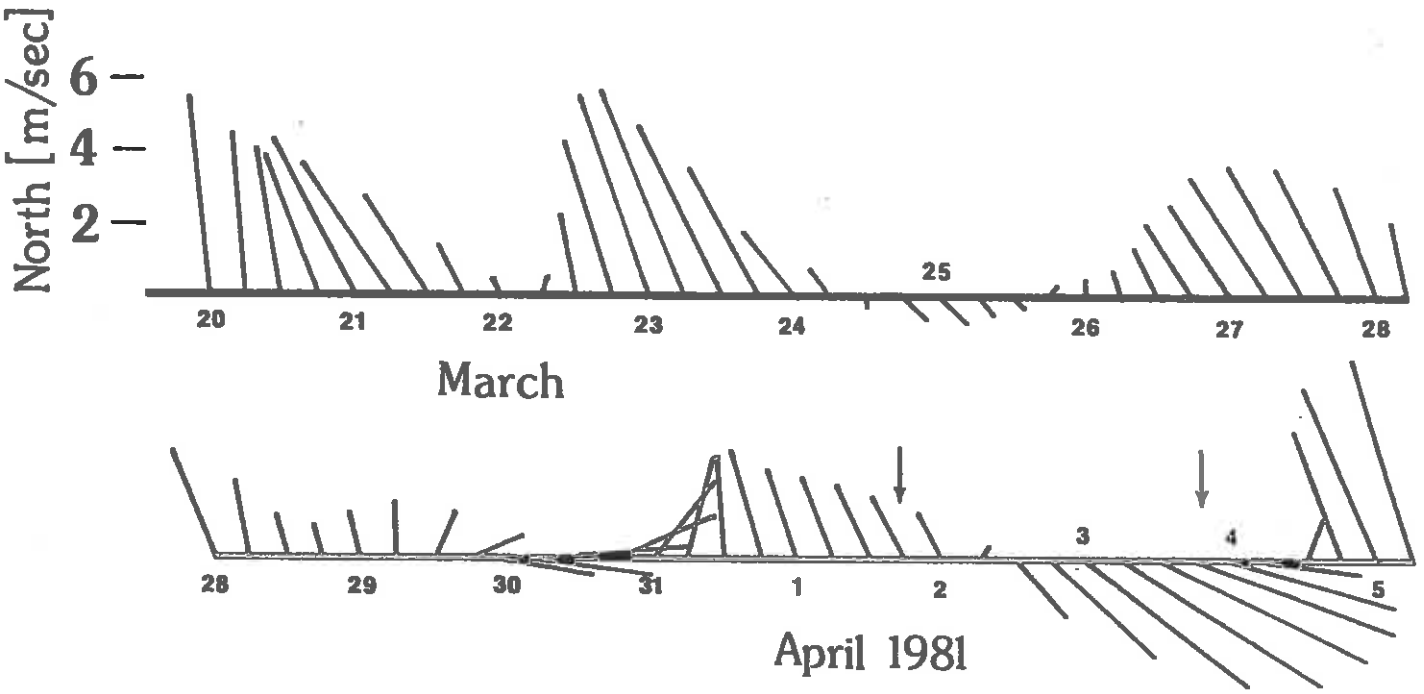

Figure 5.8. Wind speed and direction values recorded every six hours (0100, 0700, 1300, 1900 hrs.) at Callao (12°S) during late March and early April, 1981. North is upward and the ordinate provides a scale against which vector length may be related to wind speed. The arrows indicate the times of the 1 and 3 April 1981 satellite overpasses.

Plate 5.2. Satellite ocean color image showing the distribution of phytoplankton pigments along the southern Peruvian coast from Coastal Zone Color Scanner data acquired on 1 April 1981 (Nimbus-7 orbit 12306). The coastline runs diagonally through the center of the image.

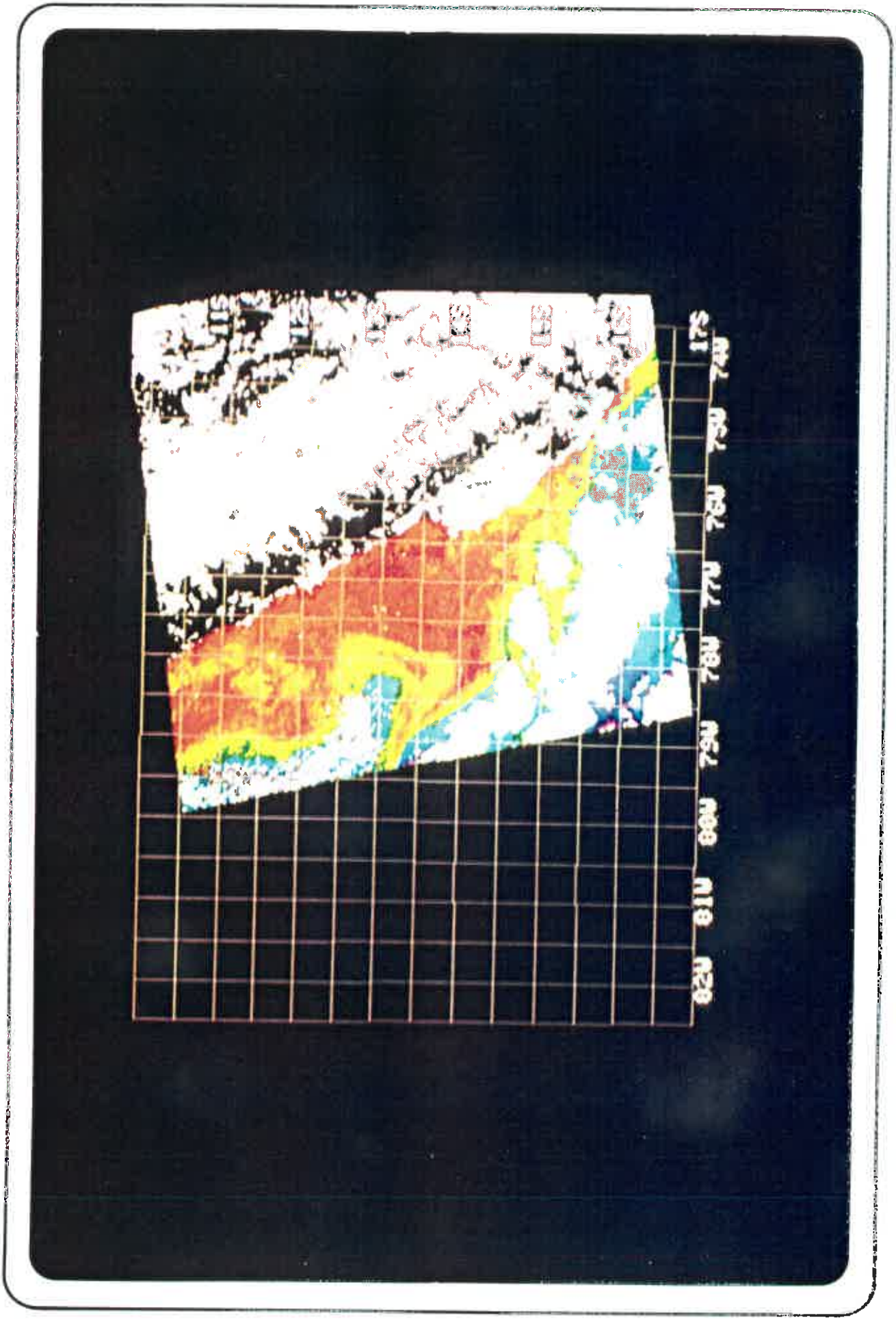
175
170
165
160
155
150
145
140
135
130

Plate 5.3. Satellite ocean color image showing the distribution of phytoplankton pigments along the southern Peruvian coast from Coastal Zone Color Scanner data acquired on 3 April 1981 (Nimbus-7 orbit 12334). The coastline runs diagonally along the right side of the image. A large cloud obscures the near-shore waters from Pisco to Callao. This scene has been remapped to the same spatial coordinates as the preceeding image.

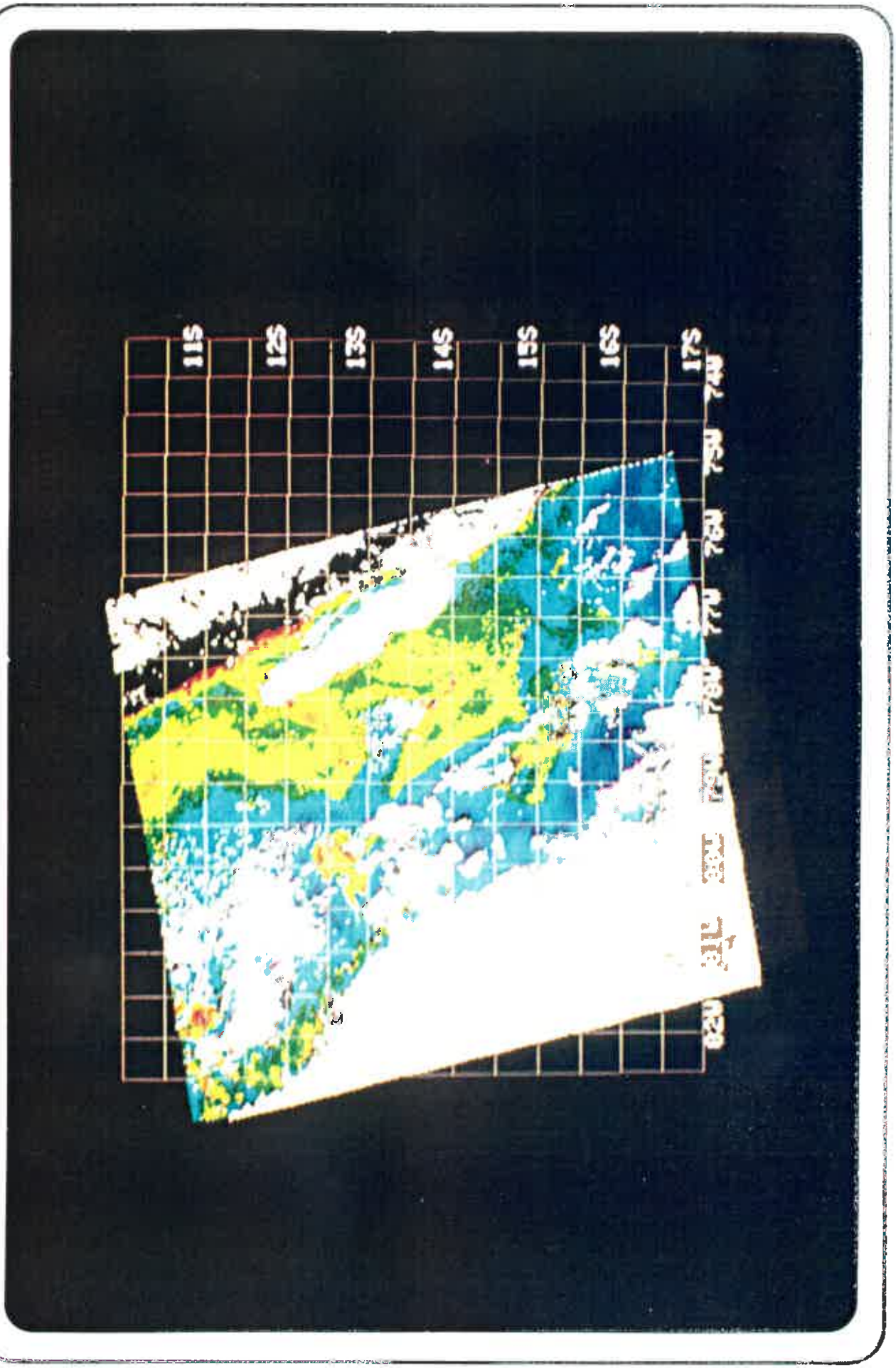
S1
S2
S3
S4
S5
S6
S7

pixel and line which enabled a larger geographic area to be displayed in a single image. The two images were then remapped to the same spatial coordinates as described in the Appendix so that statistical comparisons could be made. The apparent shift in image location between the two scenes is due to the fact that the satellite's ground track was further to the west when the 3 April data was collected.

The first thing that is apparent when comparing these two images is that a significant reduction in near-surface phytoplankton abundance occurred between 1 and 3 April. Frequency distributions of pigment concentration vs. percent total cloud-free surface area (Figure 5.9) derived from these scenes clearly illustrate this point. Mean pigment concentrations for the entire region decreased from 1.71 mg/m3 (SD = 1.53 mg/m3, n = 25,813 pixels) on 1 April to 0.68 mg/m3 (SD = 1.03 mg/m3, n = 24,947 pixels) on 3 April. Waters in which pigment concentrations exceeded 1.0 mg/m3 comprise nearly 70% (45,000 km^2) of the total cloud-free ocean surface in the 1 April image as compared with less than 7% (4,200 km^2) on 3 April.

Although overall phytoplankton abundances decreased significantly over the two days between the satellite passes, the patterns of phytoplankton distributions do not appear to have changed significantly. In both images, a broad band (150-350 km) of pigment-rich water extends along the coast from 10 - 15^{0}S. A large, plume-like structure centered about 14^{0}S is prominent

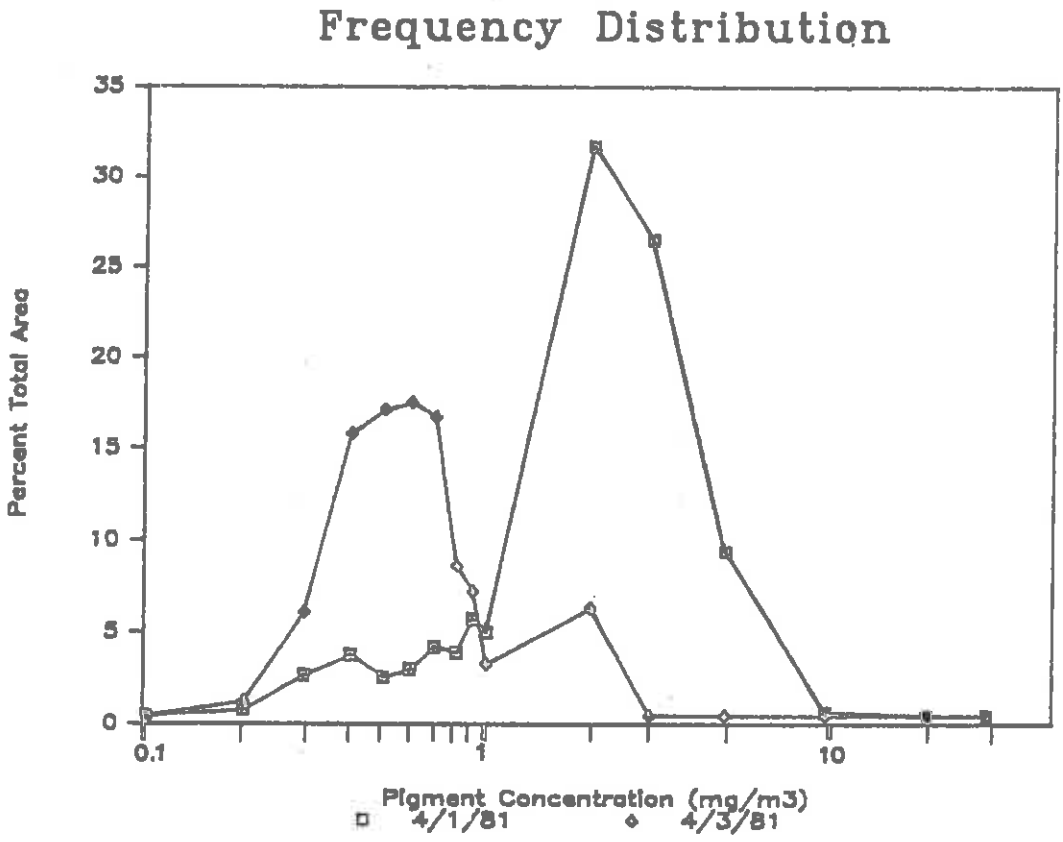

Figure 5.9. Frequency distributions of satellite-derived phytoplankton pigment concentrations (mg/m3) versus the percentage of total cloud-free surface area covered by each concentration range for the southern Peruvian coastal region seen in Plates 5.2. and 5.3. as observed by the Coastal Zone Color Scanner on 1 and 3 April 1981. Mean pigment concentration for the entire region decreased from 1.71 mg.m3 (SD = 1.53 mg/m3) on 1 April to 0.68 mg/m3 (SD = 1.03 mg/m3) on 3 April 1981.

in both images. These features, specifically the sharp color fronts that delineate the coastal/oceanic boundary are graphically represented in Figure 5.10 along with the approximate location of the 200 meter isobath. The band of plankton-rich water and the plume clearly extend beyond the continental shelf throughout most of the region. It appears, however, based upon these images and others that were examined but not included for detailed discussion, that the offshore extent of this band decreases as one progresses south along the coast below 14-15°S. For the April 1981 period at least, it seems as if the offshore extent of the zone of enhanced phytoplankton concentrations is influenced by the change in coastal orientation that occurs at 14°S.

The displacements of the most clearly defined color fronts and those least likely to have been influenced by cloud contamination are depicted in Figure 5.10. There appears to be little change in the locations of the fronts that are oriented in the alongshore direction. However, fronts which are oriented in an east-west direction, perpendicular to the direction of the rapidly shifting wind field, are displaced approximately 30 km to the south between 1 and 3 April. This southward displacement of the fronts, which is in sharp contrast to the typically northwesterly flow of the surface layer, most probably resulted from a change in near-surface current patterns associated with the wind reversal seen in Figure 5.8. Studies have shown that there are significant variations in flow associated with changing wind

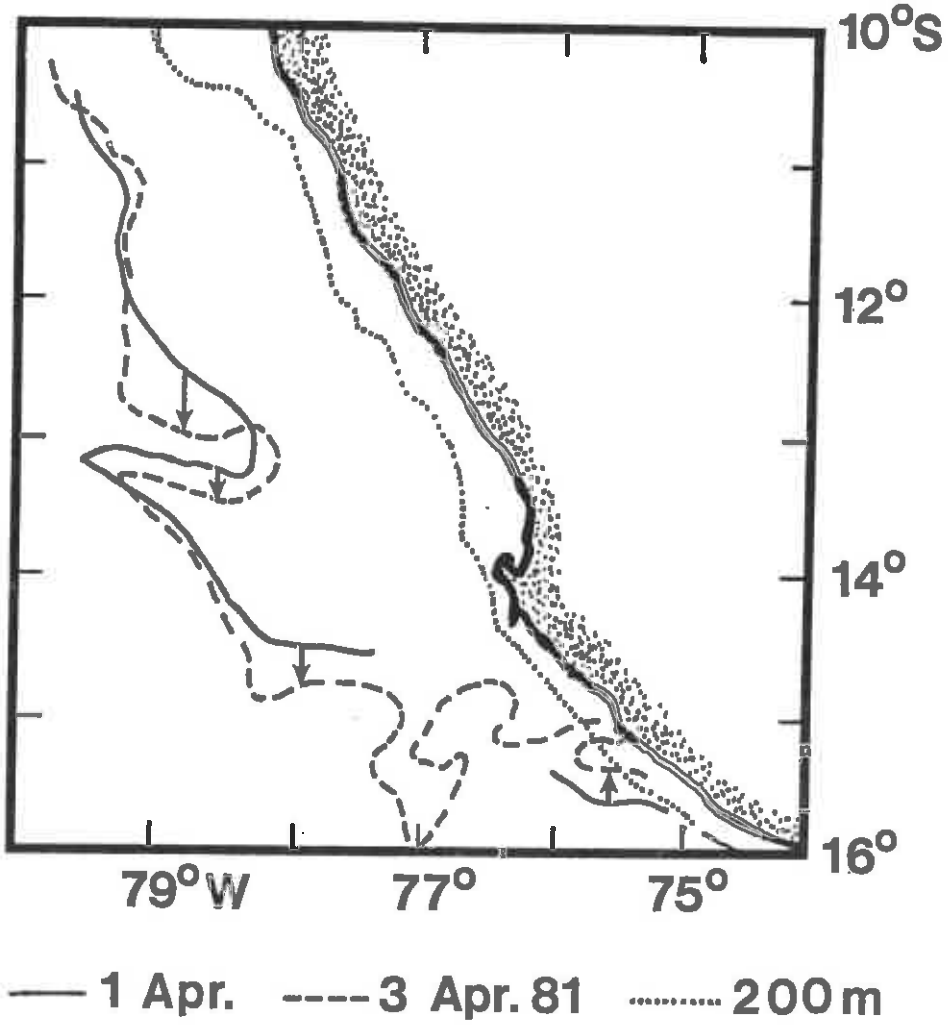

Figure 5.10. Graphical representation of the positions and displacements of the most clearly defined ocean color fronts seen in the Coastal Zone Color Scanner images of the southern Peruvian coastal region on 1 and 3 April 1981. The location of the 200 meter isobath (dotted line) marks the approximate offshore edge of the continental shelf.

forcing (Halpern, 1976) and with the passing of coastally trapped waves (Brink et al., 1981).

Significant reductions in near-surface (10 to 20m) chlorophyll concentrations after strong wind events off Peru have been reported by Walsh et al. (1980). Changes in water column flow patterns associated with the wind events were sufficient to dilute both the observed phytoplankton concentrations and those simulated in a 20m Ekman layer model of the Peru ecosystem by an order of magnitude at 15°S (Walsh et al., 1980). They reported that integrated chlorophyll concentrations decreased by 50 to 75 percent during the March and April 1977 wind events, and they concluded that horizontal advective losses of chlorophyll rather than just vertical mixing and dilution of phytoplankton beneath the euphotic zone were responsible for the reduction. The wind events discussed by Walsh et al. (1980) involved changes between calm periods and events of strong, upwelling favorable conditions, similar to the event that occured between 20 and 24 March 1981 (Figure 5.8). The wind event that took place between the times of the two satellite images presented in this section differed from the above in that a reversal in wind direction took place, rather than just a change in intensity.

While advective losses may have contributed to the decrease in overall phytoplankton concentrations that occured between 1 and 3 April 1981, it is more likely that increased vertical mixing associated with the wind reversal, reduced growth rates and losses

due to sinking were the cause. A typical mixed layer depth of 14.5m and euphotic zone depth of 18.7m have been reported for the Callao (12°-13°S) region (Guillen & Calienes, 1981). Increasing the depth of the mixed layer would significantly decrease the amount of light available for phytoplankton growth. Under such conditions, phytoplankton growth would no longer be able to compensate for loss of phytoplankton that sink rapidly out of the euphotic zone (Barber & Smith, 1981a). In addition to the physiological changes that the phytoplankton would undergo as a result of their transport to a region of lower light intensities, a mixing event of significant duration could reduce the chances of those phytoplankton ever being brought back into the near-surface environment and could result in the breakdown of the reseeding mechanism typical of coastal upwelling systems (Barber & Smith, 1981a). Phytoplankton that sink below the 40-80 m depth of entrainment for newly upwelled water (Barber & Chavez, 1983) would most likely be lost to the system.

The changes that occurred between the 1 and 3 April CZCS images are seen in the transects along 11 and 15°S. The 11°S transect on 1 April (Figure 5.11) shows inshore (0-25 pixels) and offshore (60-120 pixels) zones of pigment-rich water separated by what appears to be a 30 km wide intrusion of water with lower pigment concentrations. Phytoplankton concentrations remain very high in the nearshore waters on 3 April but the width of this band decreased. The offshore zone, as indicated by the

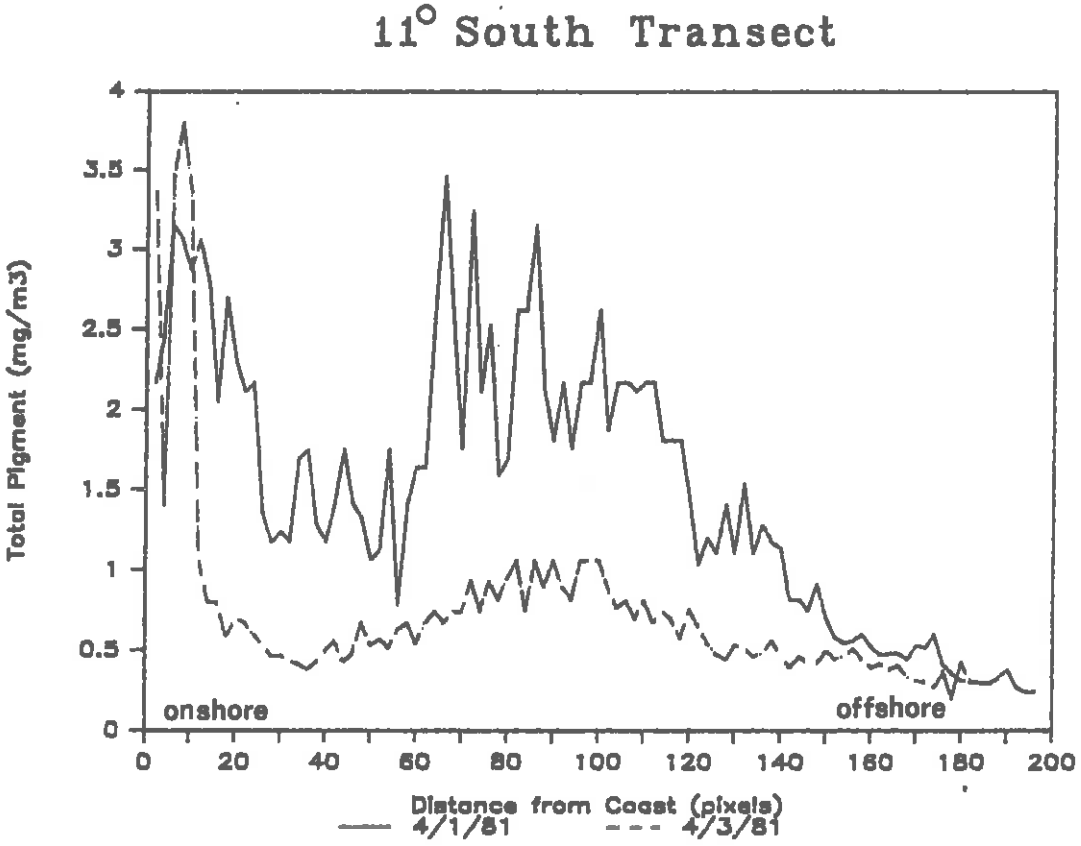

Figure 5.11. Satellite-derived phytoplankton pigment concentrations (mg/m3) versus distance (1 pixel = .825 meters) along 11°S derived from Coastal Zone Color Scanner data of the southern Peruvian coastal region acquired on 1 April (solid line) and 3 April 1981 (dashed line).

increase in pigment concentrations between pixels 60-120 is also seen on 3 April. Except for the extreme nearshore region, there was a 2-3 fold decrease in pigment concentrations along the transect between 1 and 3 April.

Along 15°S the changes are even more pronounced. The gradual decrease in phytoplankton concentrations progressing from the onshore to offshore waters on 1 April (Figure 5.12) is replaced by a relatively featureless distribution two days later. Overall mean pigment concentrations computed for the JOINT II study region decreased from 1.31 mg/m3 (SD = 1.11 mg/m3) on 1 April to 0.41 mg/m3 (SD = 0.35 mg/m3) on 3 April 1981. Close examination of the 1 April CZCS image (Plate 5.2) reveals the presence of what appear to be small plumes of pigment-rich water extending offshore from the two small capes between 15-15.5°S. The transect on 1 April is through the major axis of this plume while on 3 April the axis appears to have shifted slightly to the south.

The results of the CUEA research program clearly documented that physical processes are important in determining the observed variability in phytoplankton distributions within an upwelling region (Blasco et al., 1980). Although the satellite data presented in this chapter generally supports the CUEA findings, several new perspectives have been added. First, the satellite coverage provides a means by which the structure of the upwelling center at 15°S can be placed into its proper spatial

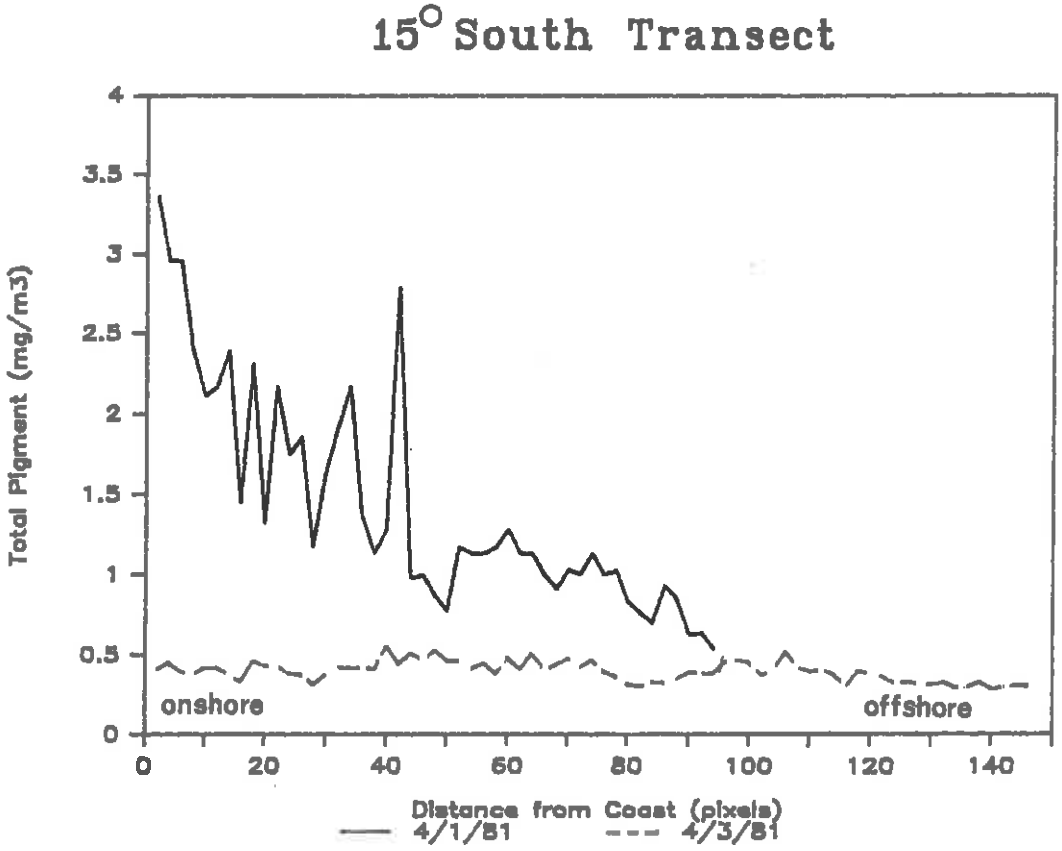

Figure 5.12. Satellite-derived phytoplankton pigment concentrations (mg/m3) versus distance (1 pixel = .825 meters) along 15°S derived from Coastal Zone Color Scanner data of the southern Peruvian coastal region acquired on 1 April (solid line) and 3 April 1981 (dashed line).

perspective. The nearly 300 km offshore extent of the plankton-rich plumes definitely broadens the scale of our concept of a narrow coastal upwelling zone (at least as defined by the biological consequences of coastal upwelling). The satellite data have also shown how short-term wind events can affect large regions along the coast and have documented how important surface observations (wind records in this case) are in the interpretation of satellite imagery.

CHAPTER 6

VARIABILITY OF THE PRODUCTIVE HABITAT IN THE EASTERN EQUATORIAL PACIFIC

In this chapter, the large-scale variability in phytoplankton distributions and abundances and the estimated primary production of the eastern equatorial Pacific are described. Individual CZCS images of the upwelling region along the western coast of South America which represent the major features of the phytoplankton distributions in this region are presented.

6.1. INTRODUCTION

There exists ample evidence supporting the link between ocean productivity and the intensity of upper ocean vertical motions (Thompson, 1981). Where these motions increase the vertical transport of nutrients to the surface waters, regions of enhanced biological production often result. This relationship has been demonstrated quite clearly for one of the most highly productive regions of the world's ocean, the coastal upwelling zone along the western coast of South America (Figure 6.1). Investigations relating changes in local winds, circulation, and the vertical distribution of density and nutrients to the patterns of enhanced biological production have shown that relatively small changes in

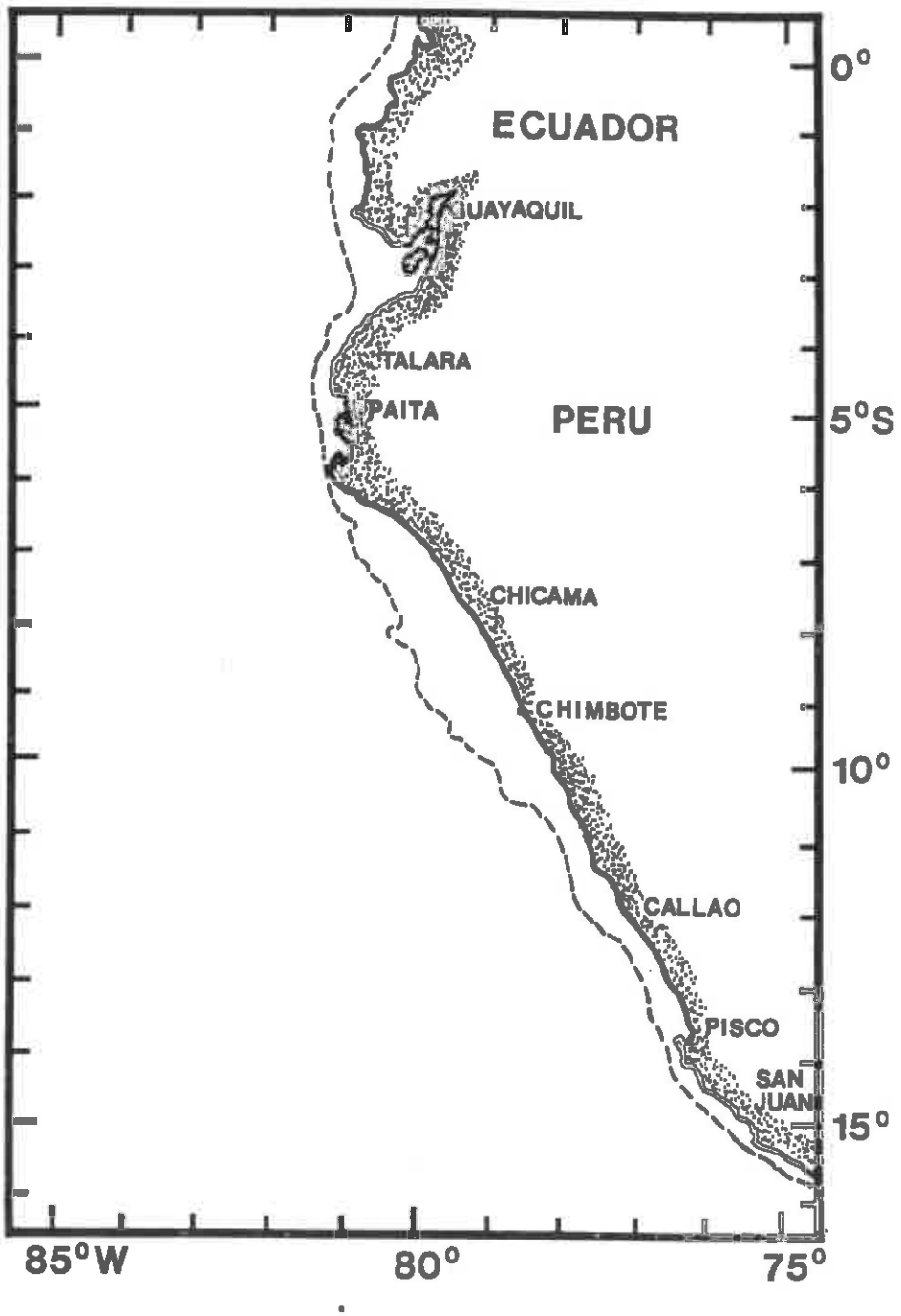

Figure 6.1. Map of the coastal upwelling regions of Ecuador and Peru. The location of the 200 meter isobath (dashed line) marks the approximate offshore edge of the continental shelf. Note that the shelf is broadest (approximately 130 Km) between 6° and 10°S.

the physical environment have large consequences for the ecosystem (Barber & Smith,1981; Smith et al.,1983). What is missing, however, is an understanding of the temporal and spatial scales of these processes and of the resulting variability in the distribution and abundances of phytoplankton. Not only do phytoplankton represent the first link in the food chain, but their patterns of distribution in time and space may provide clues as to how oceanographic processes regulate primary production (Yentsch, 1983).

The preceeding chapter discussed the structure and short-term variability of one major upwelling center along the southern Peru coast. This section focuses on a somewhat larger region covering the coasts of northern Peru and southern Ecuador and extending offshore to the Galapagos Islands. This northern region is of particular interest because of its proximity to the equator and consequently, is influenced by such features as the equatorial Front and the equatorial Undercurrent. One of the first scientific descriptions of this region was given by Schott (1931) in which the upwelling areas were classified using sea surface temperature, salinity and current observations. Love (1972) used the extensive EASTROPAC data set to describe the major physical, chemical and biological characteristics of the eastern equatorial Pacific. More recently, Lukas (1981) described the equatorial oceanic circulation patterns affecting this region, with particular emphasis on the equatorial Undercurrent and its

influence on the coastal upwelling area. A description of the hydrologic aspects of the main upwelling areas off Peru has been given by Zuta et al. (1978). Specific descriptions of the northern Peruvian upwelling area between 4° and 6° S (Fahrbach et al., 1981) and of the major upwelling center off Chimbote at 9°S (Guillen & Calienes, 1981) have described the general physical characteristics of these regions along with the observed variability in oceanographic, meteorological and biological conditions.

This chapter has two primary objectives. The first is to show that satellite ocean color data can be used to describe the major features of phytoplankton distribution as well as defining the spatial extent of the region of enhanced biological production, referred to here as the productive habitat, in the eastern equatorial Pacific. The second objective is to determine the degree of interannual variability in the areal extent of the productive habitat and in the estimated primary production of the region.

6.2. MATERIALS AND METHODS

Seventeen Coastal Zone Color Scanner images of the eastern equatorial Pacific were processed and remapped into two standard sampling grids so that statistical comparisons between images could be made and composite images produced. The 'coastal'

sampling grid encompassed the region from 2-10°S, 78.5-87.5°W. The larger 'basin-wide' sampling grid covered the region from 5°N-15°S, 74.4-94.5°W.

A method to delineate regions of enhanced biological production, making use of both the qualitative and quantitative information contained in the CZCS data, was developed. All the images were examined to determine the open ocean pigment concentration values for areas which were removed from probable coastal enhancement. Similarly, regions where the maximum gradients in pigment concentrations occured were also identified. These regions were generally associated with distinct mesoscale structures and features which could most likely be attributed to coastal or island induced processes. The images were then computer enhanced so that regions with values above and below a selected pigment concentration were clearly distinguishable. Setting the boundary at pigment concentrations between 0.8 - 1.5 mg/m3 generally produced images which satisfied the criteria described above. For this study, the 1.0 mg/m3 contour was selected as the most representative boundary separating the productive habitat from the open ocean region.

Recent work by Platt & Harrison (1985) has shown that in addition to this somewhat subjective choice of the 1.0 mg/m3 pigment contour as a means to distinguish between the productive coastal waters and the generally less productive waters further offshore, there may be biochemical evidence to support this value

as well. Their data show that the relationship between new to regenerated production saturates at nitrate concentrations of approximately 1.0 ugA/l NO_3. New production is defined as that production resulting from the injection of new nutrients into the euphotic zone (through upwelling, vertical mixing, diffusion), rather than that production supported by nutrients that have been recycled within the euphotic zone itself (Dugdale & Goering, 1967). Highly productive regions, of which upwelling systems are a good example, are characterized by the effective ratio of new production to total production being very high (roughly 80%; Platt & Harrison, 1985). In the Peruvian upwelling system, there is a general correspondance between the offshore 1.0 ugA/l NO_3 concentration and surface chlorophyll concentrations of 1.0 mg/m3 (Barber, personal communication, 1985). This relationship, when considered in light of the findings of Platt & Harrison (1985) tends to support the choice of the 1.0 mg/m3 pigment concentration contour as representing the approximate boundary between productive habitat and the open ocean region.

The selected boundary between oceanic and enhanced production also has significant ecological justification. Walsh et al. (1980) implied that chlorophyll concentrations of at least 0.7 mg/m3 would be required to satisfy the daily carbon demand of first-feeding anchovy larvae in the Peru upwelling system.

6.3. MAJOR FEATURES OF THE REGION

If monthly or seasonal composites are to be used to quantify large-scale interannual variability, it is first necessary to determine whether or not significant coherence in the distributions and abundance of phytoplankton exists in both time and space for the periods to be covered by the composites. Frequency distributions of satellite derived pigment concentrations represent one way of determining whether major changes in phytoplankton biomass have taken place from one period to the next. Changes in spatial distributions can best be assessed by a visual inspection of the satellite images. Accordingly, selected CZCS images of the eastern equatorial Pacific are described which document the major features of the region as well as those features characteristic of specific time periods.

A sequence of four CZCS images covering the region from 2° to 10°S and from 87.5° to 78.5°W are presented to document the patterns and variablity of phytoplankton abundances during the December 1978 through January 1979 period. Although this period appeared to be exceptionally cloudy, the major features of phytoplankton distribution can be seen. On 9 December 1978 (Plate 6.1) a plume of plankton-rich water nearly 100 km wide extends approximately 300 km to the northwest from Paita (5°S, Figure 6.1). A narrow (~10 km) band of high

Plate 6.1. Satellite ocean color image showing the distribution of phytoplankton pigments along the northern Peruvian coast from Coastal Zone Color Scanner data aquired on 9 December 1978 (Nimbus-7 orbit 642). The coastline is masked in black along the right side of the scene. This image has been remapped to the coastal sampling grid (see text for discussion).

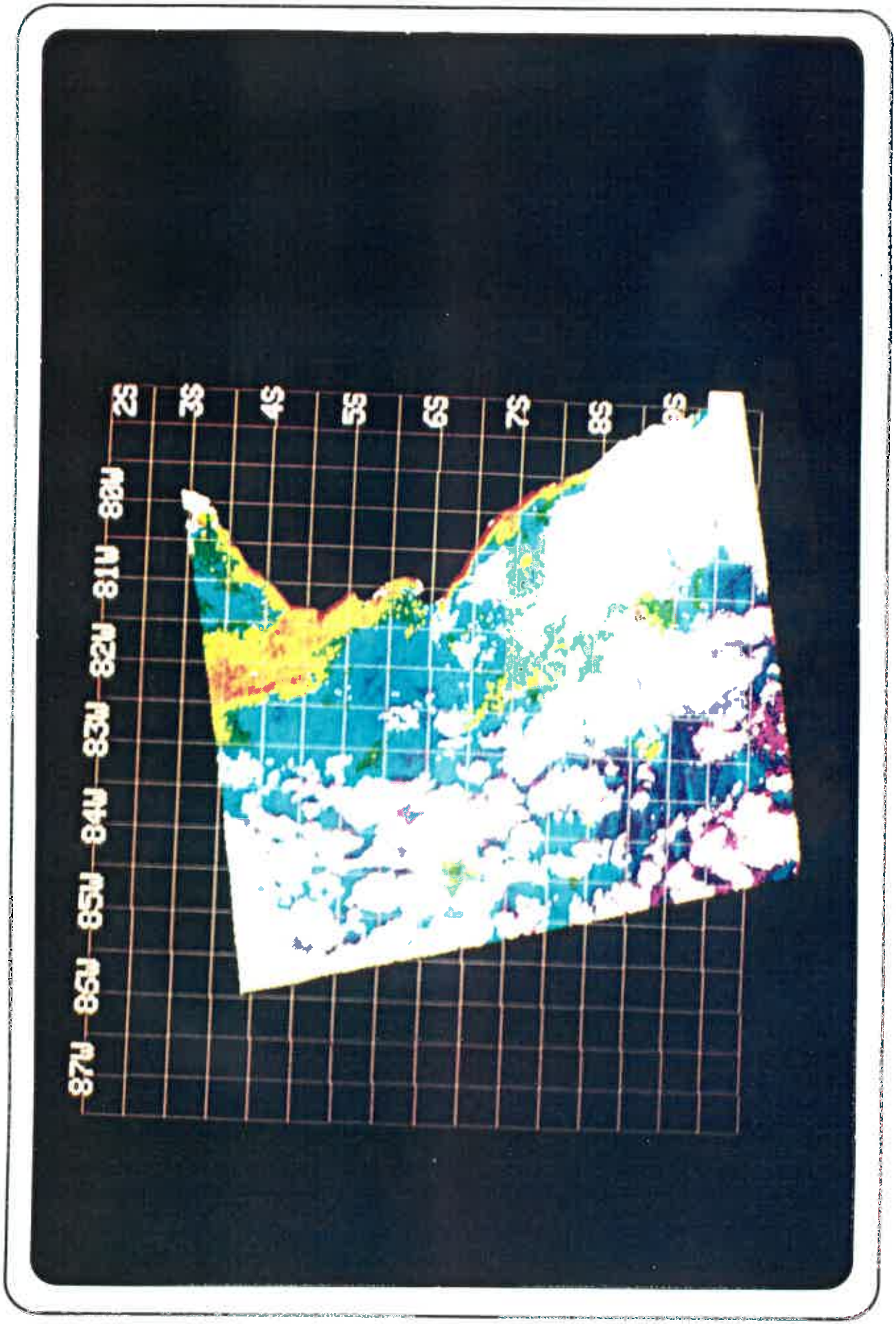
87J
86J
85J
84J
83J
82J
81J
80J
2S
3S
4S
5S
6S
7S
8S
9S

pigment concentrations can be seen along the coast to the north and south of the plume. Detailed analysis (i.e. magnifying specific areas) of the image reveals smaller plumes associated with many of the small coastal capes. One such plume extends approximately 50 km offshore from Chicama (7.5°S). There is some evidence of enhanced phytoplankton concentrations around Chimbote (9°S) as well, but that region was mostly obscured by cloud cover on that day. The coastal enhancement appears quite localized and the phytoplankton abundances in the offshore waters are fairly uniform with pigment concentrations between 0.2-0.4 mg/m3.

Another CZCS image of this region is available five days later (14 December, Plate 6.2) and distinctly shows the offshore extent of the plankton-rich plumes associated with the Chimbote upwelling center, a region that is so important to the Peruvian anchovy fishery (Guillen & Calienes, 1981). Extending over 300 km from the coast, the offshore extent of the zone of enhanced phytoplankton concentrations is between two to six times that defined by the offshore extent of the cold, upwelled water typical of this region (Guillen & Calienes, 1981). In addition to the visualization of the Chimbote upwelling, this image also shows that a southward displacement of the Paita plume occurs between the 9 and 14 December. The small plume off Talara (~4.5°S) which is oriented in a northwesterly direction on 9 December, has been displaced toward the southwest five days later. The sea

Plate 6.2. Satellite ocean color image showing the distribution of phytoplankton pigments along the northern Peruvian coast from Coastal Zone Color Scanner data aquired on 14 December 1978 (Nimbus-7 orbit 711). The coastline is masked in black along the right side of the scene. This image has been remapped to the coastal sampling grid.

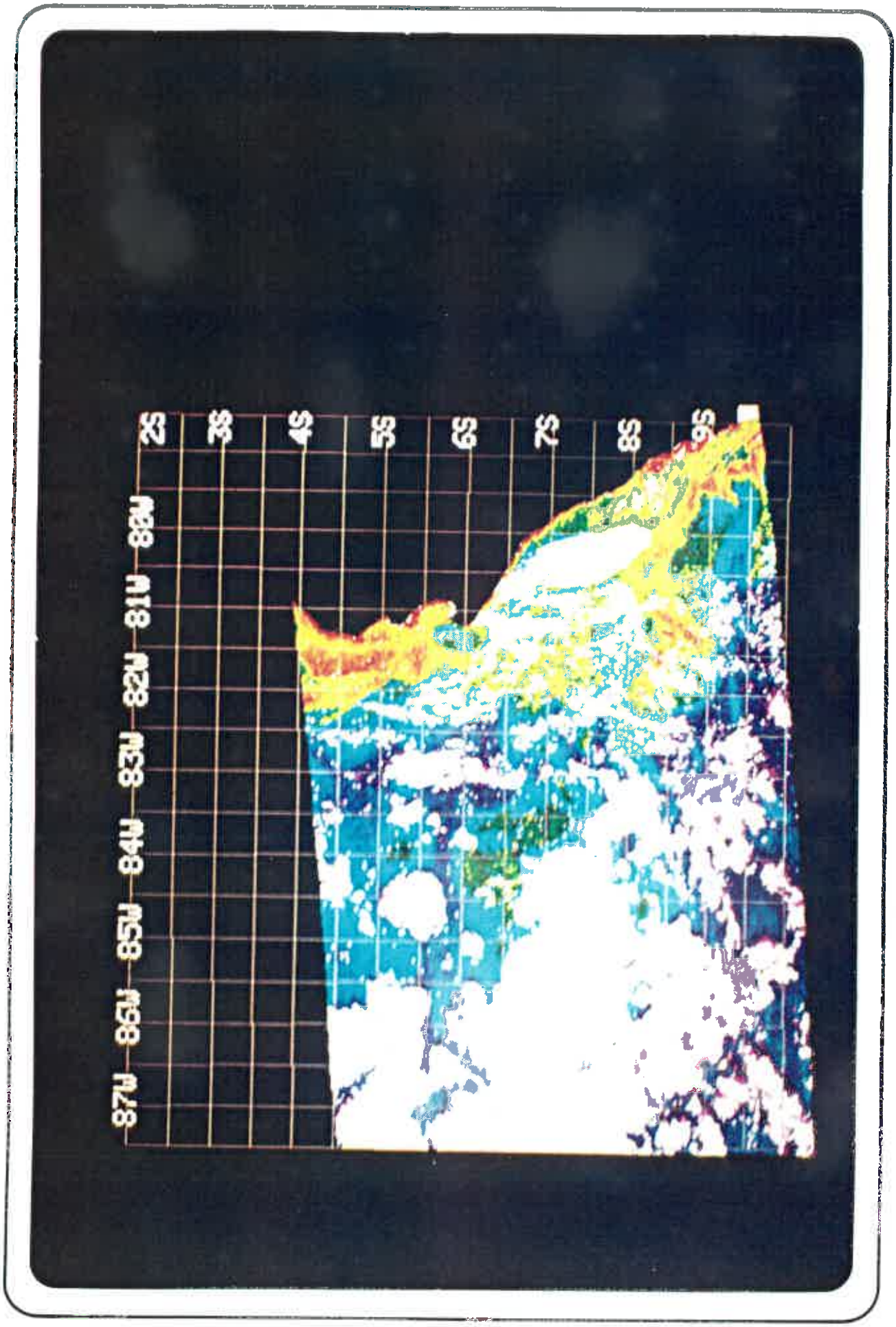
25
35
45
55
65
75
85
95
88W
81W
82W
83W
84W
85W
86W
87W

surface temperature distributions for these two days (analyzed but not presented) indicate a similar displacement in the isotherms along the coast. On 9 December, cool (~19°C) water was restricted to a narrow coastal band (<50 Km) with the exception of a distinct cold water plume, similar in location and extent to that observed in the CZCS image. Five days later, the band of cool water extended nearly 100 km offshore.

The CZCS image taken one week later (21 December 1978, Plate 6.3) shows little change in the offshore extent of the Chimbote plume, however, there is no longer any evidence of the Paita plume. Two images from January 1979 display similar features. The patterns observed on 19 January (Plate 6.4) are quite similar to those seen in the 9 December image. There is clear evidence of a northwesterly oriented Paita-Talara plume. While there is still the indication of enhancement in the Chimbote region, the offshore extent of the plume and the concentration levels appear to have been reduced. Several patches of plankton-rich water can be seen between 83° and 84°W, approximately 500 km from the coast. It is possible that these patches represent the remnants of the offshore edge of the Chimbote plume. A final scene on 31 January (not presented because of excessive cloud cover) shows the development of a broad band (~100 km) of pigment-rich water along the coast between 6° to 9°S, and an increase in pigment concentrations within the Paita plume. There is also the indication that the offshore patches observed in the 19 January

Plate 6.3. Satellite ocean color image showing the distribution of phytoplankton pigments along the northern Peruvian coast from Coastal Zone Color Scanner data acquired on 21 December 1978 (Nimbus-7 orbit 808). The coastline is masked in black along the right side of the scene. This image has been remapped to the coastal sampling grid.

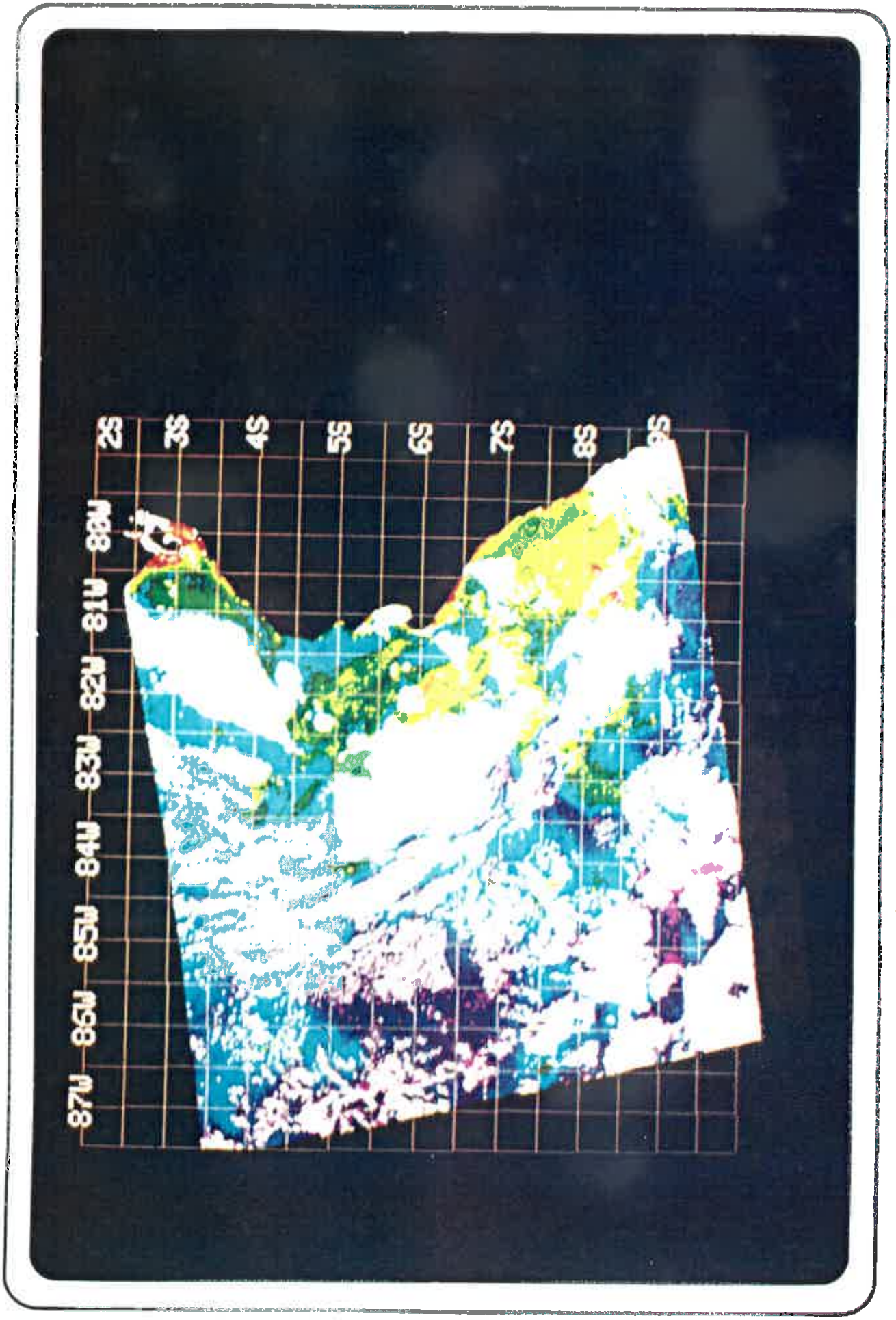
87W
86W
85W
84W
83W
82W
81W
80W

Plate 6.4. Satellite ocean color image showing the distribution of phytoplankton pigments along the northern Peruvian coast from Coastal Zone Color Scanner data acquired on 21 December 1978 (Nimbus-7 orbit 1209). The coastline is masked in black along the right side of the scene. This image has been remapped to the coastal sampling grid.

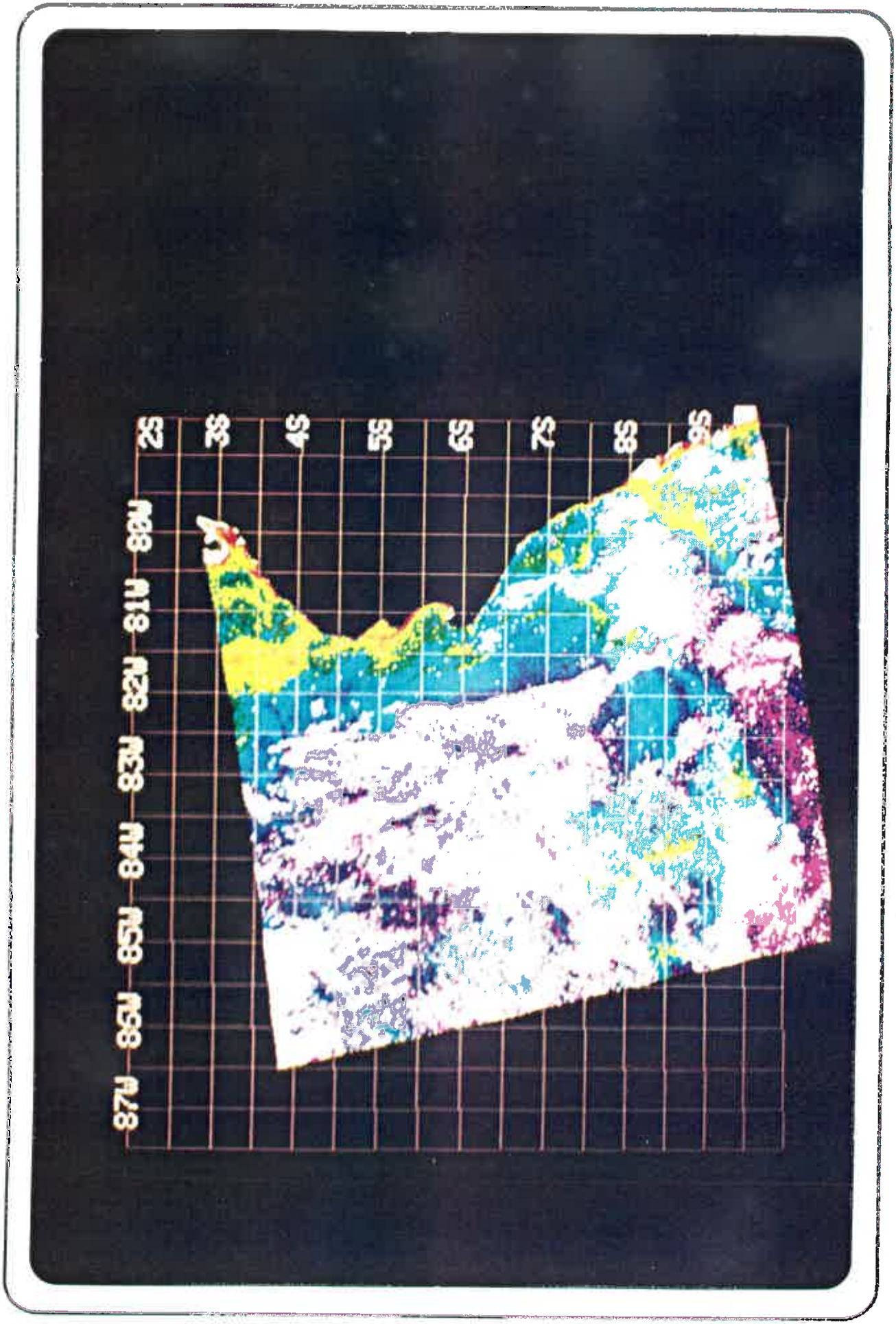
87W
86W
85W
84W
83W
82W
81W
80W
79W
78W
77W
76W
75W
74W

image may have increased in size, but the cloud cover over that region makes analysis difficult.

Four images of the eastern equatorial Pacific are available for the December 1979 through January 1980 period. The two best images (26 December 1979, Plate 6.5; 17 January 1980, Plate 6.6) are presented at full swath resolution (~1500 x 1500 km). The statistical analyses that were performed on these images for comparison with the December 1978-January 1979 period, however, made use of images that had been remapped to the same standard sampling region displayed in Plates 6.1-4.

The December 1979 image (Plate 6.5) shows that the region of enhanced phytoplankton abundances extends much further offshore than during the previous December. The most striking feature is the region of high phytoplankton biomass that extends across the entire northern portion of the image, a distance greater than 1000 km. It seems unlikely that such a broad band of enhanced production could be due solely to coastal upwelling. Also seen is a band of pigment-rich water extending ~200 km offshore along the entire coast south of 6°S. The Chimbote plume reaches nearly 350 km offshore. One feature of particular interest is the plume which originates at 6°S and curves toward the south as it progresses nearly 500 km offshore. What makes this feature particularly interesting is the fact that it occurs at a point where the coastline geometry changes sharply and at the approximate location where the Peru Coastal Current leaves the

Plate 6.5. Satellite ocean color image showing the distribution of phytoplankton pigments in the eastern equatorial Pacific from Coastal Zone Color Scanner data acquired on 26 December 1979 (Nimbus-7 orbit 5922). The Ecuadorian and Peruvian coastlines are masked in black along the right side of the scene. This image has been remapped to the basin-wide sampling grid (see text for discussion) so that the offshore extent of the plankton-rich waters can be seen.

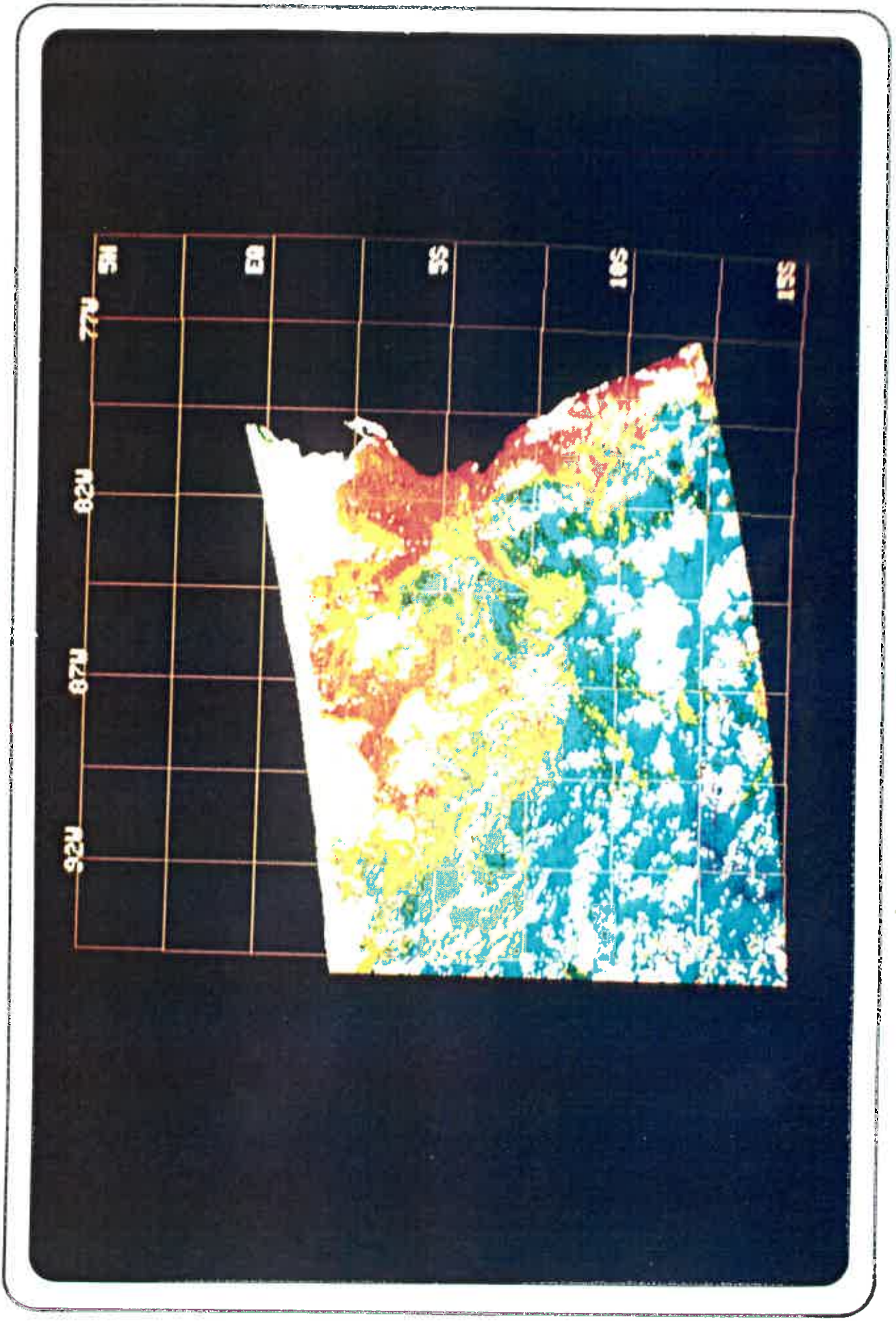
115
120
125
130
135
42N
43N
44N
45N

coast and turns west. Wyrtki (1965) notes that the shape of the coastline seems to have considerable influence on the coastal current, and that it has a tendency to leave the coast at almost every cape. He also shows that the southward flowing Peru Countercurrent is typically located about 500 km offshore and is most pronounced from November to March. From April to June, however, its location and strength are more variable. The observed shape of the above mentioned plume may be a result of the interaction between these two flow regimes.

That this period is significantly different from the preceeding year is also evident in an east to west transect performed along 5°S on this image and on the one from 9 December 1978 (Figure 6.2). In 1978, high pigment concentrations are restricted to a narrow coastal band along 5°S, dropping below 1.0 mg/m3 within 40 pixels (33Km) offshore. In December 1979, however, pigment concentrations remained above 1.0 mg/m3 at least 130Km offshore. A visual inspection of the CZCS image (Plate 6.5) shows that further offshore, concentrations increase to near coastal levels across most of the image.

As in the previous scene, the 17 January 1980 image (Plate 6.6) shows quite clearly the broad region of enhanced phytoplankton concentrations. The northern limit of this zone is quite distinct and may represent the position of the Equatorial Front. Wooster (1969) described this front between the Galapagos Islands and the coast of South America as a generally narrow,

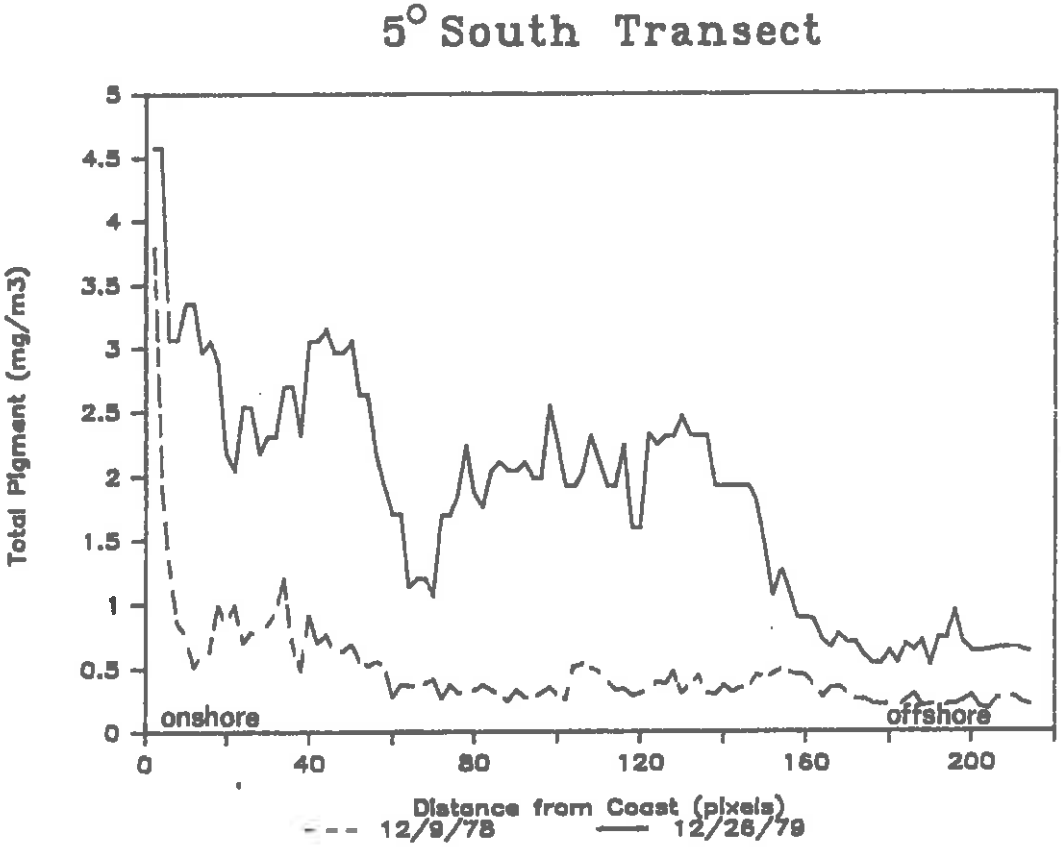

Figure 6.2. Satellite-derived phytoplankton pigment concentrations (mg/m3) versus distance (1 pixel = .825 meters) along 5°S derived from Coastal Zone Color Scanner data of the northern Peruvian coastal region acquired on 9 December 1978 (dashed line) and 26 December 1979 (solid line).

Plate 6.6. Satellite ocean color image showing the distribution of phytoplankton pigments in the eastern equatorial Pacific from Coastal Zone Color Scanner data acquired on 17 January 1980 (Nimbus-7 orbit 6226). The Ecuadorian and Peruvian coastlines are masked in black along the right side of the image and the Galapagos Islands can be seen along the equator near 92°W. This image has been remapped to the basin-wide sampling grid.

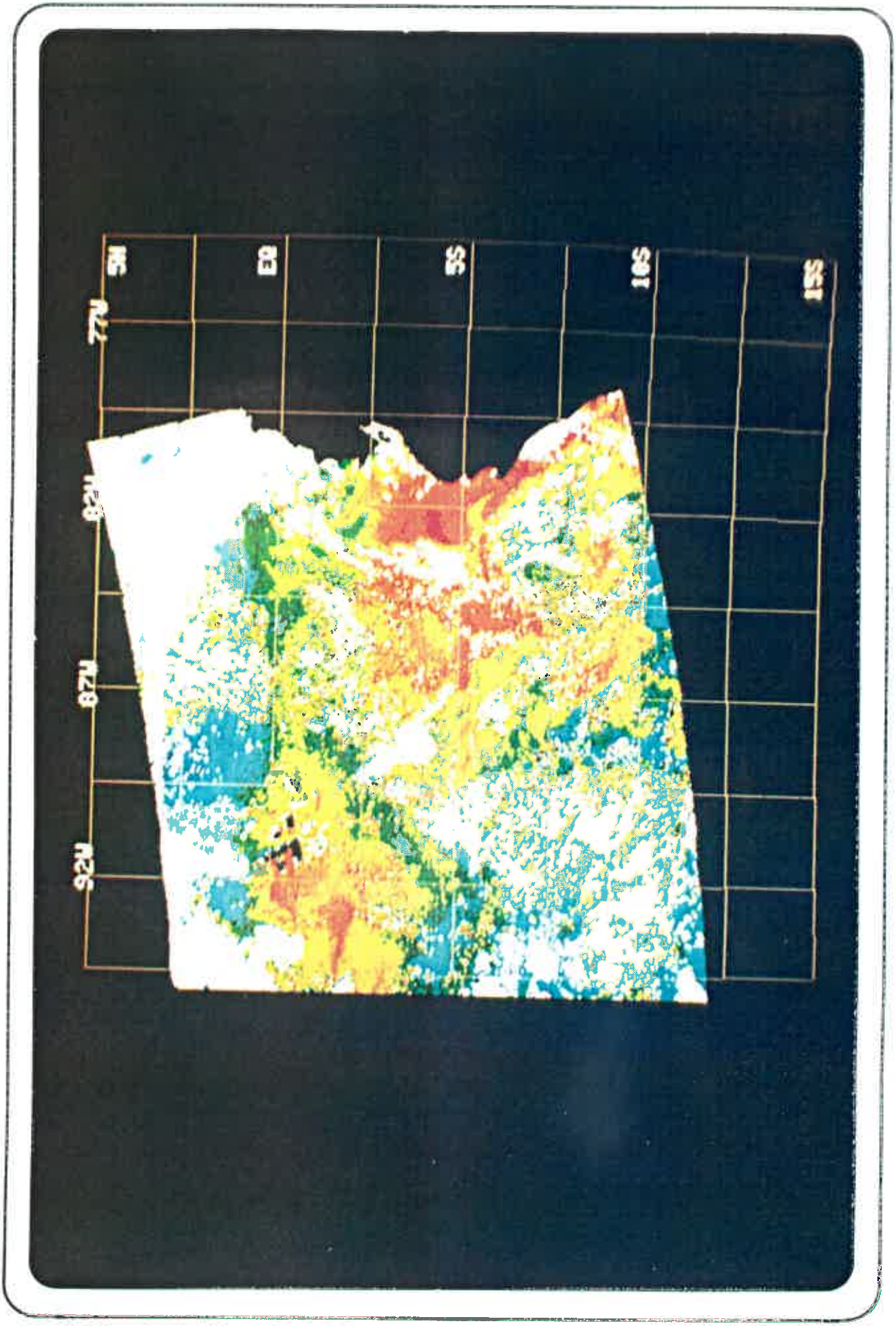
77W
82W
87W
92W

shallow feature which separates the cold, salty waters of the Peru Current from the warmer, less saline tropical waters further north. There is significant variability in the position of the Equatorial Front (Barber & Chavez, 1983), its movement determined by features of the large-scale circulation patterns of the region. The influence of the Galapagos Islands on the distributions and abundances of phytoplankton in the surrounding waters is also seen in this image. Although somewhat speculative, a detailed analysis of this image reveals what appear to be a pair counter-rotating eddies, one of which may have been shed off the western end of the archipelago. This offshore structure is approximately 75 km in diameter and is located nearly 150 km to the west of Isabela. Unfortunately, approximately 20 scan lines (17 km) covering the southern portion of the islands are missing from the raw CZCS data making quantitative analysis of these features quite difficult.

The interannual variability in phytoplankton distribution and abundance can also be seen in a comparison between the May 1979 and April 1981 periods. Frequency distributions of mean pigment concentrations for both periods (Figures 6.3 & 6.4) demonstrate the short-term (2-3 weeks) coherence in phytoplankton concentrations throughout the study area. The interannual variability is clearly greater than the changes that occured between individual images presented. The phytoplankton distributions during May 1979 are similar in most respects to the 19 January 1979 image (Plate 6.4) and do not display any features

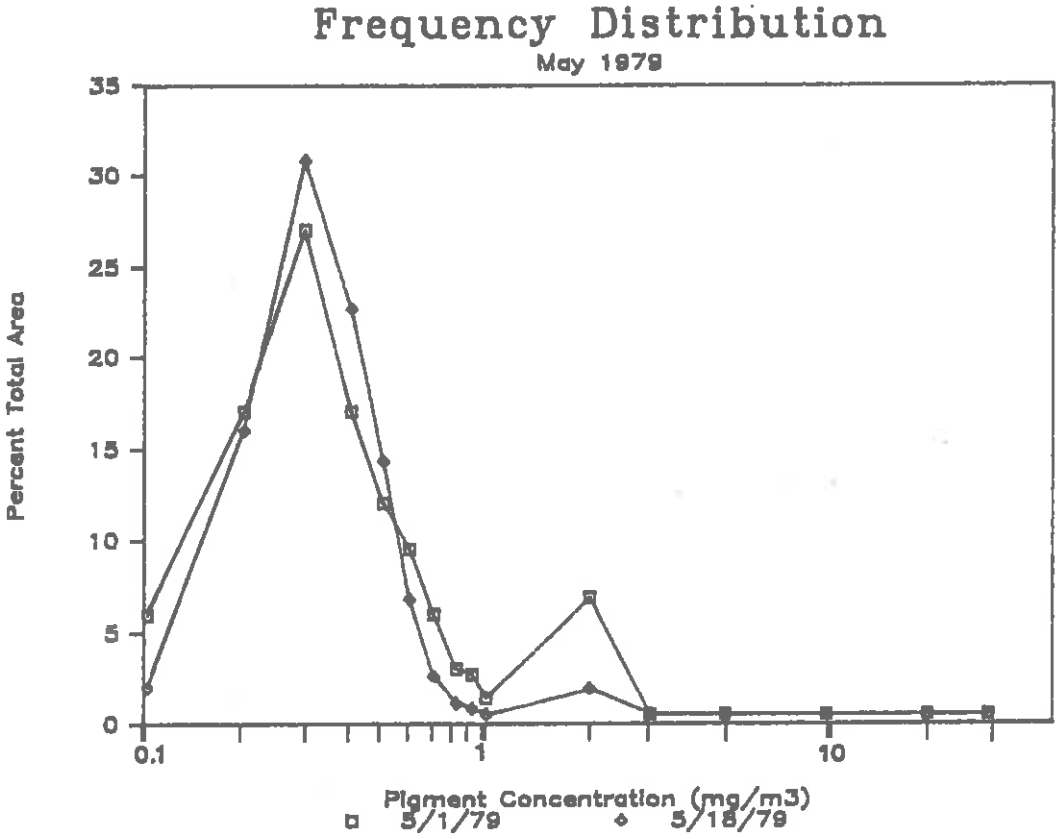

Figure 6.3. Frequency distributions of satellite-derived phytoplankton pigment concentrations (mg/m3) versus the percentage of total cloud-free surface area covered by each concentration range for the northern Peruvian coastal region (coastal sampling grid) as observed by the Coastal Zone Color Scanner on 1 May (Mean = 0.69 mg/m3, SD = 2.07 mg/m3) and 18 May 1979 (Mean = 0.41 mg/m3, SD = 0.96 mg/m3).

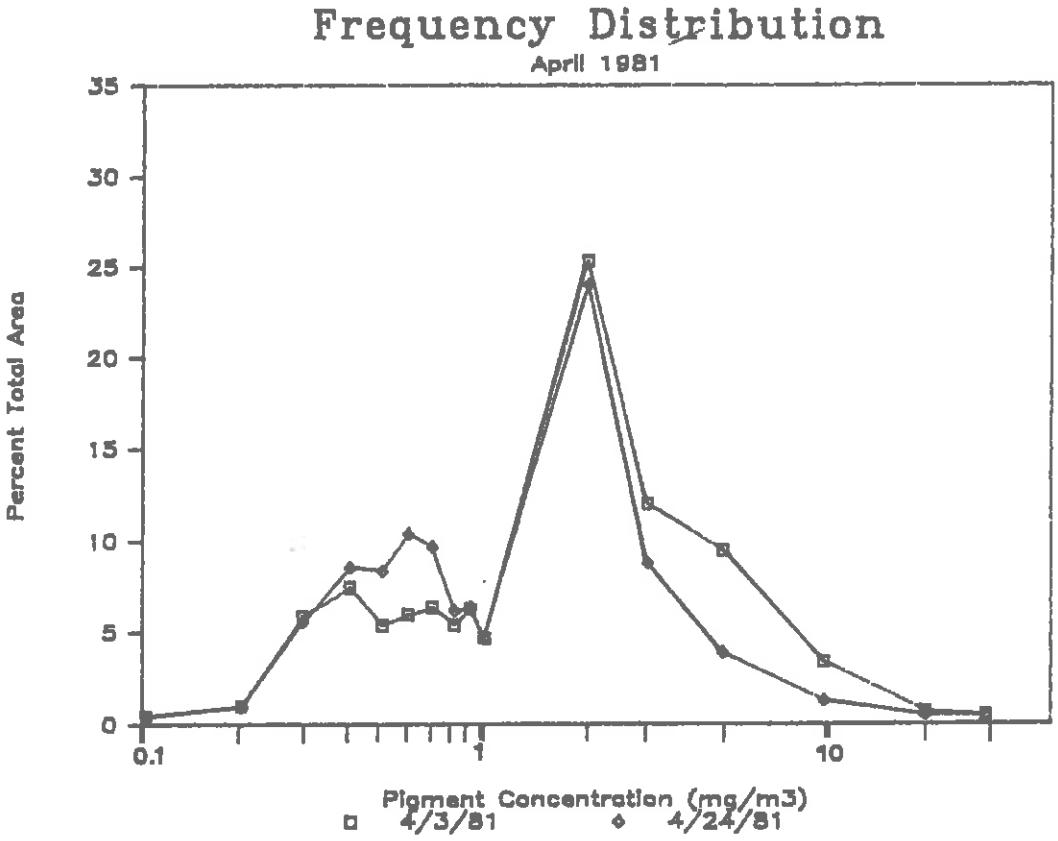

Figure 6.4. Frequency distributions of satellite-derived phytoplankton pigment concentrations (mg/m3) versus the percentage of total cloud-free surface area covered by each concentration range for the northern Peruvian coastal region (coastal sampling grid) as observed by the Coastal Zone Color Scanner on 3 April (Mean = 1.72 mg/m3, SD = 2.44 mg/m3) and 24 April 1981 (Mean = 1.24 mg/m3, SD = 1.76 mg/m3).

which are of particular interest beyond those already described. The individual scenes of the Pisco upwelling center described in Chapter 5 as well as the available hydrological data (Zuta et al., 1978) suggests that April/May is a transition period and that the differences between May 1979 (Figure 6.3) and April 1981 (Figure 6.4) may be seasonal rather than interannual. Lack of additional CZCS data for that period, however, makes it difficult to determine whether the differences are due to large-scale influences or local effects.

The April 1981 images, however, are unique and display many features which are not observed in any other CZCS images of this region. Images acquired on 3 April (Plate 6.7) and 24 April 1981 (Plate 6.8) document the richness of the Peruvian coastal system and the sharp transition that takes place between oceanic and coastal conditions. In the 3 April scene, enhanced phytoplankton concentrations are found approximately 400 km offshore in the northern portion of the image. A long band (~400 km) of exceptionally pigment-rich water (~10.0 mg/m3) is situated approximately 150 km offshore, very close to the oceanic/coastal boundary. A plume, similar in size and location to those observed in the previous two images, and with a distinct southward displacement of its offshore edge is also seen at this time. In addition, the Chimbote plume appears to be very well defined in this image. The broad region of enhanced phytoplankton concentrations that can be seen between 3° to 6°S is

Plate 6.7. Satellite ocean color image showing the distribution of phytoplankton pigments in the eastern equatorial Pacific from Coastal Zone Color Scanner data acquired on 3 April 1981 (Nimbus-7 orbit 12334). The Ecuadorian and Peruvian coastlines are masked in black along the right side of the scene. This image has been remapped to the basin-wide sampling grid. A more detailed presentation of the southern portion of this scene can be found in Plate 5.3.

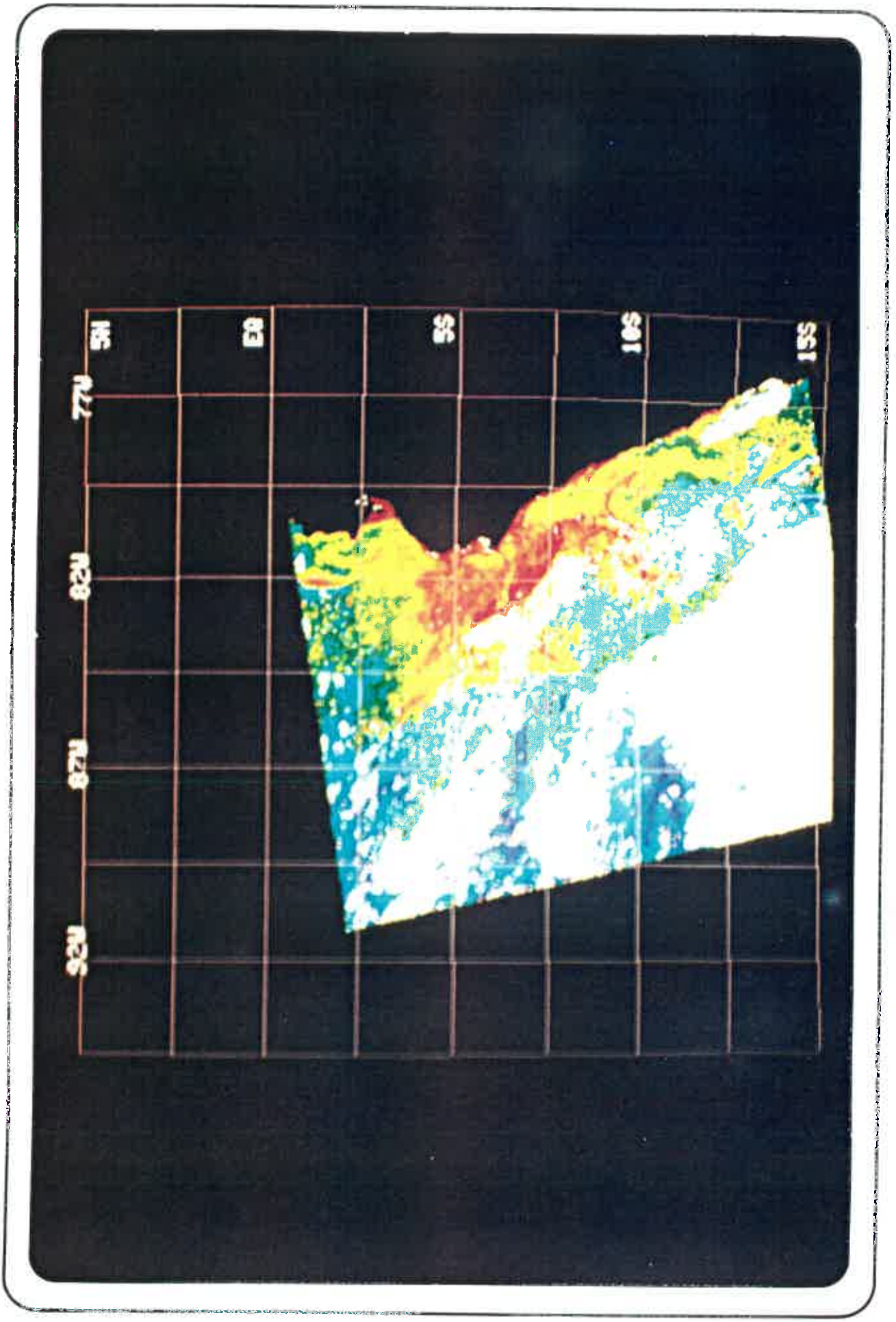
15S
10S
5S
0
5N
27
28
29
30

Plate 6.8. Satellite ocean color image showing the distribution of phytoplankton pigments along the northern Peruvian coast from Coastal Zone Color Scanner data acquired on 24 April 1981 (Nimbus-7 orbit 12624). The coastline is masked in black along the right side of the scene. This image has been remapped to the coastal sampling grid.

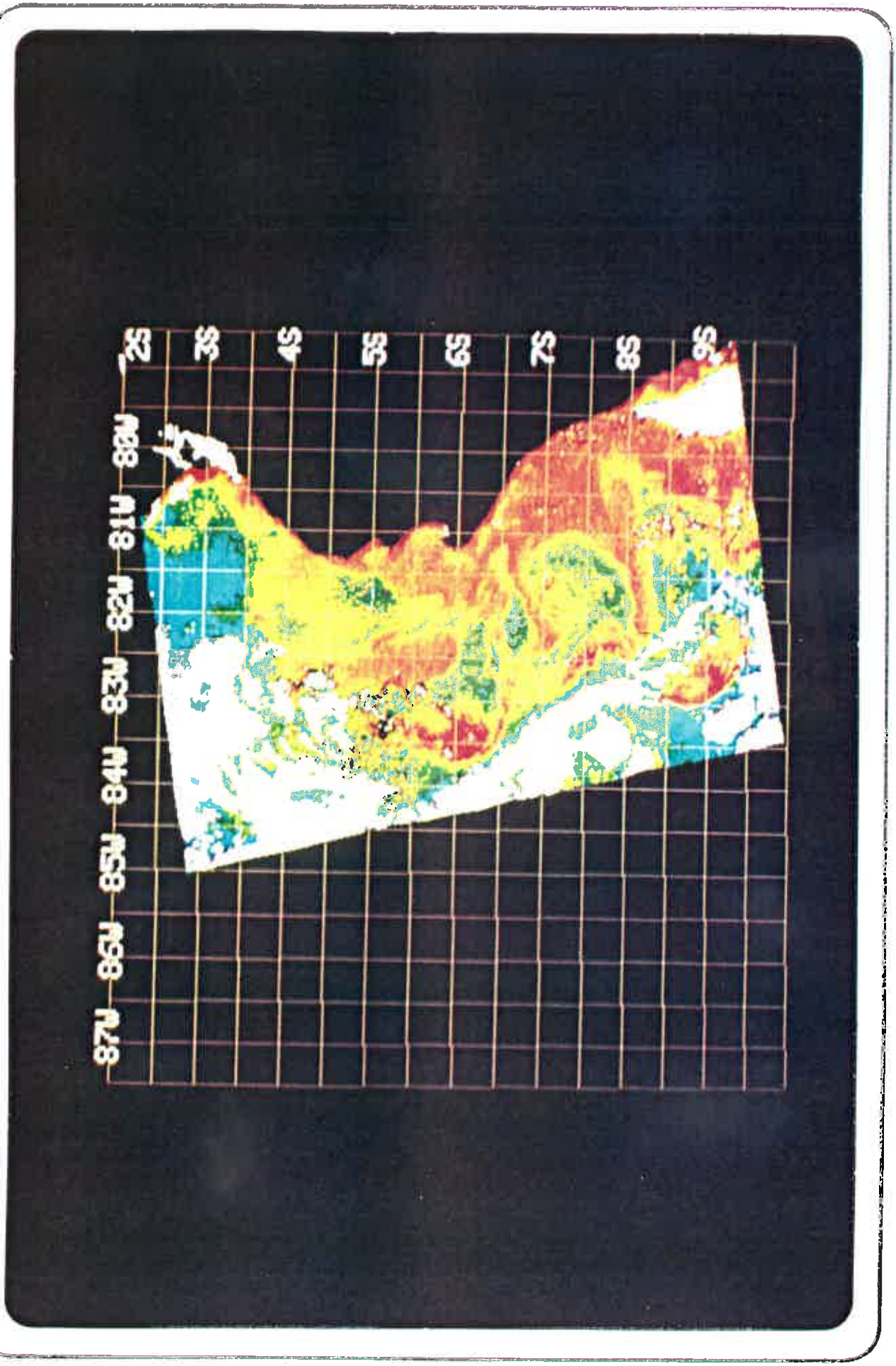
87W
86W
85W
84W
83W
82W
81W
80W

located well beyond the continental shelf. In this region, the 1000 fathom isobath is only 30 km from the coast. Phytoplankton concentrations in the southern region are lower than those to the north. Wind records from Chimbote (Enfield, personal communication, 1985) show that winds remained upwelling favorable throughout this period with no sign of the wind reversal that took place at Callao (Figure 5.7). Enfield & Newberger (1985) discussed the significance of this alongshore variability in coastal winds and the satellite images demonstrate the biological consequences quite clearly.

The patterns of phytoplankton distribution observed in the 24 April 1981 CZCS image (Plate 6.8) are unique and document just how dynamic this region is. The 400 km band along the coast seen in the previous image has broken into a series of plankton-rich filaments and eddies. One particularly distinct eddy, approximately 50 km in diameter with pigment concentrations greater than 10.0 mg/m3 is centered at 6°S, 83.5°W. A similarly sized structure with somewhat lower pigment concentrations is located approximately 100 km further inshore. A third eddy-like structure appears to be forming near 9°S, 83°W. A detailed analysis of these two offshore structures reveals a cyclonic, or clock-wise sense of rotation. If so, these features would tend to be similar to the cold core eddies described by Yentsch & Phinney (1985) in which productivity, which depends upon nutrients and light, could be enhanced by the upward

dispalcement of nutrient-rich water at the center of cyclonic eddies.

Plankton-rich streamers, filaments, and both cyclonic and anti-cyclonic eddies have been observed in recent studies of the California Current (Simpson et al., 1984; Pelaez-Hudlet, 1984; Mooers & Robinson, 1984). The role that these features play in determining the physical and biological variability of the California Current System has only recently come to light through the application of remotely sensed data. Although it would seem likely that similar features would exist in the Peru Current System as well, it was previously believed that they would be restricted to a relatively short distance in the offshore direction (Suess & Theide, 1983). The patterns observed on 24 April 1981 clearly demonstrate that the Peru System is probably as rich in meso-scale features and variability as the California System, and justifiably warrants further study.

One final point that should be made concerns the north/south extent of the region of enhanced phytoplankton production. The southern portion of the 24 April image (not presented) extends to approximately 20°S along the coast of northern Chile. Although regions of localized enhancement can be seen, they appear in this scene, and several others that have been examined, to be restricted to the near-shore waters. In fact, the change in coastal orientation that occurs around 14°S seems to represent a latitudinal boundary between the highly productive northern

region with its broad offshore extent and the significantly narrower region of enhanced production to the south. Since the Rossby radius of deformation, which is a key factor in determining the coastal boundary layer width scale (Parish et al., 1983) is inversely dependent on the sine of the latitude, one would expect a significant decrease in the width of this theoretical coastal boundary moving southward along the coast. Analysis of satellite images of the Chilean coast could help to verify this.

6.4. RESULTS AND DISCUSSION

Representative frequency distributions of the percent total surface area versus CZCS-derived pigment concentration of some of the CZCS images covering the December 1978 through January 1979 (Dec78-Jan79), December 1979 through January 1980 (Dec79-Jan80) and November 1982 through February 1983 (Nov82-Feb83, El Nino) periods are presented in Figures 6.5, 6.6 and 6.7 respectively. In addition, Table 6.1 gives the mean pigment concentrations and standard deviations as well as the percent of the total cloud-free surface area with pigment concentrations greater than 1.0 mg/m3 which are derived from the coastal sampling grid for most of the CZCS scenes which are discussed in this section. Although the patterns of phytoplankton distribution observed in the satellite images display significant mesoscale variability, there is sufficient similarity in the shapes of the curves within each time

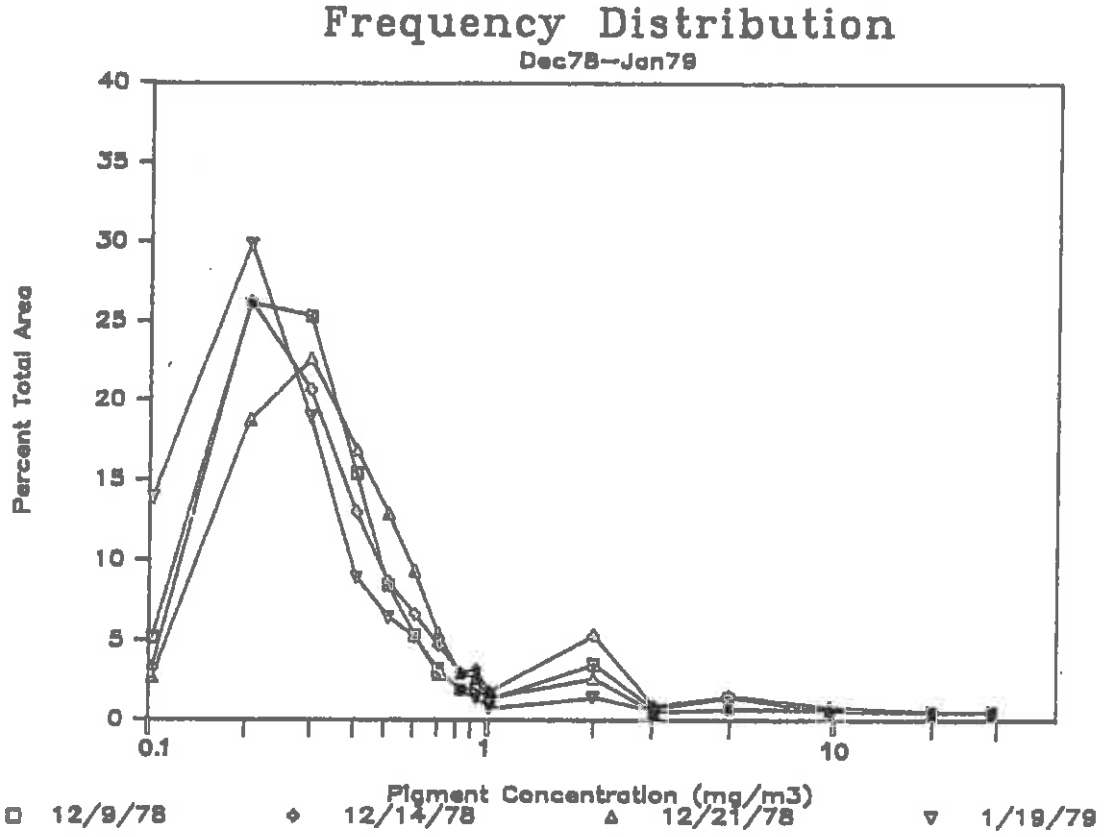

Figure 6.5. Frequency distributions of satellite-derived phytoplankton pigment concentrations (mg/m3) versus the percentage of total cloud-free surface area covered by each concentration range for the northern Peruvian coastal region (coastal sampling grid) as observed by the Coastal Zone Color Scanner on 9 December (Mean = 0.48 mg/m3, SD = 1.04 mg/m3), 14 December (Mean = 0.61 mg/m3, SD = 1.62 mg/m3), 21 December 1978 (Mean = 0.53 mg/m3, SD = 1.37 mg/m3) and 19 January 1979 (Mean = 0.38 mg/m3, SD = 1.08 mg/m3).

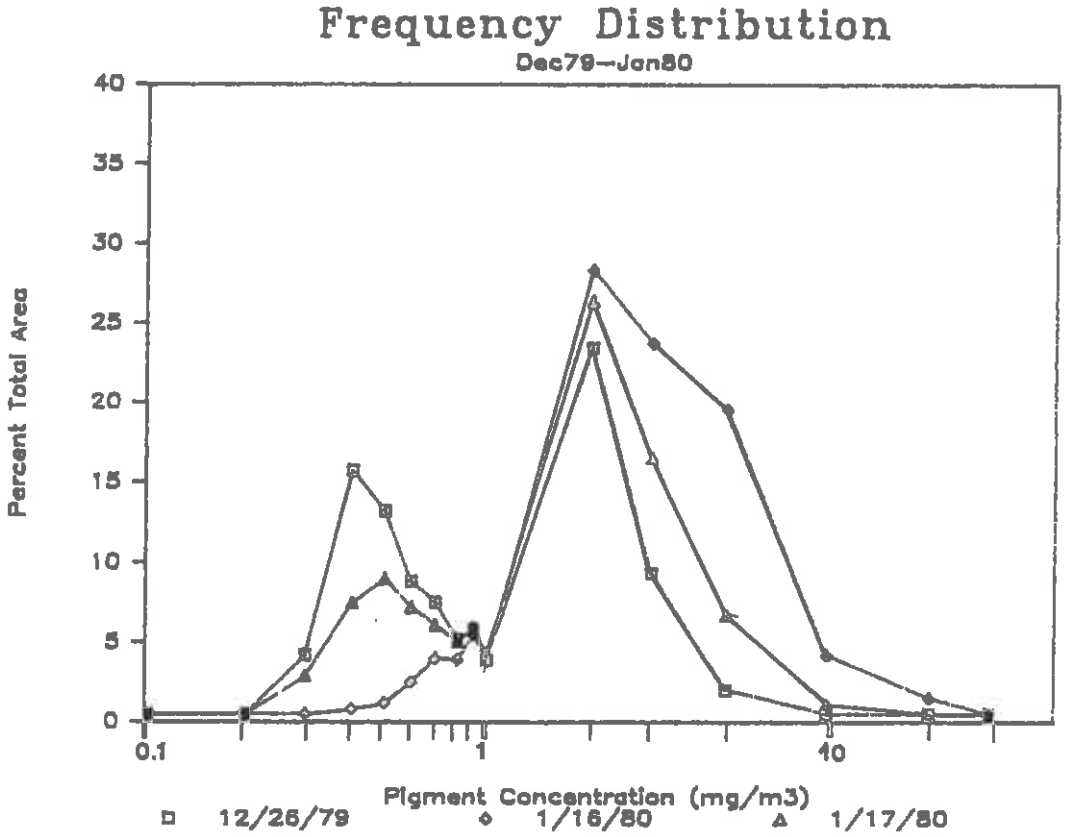

Figure 6.6. Frequency distributions of satellite-derived phytoplankton pigment concentrations (mg/m3) versus the percentage of total cloud-free surface area covered by each concentration range for the northern Peruvian coastal region (coastal sampling grid) as observed by the Coastal Zone Color Scanner on 26 December 1979 (Mean = 1.04 mg/m3, SD = 1.04 mg/m3), 16 January (Mean = 2.53 mg/m3, SD = 2.88 mg/m3) and 17 January 1980 (Mean = 1.54 mg/m3, SD = 1.89 mg/m3).

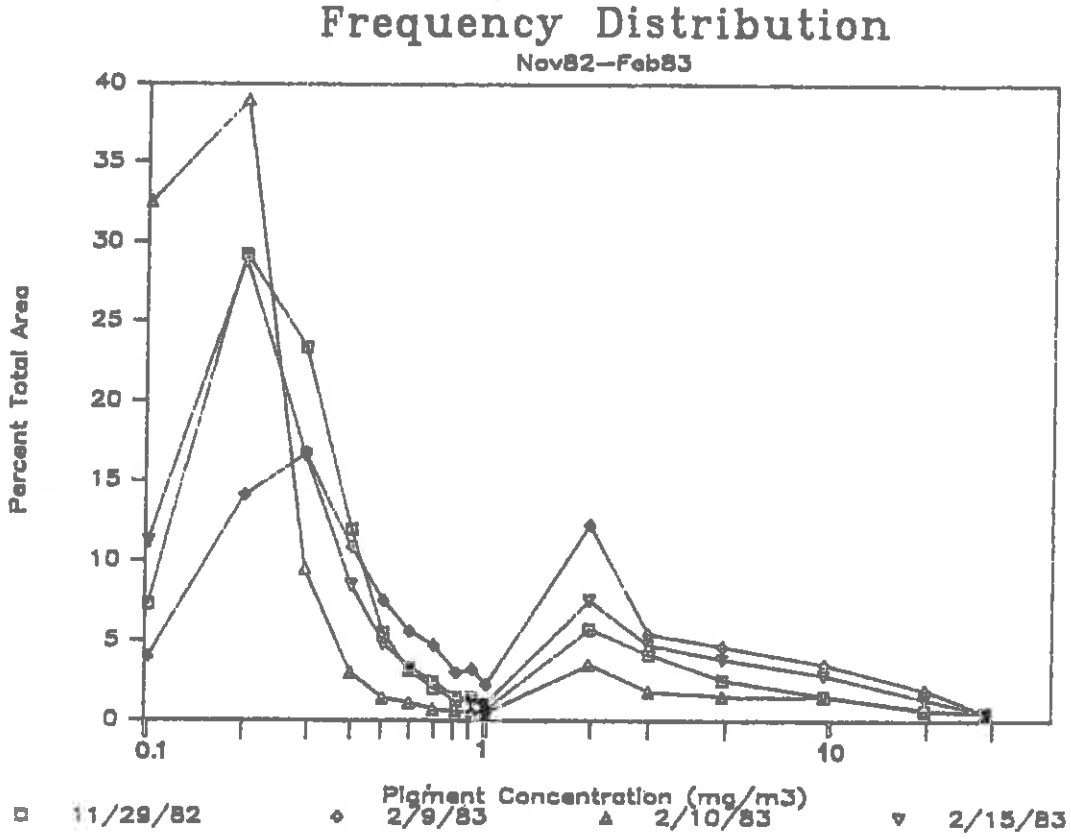

Figure 6.7. Frequency distributions of satellite-derived phytoplankton pigment concentrations (mg/m3) versus the percentage of total cloud-free surface area covered by each concentration range for the northern Peruvian coastal region (coastal sampling grid) as observed by the Coastal Zone Color Scanner on 29 November 1982 (Mean = 0.74 mg/m3, SD = 2.08 mg/m3), 9 February (Mean = 1.29 mg/m3, SD = 2.94 mg/m3), 10 February (Mean = 0.66 mg/m3, SD = 1.93 mg/m3) and 15 February 1983 (Mean = 1.07 mg/m3, SD = 2.68 mg/m3).

Date	C_{SAT}	S.D.	Per Cent Area > 1.0mg/m3
12-09-78	0.48	1.04	6.3
12-14-78	0.61	1.62	9.0
12-21-78	0.53	1.37	4.7
1-19-79	0.38	1.08	3.0
1-31-79	0.93	2.36	15.8
5-01-79	0.69	2.07	6.9
5-18-79	0.41	0.96	1.9
12-26-79	1.01	1.04	35.0
1-16-80	2.53	2.38	77.6
1-17-80	1.54	1.89	51.3
9-15-80	0.84	1.45	20.3
4-03-81	1.72	2.44	51.1
4-24-81	1.24	1.76	38.3
11-29-82	0.74	2.02	14.6
2-09-83	1.29	2.94	28.2
2-10-83	0.66	1.93	9.1
2-15-83	1.07	2.68	20.5

Table 6.1. Mean overall phytoplankton pigment concentrations (C_{SAT} in mg/m3), Standard Deviations (SD in mg/m3) and the percentage of total cloud-free surface area where pigment concentrations were greater than 1.0 mg/m3 computed for seventeen Coastal Zone Color Scanner images of the northern Peruvian coastal region (coastal sampling grid) from December 1978 through February 1983.

period to justify producing 'seasonal' mean composites. These composites retain the major structures and features observed during their respective periods and appear to be the best means for quantifying the degree of interannual variability. Figures 6.5 and 6.6 clearly show that the interannual signal between these years is greater than that observed over the shorter time scales used to construct the composites. The frequency distributions for the individual CZCS images covering the El Nino period (Figure 6.7) were similar to those from the Dec78-Jan79 period with the exception of a general increase in the 1-5.0 mg/m3 range. As is discussed later, high levels of phytoplankton biomass along a narrow coastal band were observed throughout the 1982 El Nino.

Cumulative distributions derived from the composited images remapped to the basin-wide sampling grid (Figure 6.8), document the large-scale, interannual variability observed during the three time periods considered in this study. As described earlier, if it is assumed that the area of enhanced biological production is represented by those waters in which pigment concentrations exceeded 1.0 mg/m3, the data shows that this region constitutes less than 3% of the total area in Dec78-Jan79, greater than 30% one year later, and approximately 10% of the total during El Nino (also see Table 6.2).

The distributions for the Dec78-Jan79 and El Nino periods are surprisingly similar while their contrast with the Dec79-Jan80 period is striking. The major question raised by these findings

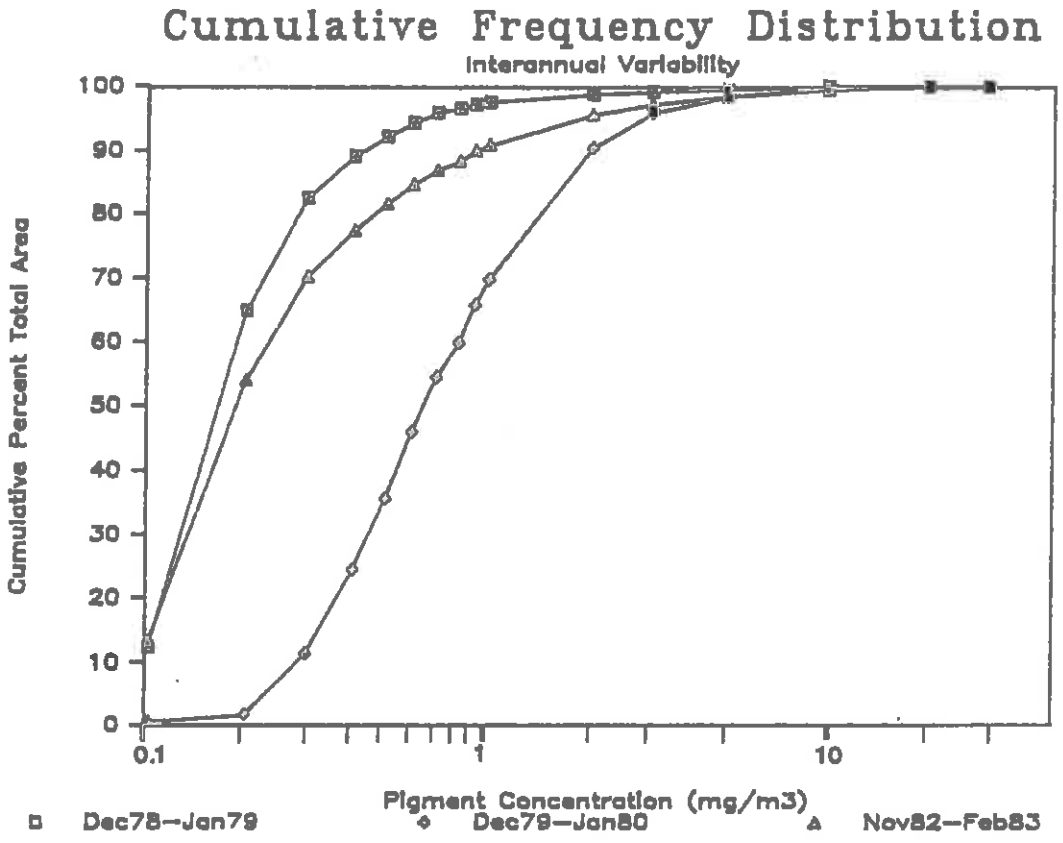

Figure 6.8. Cumulative frequency distributions of satellite-derived phytoplankton pigment concentrations (mg/m3) versus the percentage of total cloud-free surface area covered by each concentration range for the eastern equatorial Pacific (basin-wide sampling grid) as observed by the Coastal Zone Color Scanner during the December 1978 through January 1979 (Mean = 0.29 mg/m3, SD = 0.80 mg/m3), December 1979 through January 1980 (Mean = 1.04 mg/m3, SD = 1.44 mg/m3) and November 1982 through February 1983 (Mean = 0.53 mg/m3, SD = 1.52 mg/m3)periods.

does not revolve around El Nino, but rather in trying to understand the reasons behind the apparent degree of interannual variability experienced between the Dec78-Jan79 and Dec79-Jan80 periods; two periods during which conditions throughout the region have been characterized as being close to normal (Zuta & Quispe,1981). There is evidence to suggest that there may have been significant large-scale oceanic and atmospheric differences between the two periods (Sadler & Kilonsky, 1981; Donguy et al.,1982; Mangum & Hayes,1984).

While data from which strong correlations between large-scale variations in circulation and interannual variability in phytoplankton production are particularly scarce for this region, a recent study by Chelton et al. (1982) of the California Current System may provide some insight into this question. They conclude that large-scale changes in circulation patterns altered the nutrient supply available for primary production through either horizontal or vertical advection. Although not as well documented as the California System, significant variabilty in circulation patterns have been shown to occur in the eastern equatorial Pacific as well. Lukas (1981) demonstrated the variablity in the strength of the equatorial Undercurrent which could be significant because of the Undercurrent's role in supplying the Peru Undercurrent; the major source of water that upwells along the Peru coast. In addition to supplying the coastal upwelling system, variations in the strength, location, and timing of

intensified Undercurrent flows could alter the large-scale patterns of vertical mixing and nutrient supply, thereby influencing phytoplankton production. Recent improvements in large-scale ocean models (O'Brien, personal communiction, 1985) have begun to provide information about many of the parameters that could help explain the observed interannual variablity in phytoplankton abundances throughout this region.

6.5. THE PRODUCTIVE HABITAT: SEASONAL COMPOSITES

The concept of a productive habitat is somewhat different than the traditionally defined coastal zone or more specifically, coastal upwelling region. The coastal zone is often defined by submarine topography and extends generally to the edge of the continental shelf. The coastal upwelling region, however, is generally restricted to a narrow band within 50km of the coast (Smith, 1968), its width dictated by the offshore extent to which the physical process of coastal upwelling can occur. The size that one ascribes to the upwelling area is particularly important when estimates of total ecosystem production based on discrete measurements of primary production are extrapolated over the entire region. Although Smith cautioned against confusing the physical process of upwelling with its effects, most estimates of total ecosystem production for this region have relied upon the physical description of the upwelling zone rather than the area

defined by levels of enhanced biological production resulting from these processes. It is this region which can now be defined and monitored through the use of satellite ocean color measurements.

As seen in the composited CZCS image of the Dec78-Jan79 period (Plate 6.9), the productive habitat (the yellow and red regions) is generally restricted to a narrow coastal band approximately 50-75 km in width. The highest pigment concentrations (5-10.0 mg/m3) are found within 20Km of the coast near the Chimbote upwelling center (9°S). Associated with this region is a plume of pigment-rich water that extends nearly 250 km offshore. A plume of similar dimension is also seen at 5°S (Paita). Although the offshore extent of these plumes is generally greater than had been previously described, the region of biological enhancement during this period is primarily near-shore. This is in general agreement with the traditional definition of the coastal upwelling zone for this region where the spatial distribution of phytoplankton biomass has been shown to be determined by the advective supply of new nutrients to the surface layer (Barber & Chavez,1983).

The size of the productive habitat observed in the composite of the Dec79-Jan80 period (Plate 6.10) is nearly 14 times larger than was observed during the preceeding year. Enhancement appears to have occured on a much broader scale with the offshore boundary of the productive habitat extending nearly 400 km from the coast at 10°S and, nearly 1000 km from the coast at 2.5°S.

Plate 6.9. Seasonal composited satellite ocean color image showing the distribution of phytoplankton pigments in the eastern equatorial Pacific from Coastal Zone Color Scanner data acquired during December 1978 and January 1979 (composited from six orbits). The Ecuadorian and Peruvian coastlines are masked in black along the right side of the image and the Galapagos Islands can be seen along the equator near 92°W. This image has been remapped to the basin-wide sampling grid.

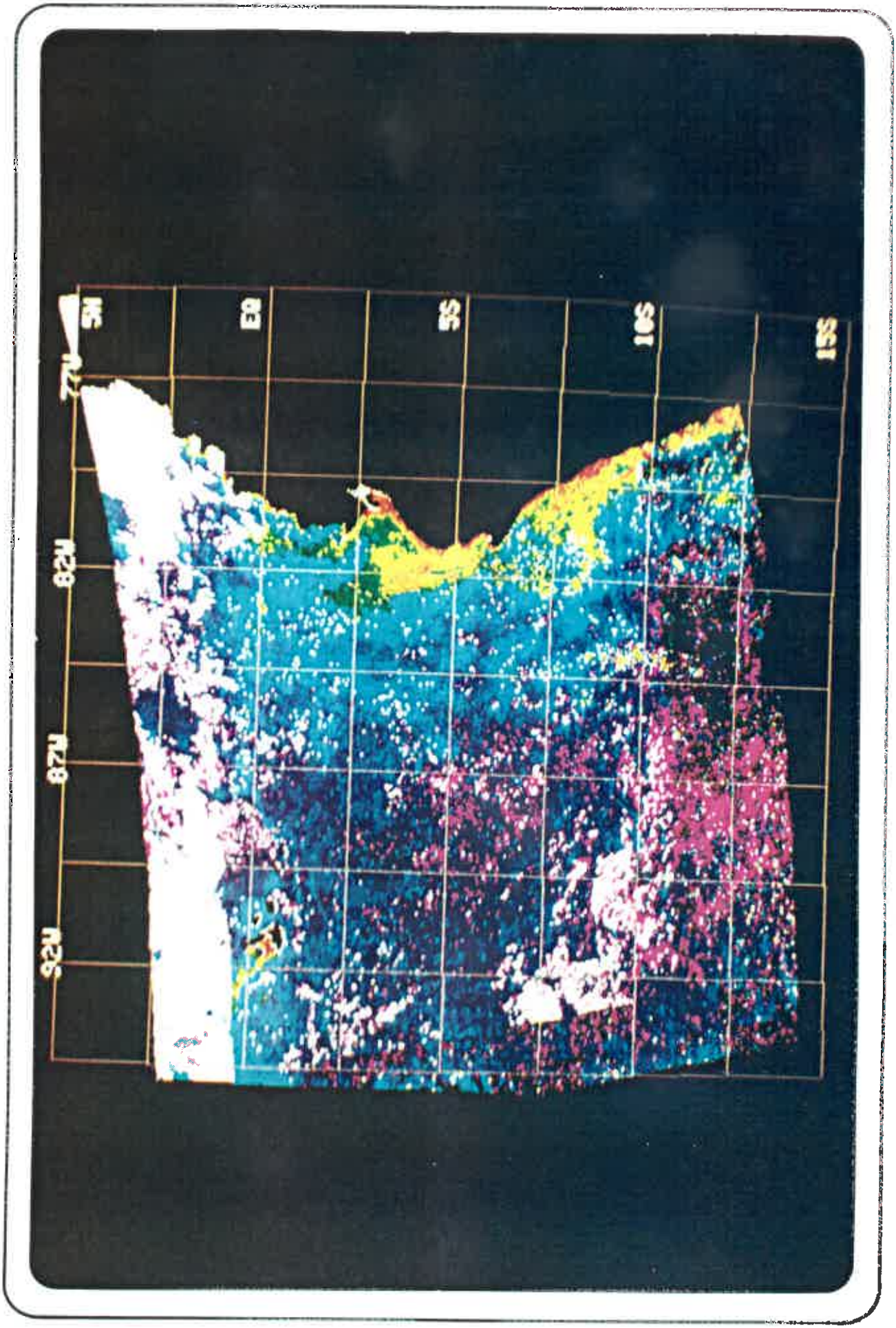
5S
0
5S
10S
15S
77W
82W
87W
92W

Plate 6.10. Seasonal composited satellite ocean color image showing the distribution of phytoplankton pigments in the eastern equatorial Pacific from Coastal Zone Color Scanner data acquired during December 1979 and January 1980 (composited from four orbits). The Ecuadorian and Peruvian coastlines are masked in black along the right side of the image and the Galapagos Islands can be seen along the equator near 92°W. This image has been remapped to the basin-wide sampling grid.

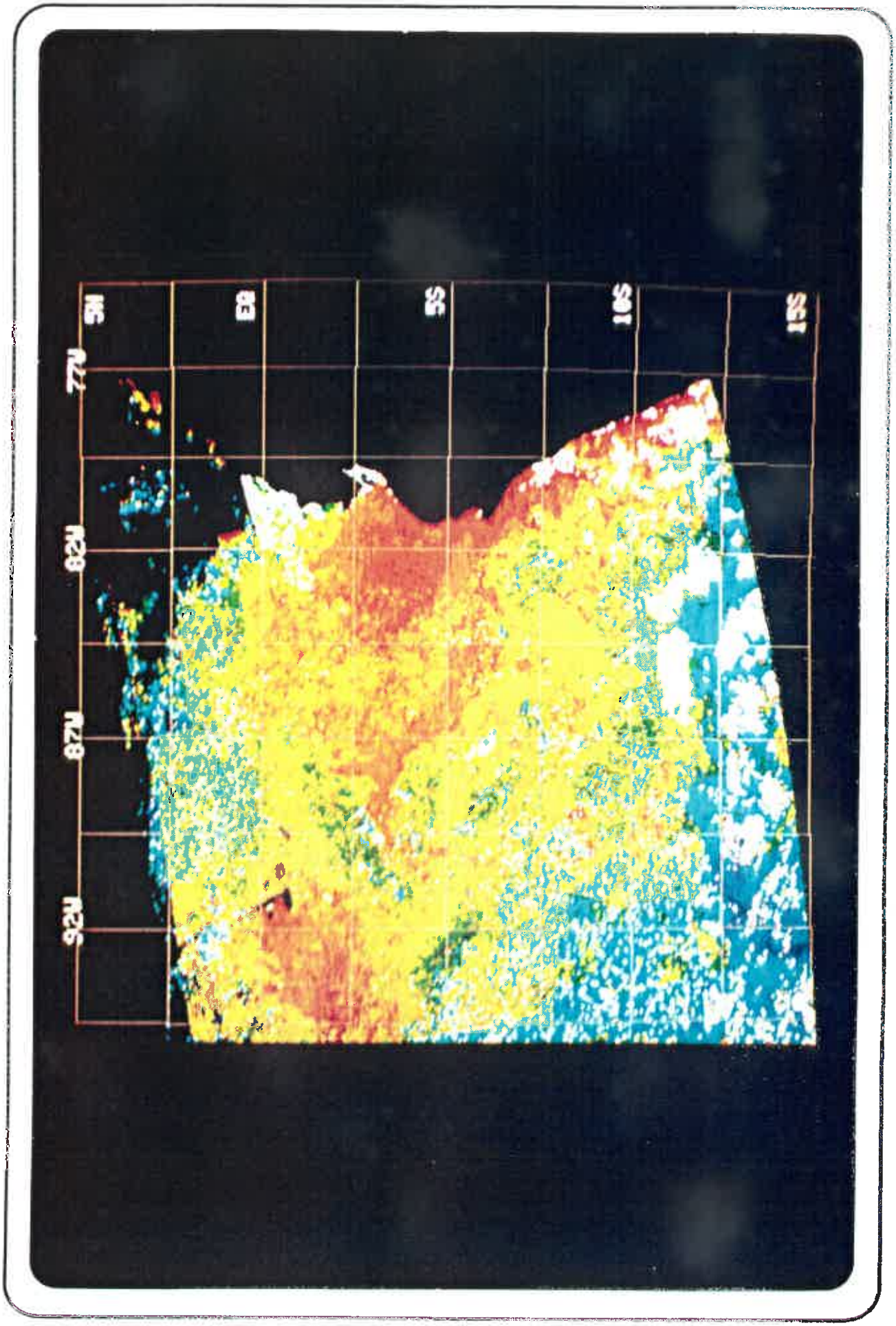
-77
-82
-87
-92
-96
-91
-86
-81
-76

These values agree quite well with the 'potential upwelling region' described by Yoshida (1967) for the eastern Pacific. The spatial distribution of phytoplankton biomass during this period suggests that processes other than coastal upwelling may have been responsible for supplying the nutrients necessary to support the levels of phytoplankton biomass observed at that time.

The size of the productive habitat is reduced during the Nov82-Feb83 phase of El Nino (Plate 6.11) when compared with the Dec79-Jan80 period; a similar reduction was observed during the 1975 El Nino (Cowles et al.,1977). Although its offshore extent closely resembles that which is observed during Dec78-Jan79, there are three notable exceptions. While high levels of phytoplankton biomass along a narrow coastal band (less than 50km) are still observed during El Nino, the offshore extent of the plankton-rich plumes is greatly reduced. Shipboard estimates of the mean chlorophyll concentrations in the 100 km wide Peruvian coastal band for Jan-Feb 1983 (1.04 mg/m3, Guillen, 1985) agreed quite well with the satellite estimate (1.01 mg/m3, SD = 0.32 mg/m3). In place of the gradual transition from enhanced to open ocean pigment concentrations which is observed in previous years, waters with very low pigment concentrations are found closer to the coast during El Nino than at any other time. During the non-Nino periods, distinct regions of enhanced production are observed to the west of the Galapagos Islands. During this phase of El Nino, however, the region of enhancement appears to shift

Plate 6.11. Satellite ocean color image showing the distribution of phytoplankton pigments in the eastern equatorial Pacific from Coastal Zone Color Scanner data acquired from November 1982 through February 1983 (El Nino, composited from eight orbits). The Ecuadorian and Peruvian coastlines are masked in black along the right side of the image and the Galapagos Islands can be seen along the equator near 92°W. This image has been remapped to the basin-wide sampling grid.

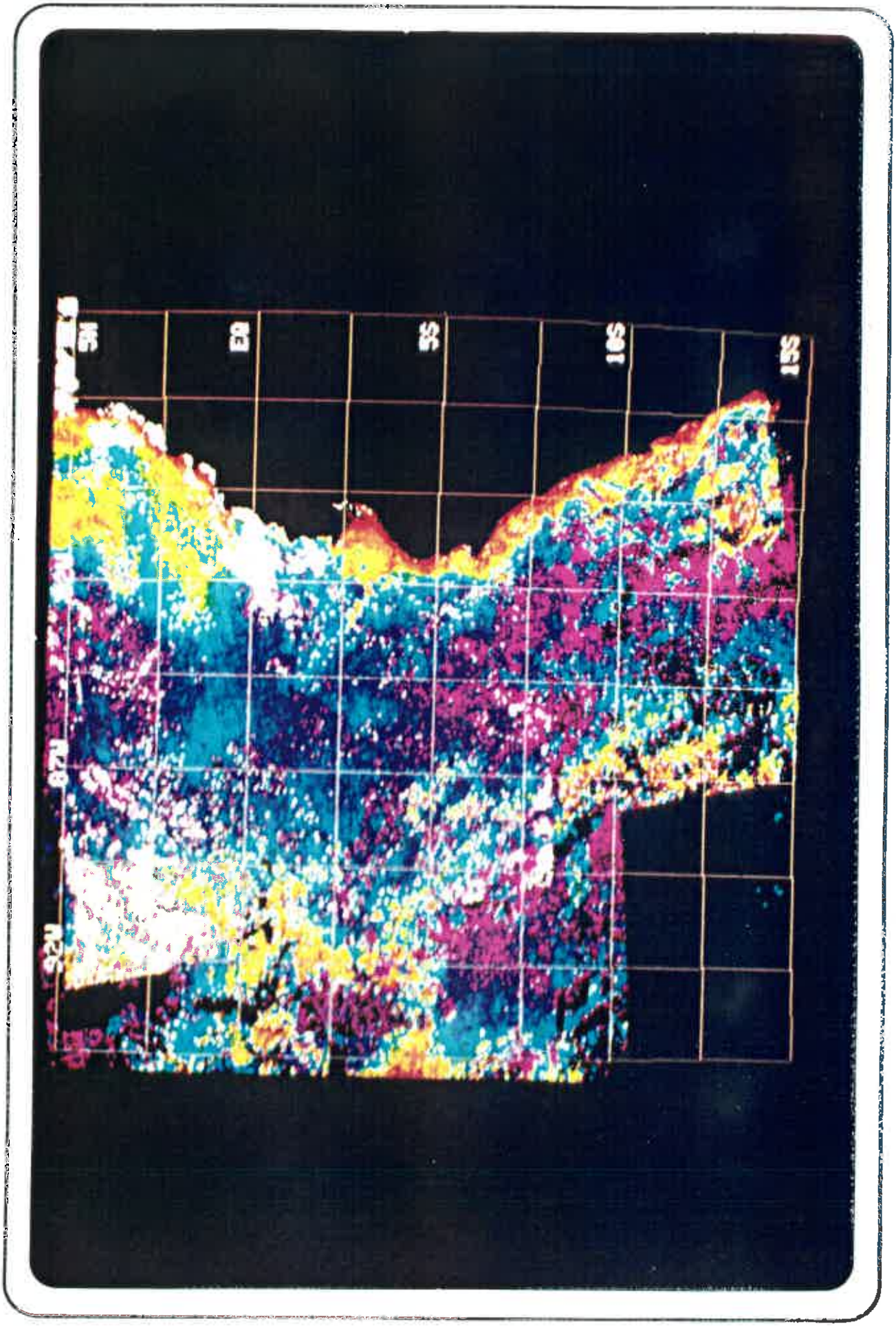
1.5S
1.0S
0.5S
0.0S
0.5N
1.0N
1.5N

from one side of the archipelago to the other reflecting the changing patterns of ocean circulation observed during that time (Feldman et al.,1984).

6.6. PRIMARY PRODUCTION

The use of remotely-sensed pigment measurements for the estimation of primary production on a regional and even global scale is growing. The principal advantage to be gained by the use of satellites is the vastly increased spatial and temporal coverage possible as compared with that available from ships. The errors imposed by the inherent limitations of the satellite measurements appear to be comparable to the errors caused by the spatial inhomogeneities in the biomass fields which are not accurrately assessed by ship surveys (Platt & Herman,1983). The quantitative information contained in the satellite images allows the primary production to be estimated for the entire study area as well as the production arising specifically from the open ocean and enhanced regions. Primary production was estimated by

$$P = C_{SAT} \times A \times D \times PI$$

where P is the total primary production (mgC/d) calculated to a depth of 1 optical attenuation length, C_{SAT} is the satellite derived pigment concentration (mgChl/m3), A is the total surface

area (m^2) covered by that pigment concentration, D is the optical depth (m) to which the satellite measurement applies as estimated from Smith & Baker (1978), and PI is the productivity index for this region (50 $mgC/mgChld^{-1}$) based on measured values from Barber & Smith (1981) and Barber & Chavez (1983). The use of a single value for the productivity index throughout the entire region obviously neglects much of the physiological variability in phytoplankton production. Region specific productivity indices based upon temperature, seasonal variability in solar insolation and perhaps a better knowledge of the spatial and temporal variability in mixing (Eppley et al. 1985) should significantly improve our large-scale productivity estimates. The results presented in Table 6.2 therfore, represent a first approximation of satellite-derived primary production for this region. It must be emphasized that these values represent the primary production to a depth of 1 optical attenuation length, the depth from which the satellite measurements actually apply. Inferences beyond this depth to the base of the euphotic zone (approximately 4.6 optical depths) are based upon regressions derived from vertical profile data (Brown et al.1984). The values given in Table 6.2 represent approximately 40% of the total water column production which is estimated when the relationship between C_{SAT} and total production described by Eppley (1984, Fig. 2) is applied .

The satellite derived production estimate for the productive

	PRODUCTIVE HABITAT		OPEN OCEAN	
	AREA ($10^3 km^2$)	PRODUCTION ($10^{10} gC/d$)	AREA ($10^3 km^2$)	PRODUCTION ($10^{10} gC/d$)
Dec78-Jan79	34 (3)	2.1 (10)	1326 (97)	19.2 (90)
Dec79-Jan80	468 (30)	27.7 (47)	1082 (70)	31.5 (53)
Dec82-Feb83	138 (9)	8.7 (30)	1379 (91)	20.7 (70)

TABLE 6.2. Surface area and the estimated primary production to a depth of 1 optical attenuation length (approximately the top 22% of the euphotic zone) for the Productive and Open Ocean habitats of the eastern equatorial Pacific. The numbers in parentheses give the percentage of total surface area and total production represented by each value.

habitat during El Nino (8.7×10^{10}gC/d) is similar to the estimate of 12×10^{10}gC/d presented by Chavez et al.(1984) in which the area of the coastal zone (assumed to extend 50 km offshore) was estimated at approximately 78×10^{3}km^{2}. However, if their productivity estimates are extrapolated over the satellite-derived area of the productive habitat given in Table 6.2 the estimated total primary production is then 20.7×10^{10}gC/d. The estimated production given in Table 6.2 is roughly 40% of this value, or what the relationship between total water column production and upper optical depth production appears to be, based on Eppley's (1984) findings.

The 1982-83 El Nino was the best documented and most intensively sampled event of its kind. It is not surprising, therefore, to find such a close agreement between the primary production estimates from ship sampling during this period and those from the satellite data which are presented in this chapter. What is evident from this discussion, however, is that the increased spatial coverage offered by satellites may significantly reduce the errors associated with regional primary production estimates. If nothing else, satellite observations can reduce these errors by merely providing a more accurrate assessment of the region itself.

CHAPTER 7

CONCLUSIONS

"The causes of things are ever more interesting than the events themselves"

Cicero, Letters to Atticus

In this study I have demonstrated that satellite ocean color data can be used to assess the variability of phytoplankton biomass over a wide range of time and space scales. The broad spatial and high temporal resolution of the Coastal Zone Color Scanner has made possible the documentation of such features as the tight coupling that exists between the distribution of phytoplankton biomass around the Galapagos Islands and the changes in oceanic and atmospheric circulation (Chapter 4), the response of a coastal upwelling system to short term changes in atmospheric forcing (Chapter 5) and, by using both the qualitative and quantitative information contained in the CZCS data, it has been possible to define the spatial extent of the area of enhanced biological production, referred to in this study as the productive habitat, in the eastern equatorial Pacific (Chapter 6). I have also shown (Chapter 6) that by using a very simple theoretical approach, it is possible to develop what appears to be a quite accurate assessment of regional primary production based on the

CZCS data. Athough significant improvements can be made, particularly through the use of more accurate relationships between surface chlorophyll and carbon fixation, the results presented here are very encouraging.

The degree to which isolated oceanic islands, in this case the Galapagos Islands, enhance the production of the surrounding waters has been demonstrated by this study. Although highly variable, it has been shown that a region of enhanced phytoplankton concentrations extends as far as 600 km downstream from the islands and covers nearly 80,000 km^2 of ocean surface. The variability in the location and extent of this region of enhancement appears to be correlated with the features of, and the changes in, the large-scale circulation patterns. The changes in phytoplankton distribution observed during the 1982-83 El Nino (Feldman et al., 1984), when compared with the measurements of oceanic circulation at that time, most clearly demonstrate this relationship. The seasonal cycle evident in the meteorological and oceanographic data also appears to be reflected in the patterns of phytoplankton distribution, but further study is needed before a conclusive correlation can be made.

The structure of the Pisco upwelling center, one of the major upwelling regions along the coast of Peru, has been described through the use of satellite ocean color imagery. The features observed in the satellite data are in general agreement with those described for an idealized coastal upwelling center with two

notable exceptions. First, the offshore extent of the band of enhanced phytoplankton production observed in the satellite images appears to be nearly four-times that described in the literature. And second, the transition from enhanced to oceanic conditions is rather sharp, and its structure suggests that a physical rather than biological factor may control the shape and offshore extent of the region of enhanced phytoplankton abundances.

The satellite imagery has also provided a means by which the short-term variablity of the distribution and abundances of phytoplankton biomass in response to changes in the physical environment could be assessed. A nearly three-fold decrease in the mean phytoplankton pigment concentration of the southern Peruvian coastal region took place over a two day period during April 1981. In addition, a ten-fold decrease (45,000 versus 4,264 km^2) in the total ocean surface area containing pigment concentrations associated with enhanced rather than oceanic conditions (greater than 1.0 mg/m3), occured over the same two day period.

It has also been shown that one can use satellite ocean color data to define and monitor the region of enhanced biological production associated with Peru upwelling system. Significant interannual variability in the areal extent of this region has been shown to exist under non-perturbed (i.e. non-El Nino) conditions. Basing estimates of total ecosystem production on the physical description of the upwelling zone rather than on the area

defined by enhanced levels of biological production can lead to significant errors. Using some rather basic assumptions and the quantitative information contained in the CZCS data, it was demonstrated how the increased spatial coverage offered by satellites may significantly reduce the errors associated with regional primary production estimates.

7.1. UNANSWERED QUESTIONS RAISED BY THIS STUDY

Although it is the goal of any research project to provide answers to some fundemental questions, it often is the case that in the course of the investigation new questions arise, many which were neither anticipated nor able to be adequately addressed within the scope of the original project. Such is the case with this study.

An understanding of the underlying processes responsible for the degree of large-scale, interannual variability in phytoplankton biomass described in Chapter 6 is to my mind, the major unanswered question raised by this study. A similar finding in the Gulf of California (Clark, personal communication, 1985) suggests that the driving mechanisms were not just regional, but extended over a much larger scale. As mentioned elsewhere, the identification, understanding and possible prediction of such variability in the ocean/atmosphere system is a major goal of the TOGA program. That this variability has such a strong biological

signature, and that because many of the features evident in the satellite ocean color images are so clearly associated with physical processes, a stronger biological component to the TOGA program is justified.

Much of oceanography is involved with the identification of the 'mean state' from which variability, as defined by its departure from the mean, can be assessed. To answer the question of what constitutes 'normal' conditions or in fact, do such conditions really exist in the dynamic ocean/atmosphere system is not easy, but needs to be addressed. Likewise, do individual biological measurements made at discrete locations from one year to the next truly represent interannual variability. This study has demonstrated how valuable satellite ocean color observations can be in determining the significance of individual biological measurements (i.e. primary production) by placing them within the larger, synoptic perspective. Just how many years of data will be needed to adequately describe the 'mean state' of the biological system remains to be seen.

7.2. FUTURE WORK: EASTERN EQUATORIAL PACIFIC TIME SERIES

One area of research that could build directly upon the work begun with this study involves the development of a comprehensive time series of the patterns of phytoplankton distribution and abundance in the Eastern Equatorial Pacific. The data sets used in this study cover the periods from December 1978 through November 1981, and September 1982 through May 1983. Unfortunately, the data are not uniformly distributed throughout those periods resulting in some months being covered more extensively than others. In addition it would be of particular importance to fill in the missing period from November 1981 through September 1982 with data now available, to gain a better understanding of the interannual variability and conditions that prevailed prior to El Nino.

Data acquired after May 1983, and which have not yet been processed, should be extremely useful in understanding how the equatorial Pacific recovered from the major El Nino of 1982-83, and the large number of surface observations which are available from that period should facilitate the interpretation of the satellite images. There is evidence to suggest that phytoplankton abundances after this El Nino were some of the highest observed and that the region of plankton-rich water extended several hundred kilometers offshore (Barber, personal communication, 1985), in many ways similar to the change that took place between

the December 1978 and December 1979 period. One interesting line of speculation is that perhaps the system is periodically 'purged', or more specifically, periods during which primary production is low throughout most of the region, significantly reduces the abundances of the primary herbivores (i.e. copepods, anchovies). Such a reduction in grazing pressure, which would be prolonged because of the longer generation times of the herbivores relative to phytoplankton, if accompanied by sufficient nutrient levels would then allow for a large increase in phytoplankton abundances. Although speculative, it would be interesting to see if such 'boom and bust' scenarios could be identified. Through the production of monthly or seasonal CZCS composites, it may be possible to correlate the large-scale processes in the annual cycle of oceanographic and meteorological parameters derived from observational and/or ocean simulation modelling studies with the variability in biological production.

7.3. EQUATORIAL FRONT AND LONG WAVES

Linked in as yet some unexplained way to the annual cycle, there appears to be an annual variation in the strength as well as the location of the Equatorial Front and in the appearance of the westward propagating, cusp-shaped equatorial long waves. Analysis of the CZCS data demonstrates that major ocean features such as the equatorial Front and the long waves that have been observed in

Plate 7.1. Satellite-derived sea surface temperature distributions around the Galapagos Islands acquired on 23 June 1979 (Nimbus-7 orbit 3352). Isabela and Fernandina Islands (gray) are visible in the lower right corner of the image. A distinct wave form (the crest of which is located near 98.5°W) separates the warmest waters (red) to the north of the equatorial Front from waters of intermediate temperatures (yellow) along the equator. The coolest temperatures (deep blue, approximately 19°C) associated with the upwelling of the equatorial Undercurrent can be seen just to the west of the Galapagos.

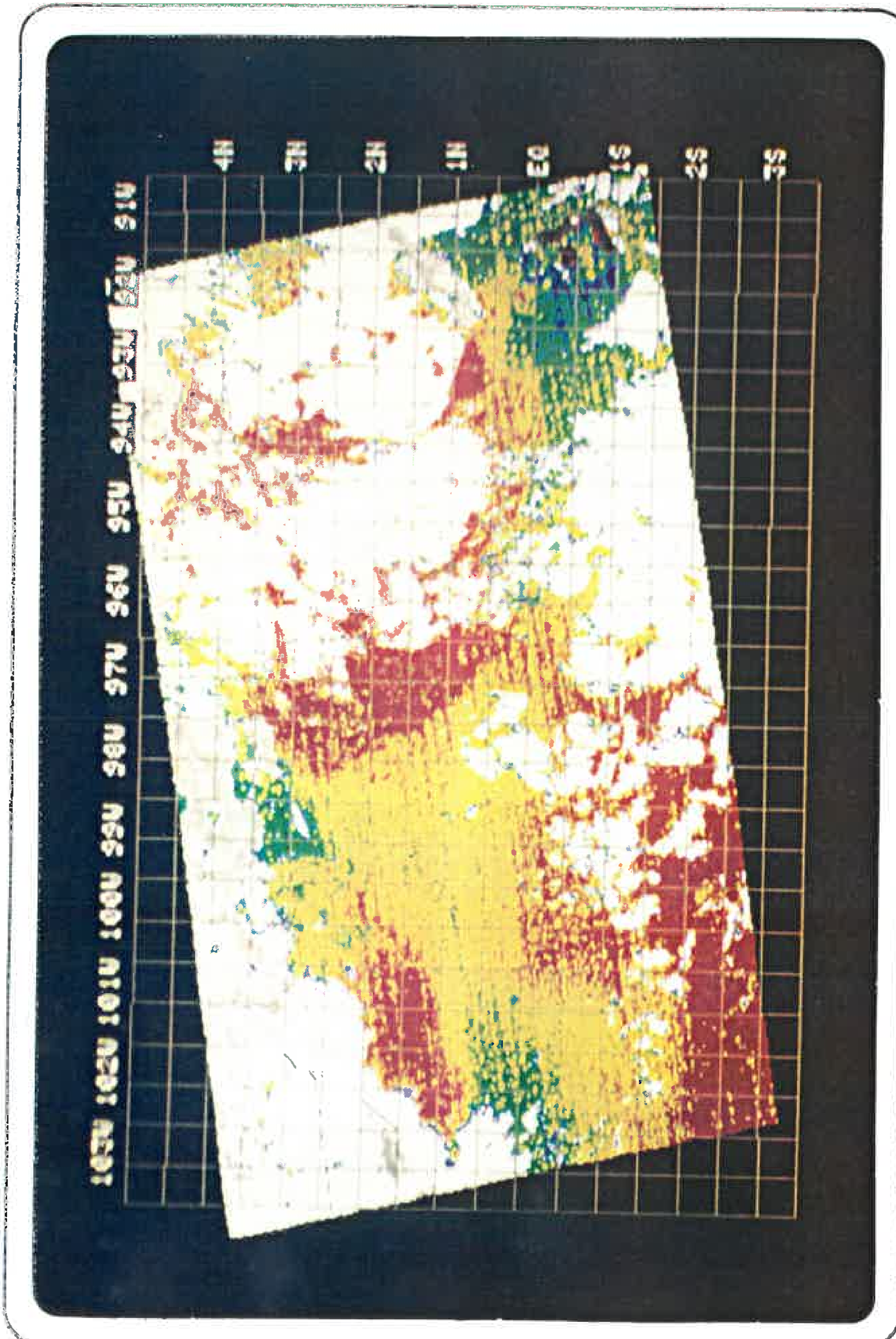
91W
92W
93W
94W
95W
96W
97W
98W
99W
100W
101W
102W
103W
4N
3N
2N
1N
EQ
1S
2S
3S

Plate 7.2. Satellite ocean color image of the distribution of phytoplankton pigments around the Galapagos Islands acquired on 23 June 1979 (Nimbus-7 orbit 3352). An ocean color front, with a form similar to the thermal front seen in Plate 7.1., separates the northern waters low in phytoplankton abundances from the richer southern waters. The highest pigment concentrations are found near the islands.

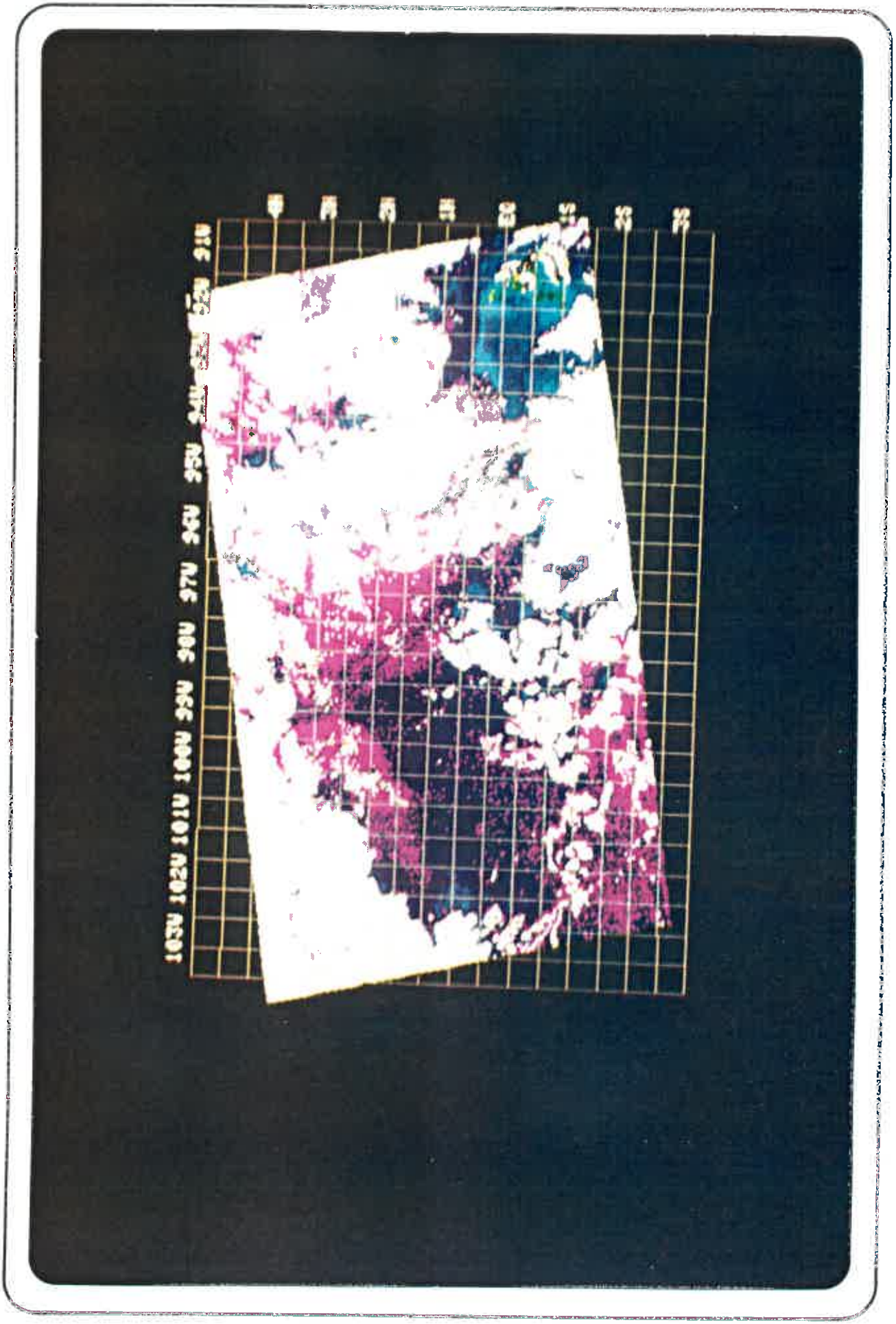

sea surface temperature (Legeckis, 1984), sea level (Lukas, personal communication, 1984), and drifting buoy data (Hansen & Paul, 1984) can be monitored by the CZCS. One example of the equatorial long waves as detected by the CZCS is given in Plates 7.1 & 7.2. The Galapagos Islands with the topographically induced upwelling of the cold (blue) waters of the equatorial Undercurrent are seen in the lower right-hand corner of the CZCS-derived sea surface temperature distributions acquired on 23 June 1979 (Plate 7.1). A distinct wave form (crest at 98.5°W) separates the warm (red) waters to the north of the equatorial Front from the cooler (yellow) waters to the south. A second, zonally oriented temperature front can be seen along the southern portion of the image. Another wave crest, located to the west of the region covered by Plates 7.1 & 7.2, is described by Hansen & Paul (1984). They monitored the eddy motions associated with this feature through the use of satellite-tracked drifting buoys on the same day as the CZCS observation. The co-registered CZCS-derived pigment concentrations (Plate 7.2) indicate a distinct ocean color front associated with the thermal front, with higher pigment concentrations found on the southern side of the front. It is believed that this is the first observation of a biological indicator of the equatorial long waves. The eddy motions associated with the waves and their possible influence on the heat flux near the equator may have a similar effect on the flux of nutrients and, hence, their ocean color signature. The patterns

observed by the CZCS may, therefore, provide further insight into the dynamics of these features and possibly offer a way of monitoring the long waves when their thermal signature is masked. Some specific questions which could be addressed through further study include:

1- with what frequency do the waves appear in the satellite ocean color data?
2- what is the relationship between the ocean color front and the physical structure of the front?
3- are there times when the front and/or waves appear in either the ocean color data or sea surface temperature data, but not in both?
4- are there indications in the CZCS images of the eddy motions observed in the buoy data (i.e. is the eddy located to the north of the Galapagos in Plate 4.11 an example of such a feature)?

7.3. INFLUENCE OF ISLANDS AND ISLAND GROUPS ON OCEANIC PRODUCTION

The study of the circulation and mixing patterns around oceanic islands and of their influence on oceanic production is a topic worthy of further study. This investigation has clearly demonstrated that the Galapagos Islands significantly enhance the productivity of the surrounding waters and some evidence of

possible mechanisms has been offered. It would be interesting to continue this work around the Galapagos and also expand the coverage to include other oceanic islands or island groups in order to define and monitor the area of enhanced biological production associated with them. The understanding of flow patterns around islands (observational as well as theoretical) and the formation of island wakes has been the subject of much investigation. In particular, recent observations of the Galapagos Islands from the Space Shuttle (Scully-Power et al., 1985) revealed many features about the circulation around these islands not amenable to study by other means. Unfortunately, the biological consequences of such processes have been poorly quantified and are often lumped under the general term of 'island mass effect'. The visualization and quantification of island wakes and plumes in the satellite ocean color data has been demonstrated in this study. Finally, it is proposed that an island plume model (Okubo, personal communication, 1985) be developed and applied to the phytoplankton patterns observed in the CZCS imagery.

REFERENCES

Arcos, F. (1981) A dense patch of Arcartia levequei (Copepoda calanoida) in upwelled equatorial undercurrent water around the Galapagos Islands. In: Coastal Upwelling, F. A. Richards, editor, American Geophysical Union, Washington, D.C., 427-432.

Ashmole, N. P. (1971) Seabird ecology and the marine environment. In: Avian Biology, 1, D. S. Farmer and J. R. King, editors, Academic Press, New York, 233-286.

Barber, R. T. & F. Chavez (1983) Biological Consequences of El Nino. Science, 226, 1203-1210.

Barber, R. T., Huntsman, S. A., Kogelschatz, J. E., Smith, W. O., Jones, B. H. & J. C. Paul (1978) Carbon, Chlorophyll and Light Extinction from JOINT II 1976 and 1977. CUEA Data Report 49, 476 pp.

Barber, R. T. & J. H. Ryther (1969) Organic chelators: factors primary production in the Cromwell Current upwelling. Journal of Experimental Marine Biology and Ecology, 3, 191-199.

Barber, R. T. & R. Smith (1981) Coastal Upwelling Ecosystems. In: Analysis of Marine Ecosystems, editor A. R. Longhurst, Academic Press, New York, 31-68.

Barber, R. T. & W. O. Smith (1981a) The Role of Circulation, Sinking, and Vertical Migration in Physical Sorting of Phytoplankton in the Upwelling Center at 15S. In: Coastal Upwelling, F. A. Richards, editor, American Geophysical Union, Washington, D.C., 366-371.

Beebe, C. W. (1926) The Arcturus adventure. Putnam, New York.

Blasco, D., Estrada, M. & B. Jones (1980) Relationship between he phytoplankton distribution and composition and the hydrography in the northwest African upwelling region near Cabo Corbeiro. Deep-Sea Research, 27a, 799-821.

Boersma, P. D. (1978) Breeding Patterns of Galapagos penguins as an indicator of oceanographic conditions. Science, 200, 1481-1483.

Bowman, M. J., Foster, B. A. & P. P. Lapennas (1982) Ocean Water Properties. In: Maui Development Environmental Study Report on Phase Two, 1977-1981, Kibblewhite, A., Bergquist, P., Foster, B., Gregory, M. & M. Miller, editors, University of Auckland, Auckland, 77-98.

Boyd, C. M. & S. L. Smith (1983) Plankton, upwelling, and coastally trapped waves off Peru. Deep-Sea Research, 30, 723-742.

Brink, K. H., Halpern, D. & R. L. Smith (1980) Circulation in the Peruvian Upwelling System Near 15S. Journal of Geophysical Research, 85, 4036-4048.

Brink, K. H., Jones, B. H., Van Leer, J. C., Mooers, C. N. K., Stuart, D. W., Stevenson, M. R., Dugdale, R. C. & G. W. Heburn (1981) Physical and Biological Structure and Variability in an Upwelling Center off Peru Near 15S During March, 1977. In: Coastal Upwelling, F. A. Richards, editor, American Geophysical Union, Washington, D.C., 473-495.

Brown, O., Evans, R., Brown, J., Gordon, H., Smith, R. & K. Baker (1984) Blooming Off the U.S. East Coast: A Satellite Description. In: Global Ocean Flux Study, Proceeding of a Workshop, Board on Ocean Science and Policy, National Research Council, National Academy Press, Washington, D.C., 67-84.

Brown, O., Evans, R., Brown, J., Gordon, H., Smith, R. & K. Baker (1985) Phytoplankton Blooming Off the U.S. East Coast: A Satellite Description. Science, 229, 163-167.

Bubnov, V. A. & V. D. Egorikhin (1981) Central Pacific equatorial currrents. Tropical Oceans-Atmosphere Newsletter, 7, 1-3.

Campbell, J. W. & W. E. Esaias (1985) Spatial patterns in temperature and chlorophyll on Nantucket Shoals from airborne remote sensing data, May 7-9, 1981. Journal of Marine Research, 43, 139-161.

Cassie, R. M. (1959) An Experimental Study of Factors Inducing Aggregation in Marine Plankton. New Zealand Journal of Science, 2, 339-365.

Chavez, F., Barber, R., Kogelschatz, J., Thayer, V. & B. Cai (1984) El Nino and Primary Productivity: Potential Effects on Atmospheric Carbon Dioxide and Fish Production. Tropical Oceans-Atmosphere Newsletter, 28, 1-2.

Chelton, D. B., Bernal, P. A. & J. A. McGowan (1982) Large-scale interannual physical and biological interaction in the California Current. Journal of Marine Research, 40, 1095-1125.

Clark, D. K. (1981) Phytoplankton Pigment Algorithms for the Nimbus-7 CZCS. In: Oceanography from Space, J. F. R. Gower, editor, Plenum Press, New York, 227-237.

Codispoti, L. A. (1981) Temporal Nutrient Variability in Three Different Upwelling Regions. In: Coastal Upwelling, F. A. Richards, editor, American Geophysical Union, Washington, D.C., 209-220.

Codispoti, L. A. (1983) On Nutrient Variability and Sediments in Upwelling Regions. In: Coastal Upwelling: Its sediment record, Suess, E. & J. Thiede, editors, Plenum Press, New York, 125-145.

Cowles, T., Barber, R. & O. Guillen (1977) Biological Consequences of the 1975 El Nino. Science, 195, 285-287.

Cullen, J. J. (1982) The Deep Chlorophyll Maximum: Comparing Vertical Profiles of Chlorophyll a. Canadian Journal of Fisheries and Aquatic Sciences, 39, 791-803.

Denman, K. L. & A. E. Gargett. (1983) Time and Spatial Scales of Vertical Mixing and Advection of Phytoplankton in the Upper Ocean. Limnology and Oceanography, 28, 801-815.

Donguy, J. R., Henin, C., Morliere, A., Rebert, J. P., & G. Meyers (1982) Appearances in the Western Pacific of Phenomena Induced by El Nino in 1979-80. Tropical Oceans-Atmosphere Newsletter, 10, 1-2.

Doty, M. S. & M. Oguri (1956) The Island Mass Effect. J. Cons. Perm. Intl. Explor. Mer., 222, 33-37.

Dugdale, R. C. & J. J. Goering (1967) Uptake of new and regenerated forms of nitrogen in primary productivity. Limnology and Oceanography, 12, 196-206.

Enfield, D. B. & P. A. Newberger (1985) Peru Coastal Winds During 1982-83. In: Proceedings of the Ninth Annual Climate Diagnostics Workshop, Oct. 22-26, 1984, U. S. Department of Commerce, NOAA/NWS, Washington, D. C., in press.

Eppley, R. (1984) Relations Between Primary Production and Ocean Chlorophyll Determined by Satellites. In: Global Ocean Flux Study, Proceeding of a Workshop, Board on Ocean Science and Policy, National Research Council, National Academy Press, Washington, D.C., 85-102.

Eppley, R., Stewart, E., Abbott, M. & R. Owen (1985) Estimating ocean production from satellite-derived chlorophyll: insights from the EASTROPAC data set. In: Preprints from the Symposium on Vertical Motion in the Equatorial Upper Ocean and its Effects Upon Living Resources and the Atmosphere, Paris, May 1985, SCOR, UNESCO.

Eppley, R. Stewart, E., Abbott, M. & U. Heyman (1985) Estimating ocean primary production from satellite chlorophyll. Introduction to regional differences and statistics for the Southern California Bight. Journal of Plankton Research, 7, 57-70.

Esaias, W. E. (1980) Remote Sensing of Oceanic Phytoplankton: Present Capabilities and Future Goals. In: Primary Productivity in the Sea, P. Falkowski, editor, Plenum Press, New York, 321-337.

Fahrbach, E., Brockmann, C., Lostaunau, N. & W. Urquizo (1981) The Northern Peruvian Upwelling System During the ESACAN Experiment. In: Coastal Upwelling, F. A. Richards, editor, American Geophysical Union, Washington, D.C., 134-145.

Feldman, G., Clark, D., & D. Halpern (1984) Satellite Color Observations of the Phytoplankton Distribution in the Eastern Equatorial Pacific During the 1982-1983 El Nino. Science, 226, 1069-1071.

Fitz-roy, R. (1839) Narrative of the Surveying Voyages of His Majesty's Ships Adventure and Beagle between the years 1826 and 1836, London.

Gilmartin, M. & N. Revelante (1974) The 'Island Mass' Effect on the Phytoplankton and Primary Production of the Hawaiian Islands. Journal of Experimental Biology and Ecology, 16, 181-204.

Global Ocean Flux Study, Proceeding of a Workshop, Board on Ocean Science and Policy, National Research Council, National Academy Press, Washington, D.C. 359 pp.

Gordon, H. & D. H. Clark (1981) Clear Water Radiances for Atmospheric Correction of Coastal Zone Color Scanner Imagery. Applied Optics, 20, 299-313.

Gordon, H., Brown, J., Brown, O., Evans, R. & D. Clark (1983a) Nimbus-7 CZCS: reduction of its radiometric sensitivity with time. Applied Optics, 22, 3929-3931.

Gordon, H., Clark, D., Brown, J., Brown, O., Evans, R., & W. Broenkow (1983) Phytoplankton pigment concentrations in the Middle Atlantic Bight: comparison of ship determinations and CZCS estimates. Applied Optics, 22, 20-36.

Gordon, H. & A. Morel (1983) Remote Assessment of Ocean Color for Interpretation of Satellite Visible Imagery: A Review. Lecture Notes on Coastal and Estuarine Studies, Springer-Verlag, New York, 114 pp.

Guillen, O. (1985) Chemical Characteristics and Productivity Off Peru During El Nino 1982-83. In: Preprints from the Symposium on Vertical Motion in the Equatorial Upper Ocean and its Effects Upon Living Resources and the Atmosphere, Paris, May 1985, SCOR, UNESCO.

Guillen, O. & R. Calienes (1981) Upwelling Off Chimbote. In: Coastal Upwelling, F. A. Richards, editor, American Geophysical Union, Washington, D.C., 312-326.

Halpern, D. (1976) Structure of a coastal upwelling event observed off Oregon during July 1973. Deep-Sea Research, 23, 495-508.

Halpern, D. (1983) Annual and Interannual Current and Temperature Fluctuations in the Eastern Pacific Upper Ocean, 1980-1982. Tropical Oceans-Atmosphere Newsletter, 16, 18-19.

Halpern, D., Hayes, S., Leetmaa, A., Hansen, D. & S. G. H. Philander (1983) Oceanographic Observations of the 1982 Warming of the Tropical Eastern Pacific. Science, 221, 1173-1175.

Hamner, W. M. & I. R. Hauri (1981) Effects of island mass: Water flow and plankton pattern around a reef in the Great Barrier Reef lagoon, Australia. Limnology and Oceanography, 26, 1084-1102.

Hansen, D. V. & C. A. Paul (1984) Genesis and Effects of Long Waves in the Equatorial Pacific. Journal of Geophysical Research, 89, 10431-10440.

Haury, L. R., McGowan, J. A. & P. H. Wiebe (1978) Patterns and Processes in the Time-Space Scales of Plankton Distributions. In: Spatial Patterns in Plankton Communities, J. H. Steele, editor, Plenum Press, 277-327.

Hayes, S. P. (1985) Sea level and near surface temperature variability at the Galapagos Islands, 1979-1983. In: Galapagos 1982-1983: A chronicle of the effects of El Nino, G. Robinson & E. del Pino, editors, in press.

Hayes, S. P. & D. Halpern (1976) Observations of internal waves and coastal upwelling off the Oregon coast. Journal of Marine Research, 34, 247-267.

Hayes, S. P. & D. Halpern (1984) Correlation of Current and Sea Level in the Eastern Equatorial Pacific. Journal of Physical Oceanography, 14, 811-824.

Hayward, T. L. & E. L. Venrick (1982) Relation Between Surface Chlorophyll, Integrated Chlorophyll and Integrated Primary Production. Marine Biology, 69, 247-252.

Houvenaghel, O. T. (1978) Oceanographic conditions in the Galapagos Archipelago and their relationships with life on the islands. In: Upwelling Ecosystems, R. Boje and M. Tomczak, editors, Springer-Verlag, New York, 181-202.

Houvenaghel, O. T. (1984) Oceanographic Setting of the Galapagos Islands. In: Galapagos - Key environments, R. Perry, editor, Pergaman Press, Oxford, 43-54.

Hovis, W., Clark, D., Anderson, F., Austin, R., Wilson, W., Baker, E., Ball, D., Gordon, H., Mueller, J., El-Sayed, S., Sturm, B., Wrigley, R. & C. Yentsch (1980) Nimbus-7 Coastal Zone Color Scanner: System Description and Initial Imagery. Science, 210, 60-63.

Hovis, W. (1981) The Nimbus-7 Coastal Zone Color Scanner Program. In: Oceanography from Space, J. F. R. Gower, editor, Plenum Press, New York, 213-225.

Huyer, A. (1980) The Offshore Structure and Subsurface Expression of Sea Level Variations off Peru, 1976-1977. Journal of Physical Oceanography, 10, 1755-1768.

Ikeda, M. & W. J. Emery (1984) A continental shelf upwelling event off Vancouver Island as revealed by satellite infrared imagery. Journal of Marine Research, 42, 303-317.

Jimenez, R. (1981) Composition and distribution of phytoplankton in the upwelling system of the Galapagos Islands. In: Coastal Upwelling, F. A. Richards, editor, American Geophysical Union, Washington, D.C., 327-338.

Jones, B. H., Brink, K. H., Dugdale, R. C., Van Leer, J. C., Blasco, D. & J. C. Kelly (1983) Observations of a persistant upwelling center off Point Conception, California. In: Coastal Upwelling: Its sediment record, E. Suess & J. Theide, editors, 37-60.

Kogelschatz, J., Solorzano, L., Barber, R. & P. Mendoza (1985) Oceanographic Conditions in the Galapagos Islands During the 1982/1983 El Nino. In: Galapagos 1982-1983: A chronicle of the effects of the El Nino, G. Robinson and E. del Pino, editors, in press.

Kuhn, T. S. (1970) The Structure of Scientific Revolutions, University of Chicago Press, Chicago.

LaFond, E. C. & K. G. LaFond (1971) Oceanography and its relation to marine organic production. In: Fertility of the Sea, J. D. Costlow, editor, Gordon & Breach, 241-265.

Leetmaa, A. & R. L. Molinari (1984) Two Cross-Equatorial Sections at 110°W. Journal of Physical Oceanography, 14, 255-263.

Legeckis, R. (1984) Monitoring of Long Waves in the Eastern Equatorial Pacific 1981-1983 Using Satellite Multi-Channel Sea Surface Temperature Charts. NOAA Technical Report NESDIS 8 .

Limberger, D., Trillmich, F., Kooyman, G. & P. Majluf (1983) Reproductive Failure of fur seals in Galapagos and Peru in 1982-83. Tropical Oceans-Atmosphere Newsletter, 21, 16-17.

Lorenzen, C. J. (1970) Surface chlorophyll as an index of the depth, chlorophyll content and primary productivity of the euphotic layer. Limnology and Oceanography, 15, 479-480.

Love, C. M. (1972) EASTROPAC Atlas, U.S. Department of Commerce, circular 330.

Lukas, R. (1981) The termination of the equatorial undercurrent in the eastern Pacific. Ph.D. dissertation, University of Hawaii. 126 pp.

MacIsaac, J. J., Dugdale, R. C., Barber, R. T., Blasco, D. & T. T. Packard (1985) Primary Production Cycle in an Upwelling Center. Deep-Sea Research, 32, 503-529.

Mangum, L., & S. Hayes (1984) The Vertical Structure of the Zonal Pressure Gradient in the Eastern Equatorial Pacific. Journal of Geophysical Research, 89, 10441-10449.

Maxwell, D. C. (1974) Marine primary productivity of the Galapagos Archipelago. Ph.D. dissertation, Ohio State University, 163 pp.

Maxworthy, T. & S. Narimousa (1985) Experiments and Observations on the Effects of Bottom Topography on Coastal Upwelling. In: Preprints from the Symposium on Vertical Motion in the Equatorial Upper Ocean and its Effects Upon Living Resources and the Atmosphere, Paris, May 1985, SCOR, UNESCO.

McClain, C. R., Pietrafesa, L. J. & J. A. Yoder (1984) Observations of Gulf Stream-Induced and Wind-Driven Upwelling in the Georgia Bight Using Ocean Color and Infrared Imagery. Journal of Geophysical Research, 89, 3705-3723.

Melville, H. (1856) The Piazza Tales- "The Encantadas" or the Enchanted Isles, New York.

Mooers, C. N. K. & A. R. Robinson (1984) Turbulent jets and eddies in the California Current and inferred cross-shelf transports. Science, 223, 51-53.

Morel, A. & L. Prieur (1977) Analysis of Variations in Ocean Color. Limnology and Oceanography, 22, 709-722.

Owen, R. W. (1981) Fronts and Eddies in the Sea: Mechanisms, Interactions and Biological Effects. In: Analysis of Marine Ecosystems, A. R. Longhurst, editor, Academic Press, New York, 197-233.

Palmer, C. E. & R. L. Pyle (1966) The Climatological Setting of the Galapagos. In: The Galapagos, R. Bowman, editor, University of California Press, Berkeley, 108-122.

Parrish, R., Bakun, A., Husby, D. & C. Nelson (1983) Comparative Climatology of Selected Environmental Processes in Relation to Eastern Boundary Current Pelagic Fish Production. In: Proceedings of the Expert Consultation to Examine Changes in Abundance and Species of Neritic Fish Resources, Sharp, G. & J. Csirke, editors, FAO Fish Rep. 291, Vol. 3, 731-778.

Paulik, G. J. (1971) Anchovies, Birds, and Fishermen in the Peru Current. In: Environment: Resources, Pollution and Society, W. M. Murdoch, editor, Sinauer Associates, Stamford, Connecticut.

Pazos, M. C. & C. A. Paul (1984) Drifting Buoy Data From the Equatorial Pacific Ocean for the Period of August 31, 1980 through April 30, 1982. NOAA Technical Memorandum ERL AOML-60

Pelaez-Hudlet, J. (1984) Phytoplankton Pigment Concentrations and Patterns in the California Current as Determined by Satellite. Ph.D. Dissertation, University of California, 98 pp.

Philander, S. G. H., Halpern, D., Hansen, D., Legeckis, R., Miller, L., Paul, C., Watts, R., Weisberg, R. & M. Wimbush (1985) Long Waves in the Equatorial Pacific Ocean. EOS, 66, 154.

Platt, T., & A. Herman (1983) Remote sensing of phytoplankton in the sea: surface-layer chlorophyll as an estimate of water-column chlorophyll and primary production. International Journal of Remote Sensing, 4, 343-351.

Platt, T. & W. G. Harrison (1985) Carbon and Oxygen Fluxes in the Open Ocean. In: Preprints from the Symposium on Vertical Motion in the Equatorial Upper Ocean and its Effects Upon Living Resources and the Atmosphere, Paris, May 1985, SCOR, UNESCO.

Preller, R. & J. J. O'Brien (1980) The Influence of Bottom Topography on Upwelling Off Peru. Journal of Physical Oceanography, 10, 1377-1398.

Rasmusson, E. M., & J. M. Wallace (1983) Meteorological Aspects of the El Nino/Southern Oscillation. Science, 222, 1195-1202.

Robinson, W. A. (1972) Return to the Sea, John de Graff, inc., p.47.

Rowlands, P. B. (1982) The Flow of equatorial Kelvin waves and the equatorial undercurrent around islands. Journal of Marine Research, 40, 915-936.

Sadler, J. C. & B. J. Kilonsky (1981) Trade Wind Monitoring Using Satellite Observations. UHMET 81-01, Department of Meteorology, University of Hawaii.

Schneider, D. (1982) Fronts and Seabird Aggregations in the Southeastern Bering Sea, Marine Ecology - Progress Series, 10, 101-103.

Schott, G. (1931) Der Peru-Strom und seine nordlichen Nachbargebiete in normaler and abnormaler Ausbildung. Ann. Hydro. u. Mar. Met., 59, 161-169, 200-213, 240-257.

Schreiber, R. W. & E. A. Schreiber (1983) Central Pacific Seabirds and the El Nino Southern Oscillation: 1982 to 1983 Perspectives. Science, 225, 713-716.

Scully-Power, P., Hughes, J. & T. Aldinger (1985) Navy Oceanographer Shuttle Observations, STS 41-G, Quicklook Report. NUSC Technical Document 7379.

Sette, O. E. (1955) Consideration of Midocean Fish Production as Related to Oceanic Circulatory Systems. Journal of Marine Research, 14, 398-414.

Simpson, J. J., Dickey, T. D. & C. J. Koblinsky (1984) An Offshore Eddy in the California Current System Part I: Interior Dynamics. Progress in Oceanography, 13, 5-49.

Simpson, J. H. & P. B. Tett (1985) Island Stirring Effects on Phytoplankton Growth. In: Tidal Mixing and Plankton Dynamics, Bowman, M. J., Yentsch, C., & W. T. Peterson, editors, Lecture Notes on Coastal and Estuarine Studies, Springer-Verlag, New York, in press.

Simpson, J. H., Tett, P. B., Argote-Espinoza, M. L., Edwards, A., Jones, K. J. & G. Savidge (1982) Mixing and phytoplankton growth around an island in a stratified sea. Continental Shelf Research, 1, 15-31.

Smith, R. C. (1984) Ocean Color for the Estimation of Global Marine Primary Productivity. In: Global Ocean Flux Study, Proceeding of a Workshop, Board on Ocean Science and Policy, National Research Council, National Academy Press, Washington, D.C., 104-124.

Smith, R. C., & K. Baker (1978) The bio-optical state of ocean waters and remote sensing. Limnology and Oceanography, 23, 247-259.

Smith, R. C., Eppley, R., & K. Baker (1982) Correlation of Primary Production as Measured Abord Ship in Southern California Coastal Waters and as Estimated from Satellite Chlorophyll Images. Marine Biology, 66, 281-288.

Smith, R. C. & W. H. Wilson (1981) Ship and satellite bio-optical research in the California Bight. In: Oceanography from Space, J. F. R. Gower, editor, Plenum Press, New York, 281-294.

Smith, R. L. (1968) Upwelling. Oceanogr. Mar. Biol. Ann. Rev., 6, 11-46.

Smith, W., Heburn, G., Barber, R. & J.J. O'Brien (1983) Regulation of Phytoplankton Communities by Physical Processes in Upwelling Ecosystems. J. Mar. Res., 41, 539-556.

Sorokin, Y. I., Sukhanova, I. N., Konovalova, G. V. & E. B. Pavel'eva (1975) Primary prodction and phytoplankton in the area of the equatorial divergence in the eastern part of the Pacific Ocean. Academy of Science of the USSR, Trudy P.P. Shirshov Institute of Oceanology, 102, 108-122.

Steele, J. H. (1978) Some Comments on Plankton Patches. In: Spatial Patterns in Plankton Communities, J. H. Steele, editor, Plenum Press, 1-20.

Stevenson, M. R. & B. A. Taft (1971) New evidence of the equatorial undercurrent east of the Galapagos Islands. Journal of Marine Research, 29, 103-115.

Suess, E. & J. Thiede (1983) Introduction. In: Coastal Upwelling: Its sediment record, Plenum Press, New York.

Targanza, E. D., Conrad, J. C. & L. C. Breaker (1981) Satellite observations of a cyclonic upwelling system and giant plume in the California Current. In: Coastal Upwelling, F. A. Richards, editor, American Geophysical Union, Washington, D.C., 228-241.

Thompson, J. Dana (1981) Climate, Upwelling, and Biological Productivity. In: Resource Management and Environmental Uncertainty: Lessons from Coastal Upwelling Fisheries, editors M. Glantz and J. Dana Thompson, John Wiley & Sons, New York, 13-33.

Viollier, M., Tanre, D. & P. Y. Deschamps (1980) An Algorithm for Remote Sensing of Water Color from Space. Boundary Layer Meteorology, 18, 247-267.

Walsh, J., Whitledge, T., Esaias, W., Smith, R., Huntsman, S., Santander, H. & B. De Mendiola (1980) The spawning habitat of the Peruvian anchovy, (Engraulis ringens), Deep-Sea Research, 27a, 1-27.

White, W. B. (1971) A Rossby Wake due to an Island in an Eastward Current. Journal of Physical Oceanography, 1, 161-168.

White, W. B. (1973) An oceanic wake in the Equatorial Undercurrent Downstream from the Galapagos Archipelago. Journal of Physical Oceanography, 3, 156-161.

Wirick, C. D. (1981) Marine Herbivores and the Spatial Distributions of the Phytoplankton. Ph.D. dissertation, University of Washington, 183 pp.

Wolanski, E., Imberger, J. & M. L. Heron (1984) Island Wakes in Shallow Coastal Waters. Journal of Geophysical Research, 89, 10,553-10,569.

Wooster, W. S. (1969) Equatorial Front Between Peru and Galapagos. Deep-Sea Research Suppl., 16, 407-419.

Wooster, W. S. & H. A. Sievers (1970) Seasonal variations of temperature, drift and heat exchange in surface waters off the west coast of South America. Limnology and Oceanography, 15, 595-605.

Wyrtki, K. (1965) Surface Currents of the Eastern Tropical Pacific Ocean. IATTC Bulletin, 9, 271-294.

Wyrtki, K. (1974) Sea level and seasonal fluctuations of equatorial currents in the western Pacific Ocean. Journal of Physical Oceanography, 4, 91-103.

Yentsch, C. S. (1983) Remote Sensing of Biological Substances. In: Remote Sensing Applications in Marine Science and Technology, A. P. Cracknell, editor, Reidel Publishing Company, Boston, 263-297.

Yentsch, C. S. (1984) Satellite representaion of features of ocean circulation indicated by CZCS colorimetry. In: Remote Sensing of Shelf Sea Hydrodynamics, J. Nihoul, editor, Elsevier, Amsterdam.

Yentsch, C. S. & D. A. Phinney (1985) Rotary Motions and Convection as a Means of Regulating Primary Production in Warm Core Rings. Journal of Geophysical Research, 90, 3237-3248.

Yoshida, K. (1967) Circulation in the eastern tropical oceans with special reference to upwelling and undercurrents. Japan. J. Geophys.,4, 1-75.

Zuta, S. & J. Quispe (1981) Hydrographic Features Off Peru in 1979-1980 In: Recent Progress in Equatorial Oceanography, McCreary Jr. J., Moore, D. & J. Witte, editors, Nova University/N.Y.I.T. Press, 61-73.

Zuta, S., Rivera, T. & A. Bustamante (1978) Hydrologic Aspects of the Main Upwelling Areas off Peru. In: Upwelling Ecosystems, Boje, R. & M. Tomczak, editors, Springer-Verlag, New York, 235-257.